AGGLOMERATION IN SUSPENSION:

A STUDY OF MECHANISMS AND KINETICS

G.G. BEMER

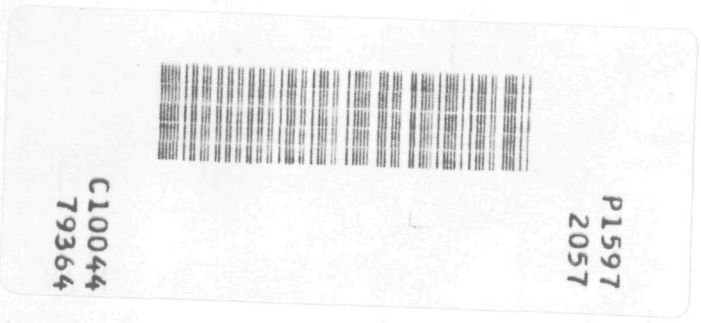

AGGLOMERATION IN SUSPENSION:

A STUDY OF MECHANISMS AND KINETICS

PROEFSCHRIFT

TER VERKRIJGING VAN DE GRAAD VAN DOCTOR IN DE TECHNISCHE WETENSCHAPPEN AAN DE TECHNISCHE HOGESCHOOL DELFT, OP GEZAG VAN DE RECTOR MAGNIFICUS PROF. DR. IR. F.J. KIEVITS VOOR EEN COMMISSIE AANGEWEZEN DOOR HET COLLEGE VAN DEKANEN, TE VERDEDIGEN OP WOENSDAG 31 OKTOBER 1979 DES MIDDAGS OM 16.00 UUR

DOOR

GERARDUS GUILLAUME BEMER

scheikundig ingenieur

geboren te Maastricht

Dit proefschrift is goedgekeurd door de promotor
PROF. F.J. ZUIDERWEG

ACKNOWLEDGEMENT

I wish to express my gratitude to Prof. F.J. Zuiderweg for his encouragement to undertake this study. Working with him has been a unique experience for me and I am particularly indepted to him for showing me that chemical engineering can be an art as well as science.

Further, I gratefully acknowledge the enthousiasm and contributions I received from my students: J. Dijckmeester, M. Hoogmoed, G. van Laar, T. Nauta, M. Nienoord, A. Palstra, M. v.d. Schoot, H. Smit, A. Spruyt and W. de Vries.

My thanks are also due to the entire staff of the "Laboratorium voor Apparatenbouw Procesindustrie" for the pleasant years of cooperation and the many contributions to this work. In particular: A. de Bruin for his help in computing work, H. Clemens for her typing the manuscript, J. Heerens for the development of measurement techniques, W. Hoogstad for the design and drawing the figures, R. Komen-Zimmerman for her bibliographical efforts and J. de Vries for carefully constructing the experimental equipment.

My special appreciation goes to Ir. P. Sonneveld of the Department of Mathematics for taking sincere interest in the subject and his outstanding work on the numerical solutions of population balance equations. My thanks are also due to Ir. Luyerink of the Department of Civil Engineering for his cooperation on the Quantimet particle size analyser.

Finally, I am indepted to the Koninklijk Shell Laboratory, Amsterdam and to Unilever Research, Vlaardingen for useful discussions. I am very pleased that their interest in this work led to sponsorship for the continuation of this project.

CONTENTS

Summary and Conclusions

Samenvatting en Conclusies

Chapter 1 Introduction

Chapter 2 Materials and methods

2.1 Introduction 5
2.2 Model systems 5
2.3 Equipment for batch-wise experiments 7
2.4 Equipment for continuous experiments 7
2.5 Light-backscattering as a method of determining growth kinetics 8

2.5.1 Introduction 8
2.5.2 Initial Equipment 9
2.5.3 Dependence of backscatter intensity on particle size and concentration 9
2.5.4 Experimental program and results obtained with narrow sized fractions of glass beads and Al-silicate powder 10
2.5.5 Light backscattering to determine large particle sizes and high slurry concentrations 12

2.6 A method of determining particle-impeller impact forces and collision frequencies 14

2.6.1 Introduction 14
2.6.2 Experimental equipment 15
2.6.3 Calibration and results 15

2.7 Other measuring methods 17

Chapter 3 Agglomeration kinetics in a batch system

3.1 Introduction 21
3.2 Kinetics and growth mechanisms in granulation 21
3.3 Experimental results 24

3.3.1 Experimental procedure 24
3.3.2 Growth regimes in agglomeration in suspension 25
3.3.3 Growth rate as a function of operating variables 27

3.4 Discussion of the 'zero-growth-rate' regime 31
3.5 Mechanisms with respect to the fast growth regime 33
3.6 A coalescence-breakage model for the fast growth regime 34

3.6.1 Introduction 34
3.6.2 Models used in granulation 34
3.6.3 The population balance approach to agglomeration in suspension 36
3.6.4 The functional form for the coalescence frequency 36
3.6.5 The functional form for the breakage frequency 38
3.6.6 Numerical analysis and results 40

3.7 Discussion of the fast growth regime 42

Chapter 4 Steady state pellet size and size distribution

4.1 Introduction 43
4.2 Mechanisms responsible for the development of the steady state regime 43
4.2.1 Introduction 43
4.2.2 Pellet strength 43
4.2.3 Pellet breakage 46
4.2.4 Forces acting on agglomerates in a stirred vessel 48
4.2.5 Other mechanisms responsible for steady state size 50
4.2.6 Discussion 50
4.3 Agglomerate size distribution 52
4.3.1 ASD at steady state 52
4.3.2 Time-evolution of ASD 55

Chapter 5 A preliminary study on a continuously operated pelletizer

5.1 Introduction 59
5.2 Experimental system and procedure 60
5.3 Results 62
5.4 Discussion 62

Appendices

I Expression for the growth rate derived from the coalescence model 65
Similarity transformation with respect to the coalescence-breakage model

II Numerical simulation procedure of the coalescence-breakage model 67

III a. Results of breakage experiments 71
b. Experimental breakage

Notation

References

Summary and Conclusions

Agglomeration in suspension, or pelletizing, is a unit operation which has promising prospectives for the separation of very fine particles (< 100 μm) from liquids and for the benefication of coal and various ores. It involves the addition of a second liquid which should be immiscible with the suspension liquid and wet the solid particles to be separated preferentially. Adhesion of the solid particles is then caused by capillary interfacial forces, whereby the second liquid or binding liquid acts as the interparticle bridging substance. When the process is carried out in suitably stirred equipment, highly spherical dense pellets are formed, which can be easily separated from the suspension liquid. Large scale technical feasibility is already established, but the knowledge on the prevailing mechanisms in batch and continuous systems, essentially for a rational design, is still lacking.
In this work, small scale batch agglomeration was studied, since it represents an essential stage in the development of properly designed process equipment. The general objectives of the major part of this study are to obtain insight in growth kinetics and mechanisms of batch agglomeration in suspension. Subsequently a preliminary study on a continuously operating pelletizer is presented.

To determine growth kinetics, a light backscatter method has been developed, which enables the increase of average particle size from 1-5000 μm to be followed in situ. Growth curves, i.e. development of the average pellet size with agglomeration time, were determined in a 1.1 liter stirred vessel as a function of various operating conditions. Glass and Al-silicate powders were most frequently used as model substances. Both solids were suspended in carbon tetrachloride whereby mixtures of water and glycerol were used as binding liquids.
Four distinct growth regimes are identified. After an immediate flocculation step where flocs of 200-300 μm in size are formed (flocculation regime), an extended period of almost zero growth is observed (zero growth regime). Then growth rate may change quite abruptly, marking the beginning of a period of fast growth (fast growth regime). Subsequently, a steady state pellet size (3-4 mm) is reached (steady state regime).
It is observed that the zero growth regime often dominates agglomeration kinetics. The duration of the z-regime ranges from almost zero to 180 minutes and more and is very sensitive to both particle properties and operating conditions (e.g. binding-liquid to solid ratio, stirrer speed, solid concentration and binding liquid viscosity). During this regime the pellet surface is deficient of binding liquid, which apparently causes the very low growth rate. It is suggested that the squeezing of the binding liquid out of the pores of the pellets controls the duration of the z-regime. The velocity of the liquid in the pores, induced by external forces, would be the rate controlling step.
The fast growth regime starts when the binding liquid appears at the surface of the pellet. It was observed that pellet-pellet coalescence was the prevailing mechanism for this regime, whereby the rate controlling factor is the deformation ability of a pair of coalescing pellets. Maximum growth rate in the fast growth regime shows to be almost independent of operating variables, but particle properties have a marked influence. However, another phenomenon also plays an important role, i.e. breakage of pellets. Therefore, the breakage of single pellets was studied in more detail. Both a stirred and a flow system were investigated. It is shown that, at typical values for the power-input, breakage occurs for most model systems. Brittle breakage as well as breakage by deformation were observed. Subsequently, it was attempted to identify which of the forces in a stirred system may cause destruction of pellets. From pellet-impeller impact force measurements, whereby a specially developed in situ method was used, it is concluded that breakage may indeed occur due to pellet-pellet collisions. It is further derived that pressure differences in the impeller vortex can also contribute to breakage.

The population balance approach was chosen for the quantitative description of agglomeration kinetics as well as for the prediction of the agglomerate size distribution (ASD) at steady state and the time evolution of the ASD. A model is described which includes coalescence and breakage of pellets. Functional forms for the coalescence and breakage rate are deduced and they both show to depend on pellet size. Numerical simulations of the model are presented and the agreement with experimental growth curves is satisfactorily. Pellet growth can be described by only two parameters which control respectively the shape and the slope of the growth curve. The coalescence breakage model predicts the experimentally observed maximum pellet size when breakage rate equals the coalescence rate. For some experiments, however, the steady state regime is due to a coalescence rate which approximates zero.
Agglomerate size distributions at steady state were determined whereby it shows that the dimensionless ASD is identical for all operating variables as well as independent of system properties. The dimensionless pellet size D/D_M (D_M is the median size) ranges between 0.6 and 1.4. An excellent fit of the ASD, predicted by the coalescence-breakage model, with experimental results was obtained for the same set of constants which yielded realistic growth curves. The relative insensitivity of the ASD is explained in terms of the model used. Also the development of the ASD with time was assessed. Experimental results do confirm the narrowing of the dimensionless ASD with time as is predicted by the coalescence-breakage model.

Finally, a preliminary study on a continuously operating pelletizer is presented. Ideas are given concerning the design of continuously operating equipment which however require experimental confirmation. A preliminary study was therefore set-up. A configuration of 3 one-liter CSTR's was used for the relative simplicity from a hydrodynamic point of view. $CaCO_3$ powder suspended in water and agglomerated with a mixture of kerosine and oleic acid was used as the model system. The $CaCO_3$ system was firstly tested batch-wise and some differences with the silica systems are discussed.
The operating conditions which ensured successful batch operation also proved to give satisfactory results in the continuous system. In general, the feed particles were removed from the liquid with an efficiency of 99-99.8%. Required solid- and liquid residence times are discussed and it is tentatively concluded that for powders that exhibite a long zero-growth regime in batch experiments, a long solid residence time is required. However, a way to overcome this problem is indicated. It is further outlined that in continuous operation, due to differences in solid- and liquid residence times, an additional mechanism i.e. layering of feed particles onto established pellets, may occur. Conditions whereby this mechanism occurs are identified.
The influence of pellet hold-up on the performance of a pelletizer shows to be important but complicated. E.g. the relative occurence of the coalescence and layering mechanisms strongly depends on hold-up. As a consequence also the stability of the process may be controlled by pellet hold-up. It is therefore emphasized to carefully examine the effect of pellet hold-up in future work.

Samenvatting en Conclusies

Agglomeratie in suspensie, of pelletizing, is een werkwijze die goede vooruitzichten biedt voor een verbeterde afscheiding van kleine in vloeistof gesuspendeerde vaste stof deeltjes (<100μm).Ook voor de zuivering van steenkool en diverse ertsen is de werkwijze veelbelovend. Aan de suspensie wordt een hulpvloeistof toegevoegd die de af te scheiden vaste stof deeltjes preferent bevochtigt maar die niet mengbaar is met de suspensie vloeistof. Deze hulpvloeistof of bindervloeistof verzorgt de adhesie tussen deeltjes welke aldus door capillaire krachten bij elkaar gehouden worden. Indien het proces uitgevoerd wordt in een geschikt geroerd apparaat, worden pilvormige kompakte agglomeraten (1-10 mm) gevormd, welke veel gemakkelijker van de vloeistof te scheiden zijn dan de oorspronkelijke deeltjes.
De technische uitvoerbaarheid van het proces is reeds aangetoond, maar de kennis omtrent groeimechanismen, die essentieel is voor een rationeel ontwerp, ontbreekt zowel voor ladingsgewijs- als kontinue werkende systemen.
In dit onderzoek is het agglomeratie proces in kleine ladingsgewijs (batch-) werkende apparaten bestudeerd, omdat dit een essentiele stap is in de ontwikkeling van gefundeerde ontwerpregels voor pelletizers. Het doel van het grootste deel van deze studie is het verkrijgen van inzicht in kinetiek en groeimechanismen zoals deze optreden bij batch agglomeratie. Tenslotte wordt over een inleidende studie betreffende een kontinu werkende pelletizer gerapporteerd.

Om de kinetiek van agglomeratie in suspensie te kunnen bepalen, is een lichtterugkaatsingsmethode ontwikkeld, die het mogelijk maakt de gemiddelde agglomeraat grootte van 1 → 5000 μm in situ te volgen. Groeikurven, te weten de verandering van de gemiddelde pellet grootte als funktie van de agglomeratietijd, zijn als funktie van een aantal proces variabelen bepaald in een 1.1 liter geroerd vat. Als modelsystemen werden voornamelijk glas- en aluminiumsilicaat poeders gebruikt. Deze werden gesuspendeerd in tetrachloorkoolstof en geagglomereerd met mengsels van water en glycerol als bindervloeistof. Vier groeiregimes zijn te onderscheiden: nadat vrijwel onmiddelijk na toevoeging van de binder flocculatie van deeltjes tot vlokken van 200-300μm (flocculation regime heeft plaats gevonden,treedt een periode op waarin nauwelijks groei plaatsvindt ('zero-growth' regime). Vervolgens kan de groeisnelheid plotseling sterk toenemen; dit is het begin van een periode van zeer snell groei (fast growth regime). Uiteindelijk wordt in het algemeen een stationaire pellet diameter (3-4 mm) bereikt (steady-state regime).
Het 'zero-growth' regime blijkt vaak het snelheidsbepalende regime te zijn. De duur van dit regime kan zich uitstrekken van bijna nul minuten tot zelfs meer dan 180 minuten en is zeer gevoelig voor zowel de deeltjes eigenschappen (grootte, grootteverdeling, ruwheid) als voor proceskondities (b.v. verhouding van de hoeveelheid bindervloeistof en vaste stof, toerental van de roerder, vaste stof koncentratie en de viscositeit van de bindervloeistof). Gedurende het z-regime wordt op het pellet oppervlak nauwelijks bindervloeistof aangetroffen.Waarschijnlijk is dit de oorzaak van de zeer lage groeisnelheid in dit regime. Aangenomen wordt dat de duur van het z-regime bepaald wordt door het uit de poriën naar het pellet oppervlak persen van de bindervloeistof. De snelheid van de vloeistof in de porien, teweeggebracht door externe krachten, zou hierbij de snelheidsbepalende stap zijn.
Het 'fast growth' regime start indien de bindervloeistof aan het oppervlak van het agglomeraat verschijnt. Waargenomen werd dat in dit regime samenvloeiing of koalescentie van agglomeraten het overheersende mechanisme is. De snelheidsbepalende faktor hierbij is de mate van deformeerbaarheid van de koalescerende pellets. Vastgesteld kon worden dat de maximale groeisnelheid in het 'fast-growth' regime praktisch onafhankelijk is van de proceskondities, maar wel duidelijk een funktie van de deeltjeseigenschappen. Echter, het bleek dat een ander fenomeen, namelijk breuk van agglomeraten hier een niet te verwaarlozen factor is.

Daarom is de breuk van agglomeraten verder onderzocht, zowel in een geroerd vat als in een stromingsmodel. Bij voor het proces typische waarden van het ingeroerde vermogen, bleek bij de meeste modelsystemen breuk van agglomeraten op te treden. Brosse breuk en breuk door deformatie werden beiden waargenomen. Vervolgens is gepoogd om vast te stellen welke krachten in een geroerd vat breuk zouden kunnen veroorzaken. Aangaande de krachten die optreden bij pellet-roerder botsingen, werden metingen verricht, m.b.v. een speciaal hiervoor ontwikkelde methode. Hieruit kan gekonkludeerd worden, dat pellet-roerder botsingen inderdaad breuk van pellets kunnen veroorzaken. Verder is afgeleid dat ook de drukverschillen die optreden in de vortex van de roerderstroming, een bijdrage leveren aan agglomeraatbreuk.
Voor de kwantitatieve beschrijving van de agglomeratiekinetiek werd gebruik gemaakt van populatie balansen. Hiermee kan zowel de groeisnelheid, de agglomeraat grootte verdeling (AGV) bij stationaire kondities en de ontwikkeling van de AGV in de tijd gesimuleerd worden. Er is een model gehanteerd, dat rekening houdt met koalescentie en breuk van agglomeraten. Relaties voor koalescentie- en breuk frequenties zijn afgeleid, waaruit blijkt dat beide grootheden funkties zijn van de agglomeraat grootte. Met behulp van deze relaties zijn met het model een aantal simulaties van het agglomeratie proces uitgevoerd; de overeenkomst met experimentele resultaten is bevredigd. Het blijkt dat de groei van agglomeraten beschreven kan worden door slechts twee parameters (volgend uit de afgeleide koalescentie/breuk relaties) die respectievelijk de vorm en de helling van de groeikurve bepalen. Het koalescentie-breuk model voorspelt de experimenteel waargenomen stationaire pelletdiameter, indien de breuksnelheid gelijk is aan de koalescentiesnelheid. Echter, bij enkele experimenten wordt het 'steady state' regime veroorzaakt doordat de koalescentiesnelheid ongeveer gelijk nul wordt. Agglomeraatgrootte verdelingen voor het geval dat de stationaire toestand bereikt is, zijn experimenteel bepaald waarbij blijkt dat indien de grootte-verdeling dimensieloos wordt uitgezet, deze identiek is voor alle proceskondities en ongevoelig voor de eigenschappen van de vaste stofdeeltjes. De dimensieloze pellet grootte D/D_M (D_M is de mediaan grootte) ligt hierbij tussen 0.6 en 1.4
De overeenstemming van de experimentele AGV en de AGV zoals deze voorspeld wordt door het koalescentie-breuk model is uitstekend te noemen. De beste overeenstemming wordt verkregen voor dezelfde waarden van de parameters die ook realistische groeikurven voorspellen. Tevens kan met behulp van het opgestelde model de relatieve ongevoeligheid van de gemeten AGV's verklaard worden. Ook de ontwikkeling van de AGV in de tijd is bestudeerd. Experimenteel verkregen resultaten bevestigen de vernauwing van de AGV in de tijd zoals deze voorspeld wordt door het koalescentie-breuk model.

Tenslotte wordt een inleidende studie gepresenteerd over een kontinu werkende pelletizer. Ideeën betreffende het ontwerp van kontinu pelletizers worden besproken. Gezien deze echter experimentele bevestiging behoeven, is een inleidend onderzoek uitgevoerd. Voor de uitvoering van deze experimenten werd gekozen voor een serie schakeling van drie 1-liter geroerde vaten, omdat dit systeem hydrodynamisch gezien vrij eenvoudig is. Als model systeem werd $CaCO_3$-poeder gebruikt, gesuspendeerd in water en geagglomereerd met een kerosine-oliezuur mengsel. Dit systeem werd allereerst getest in de bestaande batch-apparatuur; enige verschillen met de silica-systemen worden besproken.
De proceskondities, waarbij een goede batch agglomeratie verkregen werd, bleken tevens bevredigende resultaten op te leveren in het kontinu systeem. In het algemeen konden de vaste stof deeltjes voor 99 tot 99.8% uit de vloeistof afgescheiden worden. De vereiste vloeistof- en vaste stof verblijftijden worden besproken. Hieruit komt als voorlopige konklusie naar voren, dat voor die poeders, waarbij in batch experimenten een lang 'zero-growth' regime optreedt, bij kontinu experimenten een lange vast stof verblijftijd vereist is. Echter, een manier om dit probleem te omzeilen is aangegeven. Belangrijk hierbij is het optreden van

een additioneel groeimechanisme, namelijk layering, d.w.z. het zich afzetten van kleine deeltjes op reeds gevormde pellets. Dit mechanisme kan optreden, omdat de vloeistof- en vast stof verblijftijden in het apparaat aanzienlijk verschillen. De kondities waarbij het optreedt zijn geidentificeerd.
De invloed in de pellet hold-up op de werking van een pelletizer blijkt belangrijk, maar ook gekompliceerd te zijn. Als voorbeeld kan genoemd worden dat de mate waarin het coalescentie en layering mechanisme ten opzichte van elkaar optreden voor een groot deel wordt bepaald door de pellet hold-up. Als gevolg hiervan is ook de stabiliteit van het proces sterk afhankelijk van de hold-up. Het wordt daarom aanbevolen in toekomstige studies de rol van de pellet hold-up zorgvuldig te bestuderen.

Chapter 1

Introduction

Dewatering of slurries containing small particles (< 100 μm) often presents a considerable problem. In particular the mechanical separation of fine particles from liquid is difficult and expensive. An interesting alternative therefore is to include an operation whereby size enlargement of the fine particles is accomplished. The mechanical separation may then proceed more easily. Techniques such as coagulation and flocculation are well known. The additives are respectively electrolytes and polymeric flocculants. Electrolytes decrease the zeta-potential of the particles so that they can cohere, while polymeric flocculants serve as a bridging substance between the particles. The main disadvantage of these techniques lies in the weak and voluminous flocs that still contain a high percentage of liquid. Compact flocs, pellet-like in appearance are produced in the "pelleting flocculation" process [1, 2, 3], where certain organic flocculants of high molecular weight and mechanical agitation are used.

Another method involves the addition of a second liquid to act as the interparticle bridging substance. The underlying principle was reported already in 1904 [4]. In more recent literature this technique, which is the subject of this study, is refered to as "agglomeration" or more in particular "agglomeration in suspension". The latter name does distinquish the process from the classical size enlargement technique "granulation" [5, 6, 7]. With respect to the second liquid (binding liquid or binder) it is required that it is immiscible with the suspension liquid and it should wet the solid particles preferentially. When the process is carried out in suitable equipment, highly spherical dense pellets can be formed when sufficient binding liquid is added to approximately fill the pores of the agglomerate (photograph 1.1).

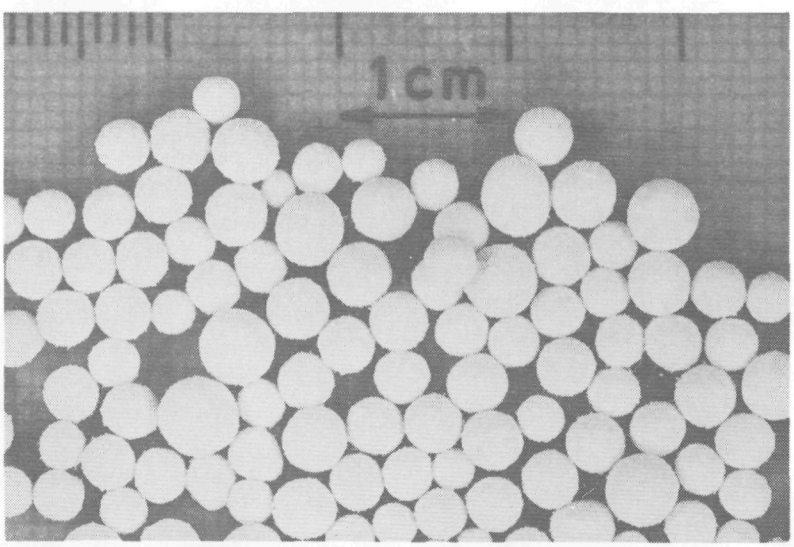

Photograph 1.1 Glass powder pellets obtained by agglomeration in suspension.

Adhesion of the particles is then caused by capillary interfacial forces. Adding too small an amount of binder results in the formation of flocs, since only liquid bridges between the particles can be formed. Addition of a relatively large amount of binding liquid causes the formation of a paste. These conditions mark the boundaries for a succesful operation of the pelletizing process.

By a suitable choice of the binding liquid, separation of mixtures of solids can also be achieved (selective agglomeration).
As early as the twenties this technique was used for separating ash from coal (Trent [8] or Converol processes [10]) or for fractionating minerals (Christensen process [9]). It was not, however, until the sixties that further developments with respect to the "spherical agglomeration process", as it is sometimes called, were published [11, 12].

In particular the National Research Council in Ottawa was concerned with studies aimed at examining the process [16-21]. It was reported that it could be successfully applied to the benefication of different ores, e.g. tin [22, 23], germanium [24], gold [25], ilmenite [26] and phosphoriferous iron ore [27]. Two reviews of their work were recently published [28, 29].
The first commercially successful operation of spherical agglomeration was reported in 1968 [13, 14, 15]. The agglomeration of soot in waste water originating from oil gasification plants was possible by mixing the sooty water with a small quantity of heavy oil. For this application the Shell Pelletizing Separator was developed (Fig. 1.1), consisting of a vertical outer cylinder with another cylinder of about half its diameter rotating within the first one. At a mean liquid residence time of 3 minutes (through-put of 20 m^3/hr) it was possible to obtain dense pellets of 1 → 7 mm in size while soot recovery was reported to be > 99,95 %.

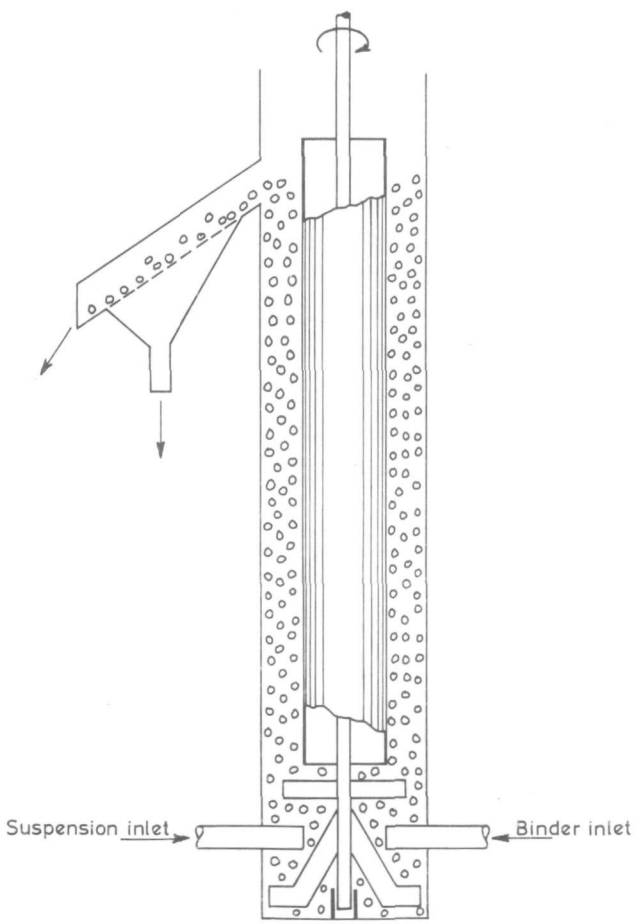

Fig. 1.1 Shell pelletizing separator.

Since the early seventies, the prospect that coal will play an increasing role as a source of primary energy and moreover that it can also become a main source of hydrocarbons has substantially increased. The benefication of coal, by means of the agglomeration in suspension process, has therefore received renewed attention [10, 30-37].

At present, mining techniques tend to become more and more mechanised and therefore the fraction of fine coal can increase to about 30 percent of the entire production. For the coal-washery this presents a tremendous problem. Classically used techniques (froth-flotation) cannot be employed in recovering superfine coal (< 100μm), in particular when there is a substantial non-coal part present. The subsequently mechanically dewatered (vacuum-filteration) coal slurry still presents a considerable handling problem due to its high moisture content. The agglomeration process can overcome both disadvantages, since it can pelletize and simultaneously de-ash fine coal and produce pellets with a low moisture content (± 15 weight percent of the entire pellet).

Therefore, in future coal technology, the major applications for the agglomeration in suspension process, are considered to be [34]:
"de-ashing, dewatering and agglomeration of fine coal orginating from:

a. fresh, run of mine coal in coal preparation plants;
b. recovery operations in existing coal preparation systems;
c. pipeline slurries".

The profitability of the process is thought [33, 34] to depend mainly on the comparative prices of coal and the oil used as binding liquid.

Until now, most experimental work was done on laboratory scale or batch pilot-scale whereby revolving drums [12], conical drums [18], shaked vessels [16] or stirred vessels [19, 20] were used. A few attempts were undertaken to assess the influence of operating conditions on growth kinetics, mechanisms and product quality [19, 20, 36, 37].
The already mentioned, commercial scale Shell Pelletizer Separator [13] operated satisfactory for lighter-than-water pellets. A high pellet hold-up (± 30 vol %) could be maintained, ensuring that all fine particles of the feed were absorbed by the pellets. The required power-input of 11 kW/m^3 is rather high.
For de-ashing of coal, the vertical pelletizer did not work satisfactorily however. A much higher residence time of about 30 minutes was required and pellet hold-up could not be maintained. Therefore, for the heavier-than-water coal pellets, a horizontal apparatus (Fig. 1.2) was developed (upto a scale of 10 tons/hr). This pelletizer is an unbaffled cylinder and features a considerable number of paddle agitators [14]. It was reported that a proper design of the equipment is essential to obtain strong pellets with a minimum amount of binding liquid, residence time and power requirement.
In this respect it was also stated that the present design is not yet optimal. In particular it does seem that reliable continuous operation is not yet ensured.

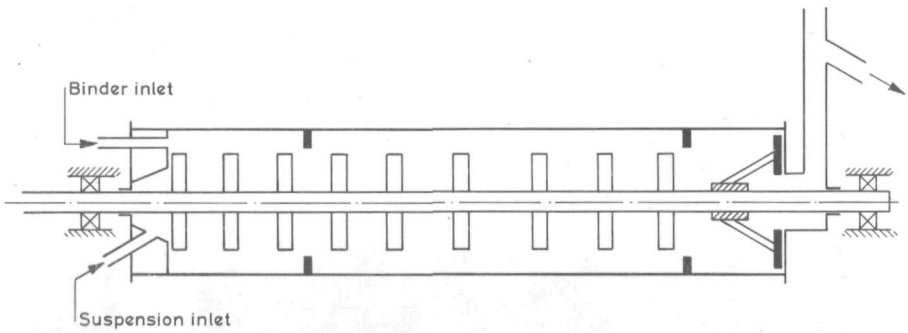

Fig. 1.2 Horizontal pelletizing separator.

With the above examples, large scale technical feasibility of the agglomeration process has been illustrated. As a consequence, more and more interest is developing for other applications, some of which have already been mentioned before.
Essential for a successful application is the determination of the binding liquid and the required particle size and size distribution of the feed particles. This is usually assessed by small scale batch experiments. Subsequently, the batch data are used for developing the design of the continuous process.
It will be clear that for a rational design, the prevailing mechanisms in both the batch and continuous systems have to be known. More in particular, we are of the opinion that for the design of satisfactorily operating pelletizing equipment knowledge is required on the following items:

- understanding of the influence of operating variables (e.g. properties and amount of binding liquid, power-input, pre-emulsification of binding liquid,

solid concentration) and particle properties (size, size-distribution, shape and wettability) on the growth kinetics and product properties;

- the internal lay-out of the apparatus with respect to the optimal staging (for both liquid and solid phase) and hydrodynamics, to ensure minimum residence time and stable operation.

From the above we need in first instance, insight in growth mechanisms and kinetics. This is the subject of this thesis. Batch-wise operation was selected because of its relative simplicity, and moreover, since it represents an essential stage in the development of properly designed process equipment. Of course, the continuous system has to be investigated subsequently, since besides the batch mechanisms additional growth mechanisms may play a role.

We define therefore the objectives of this study as follows:

- to design suitable experimental systems and techniques to study the kinetics and mechahisms of batch agglomeration;
- to obtain insight in the growth mechanism;
- to relate growth kinetics and pellet properties with relevant operating variables;
- to derive a system which enables further studies on continuously operating pelletizers.

CHAPTER 2

Materials and methods

2.1 Introduction

A number of experimental techniques will be described, enabling to meet the objectives formulated in chapter 1. Given these objectives, an agglomeration system should be used that allows significant variations of the input variables in a systematic and reproducable way. Also, an accurate determination of output variables, like growth rate, size distribution and composition of the agglomerates, is essential in studying kinetics and mechanism of this separation process.

In order to determine growth kinetics of the agglomeration process, we developed a light backscatter method for in situ determination of the average particle size. This method is described in somewhat more detail since the technique can probably also be used in other fields of technology. When studying the role of breakage of agglomerates in the process of pellet growth, as will be further outlined in chapter 4, the desirability of developing a particle-impeller impact measuring device came about. It will be demonstrated that this device can measure the impact force exerted on the particle when it hits one of the impeller blades as well as the collision frequency.

2.2 Model systems

Due to the extensiveness of possible applications of the agglomeration process to quite different solid-liquid systems, it is obvious that in order to study the kinetics and mechanism in more general terms, a model system is most desirable.

The requirements that should be put to a model system are:

- growth rate should agree approximately with that of at least one major application;
- process parameters and also the form, size and size distribution of the solid particles should allow variation over a significant range;
- the obtained experimental results should be reproducible.

With respect to this last requirement it can be mentioned that for instance coal is less suitable as a model substance due to quick oxidation of the surface causing a rapid change of the wetting properties.
Glass is a substance of which the wetting properties can be controlled rather easily. When glass particles are heated at a temperature of 400°C during 30 minutes, then allowed to cool to 20°C and stored for 12 hours [42], a quite reproducible wettability of the glass is obtained. Adjustment of the wettability is further possible by applying different heating temperatures and storage times.
A further advantage of glass as a model substance is that it can be obtained either in the form of round beads of different size and size distribution or in the form of highly irregular particles. These latter particles can be obtained by grinding larger beads. By changing grinding time in combination with sieving techniques the size and size distribution can be adjusted over a wide range. In the further text, these grinded irregular glass particles will be called "glass particles" or (interchangeable) "glass powder". In order to study a material exhibiting a quite different growth behaviour, grinded Al-silicate was frequently used.
Due to their hydrophilic nature, both the above solids were suspended in carbon tetrachloride, while water-glycerol mixtures of different composition were used

as binding liquids. For experiments in the continuously operated pelletizer a system was favoured that could be agglomerated in water.
A suitable system proved to be calcium carbonate particles, suspended in water and agglomerated with a mixture of kerosine and 5 vol % oleic acid as the binding liquid. Relevant characteristics and physical properties of the materials used are compiled in Table 2.1.

TABLE 2.1 Properties of the solids and liquids used in model experiments.

	$D_M * 10^6$ (m)	CV (%)	θ (degrees)	ρ (kg/m^3)	$\gamma * 10^3$ (N/m)	$\mu * 10^3$ (Ns/m^2)
glass powder 1 *	11	165	$75 < \theta < 90$	2910		
glass powder 2 *	9	134	$75 < \theta < 90$	2910		
glass powder 3 *	19	134	$75 < \theta < 90$	2910		
glass powder 4 *	19	165	$75 < \theta < 90$	2910		
glass powder 5 *	12	143		2910		
glass ballotini	30	71		2910		
Al-silicate	16	131		3247		
$CaCO_3$ **	15			2750		
carbon tetrachloride ***				1,595	45,1	1.7
water/glycerol 80-20				1,055	72,3	2.3
water/glycerol 60-40				1,105	70,0	5
water/glycerol 40-60				1,155	68,4	13
water/glycerol 20-80				1,205	66,3	67
kerosine/oleic acid 5vol %				800	-	1.2

* Grinded Ballotini beads of 500µm TAMSON

** Durcal 15. Plüss-Staufer AG imp. BOEKAMP BV Gouda

*** Firma Lamers en Indemans Den Bosch

Information concerning the width of the particle size distribution is given in terms of the coefficient of variation CV

$$CV = \frac{D_{84} - D_{16}}{2.D_{50}} \cdot 100\%$$

where D_{84}, D_{50} and D_{16} are the sizes corresponding to the cumulative mass of 84, 50 and 16% respectively.
Further, ρ is the solid density, μ the suspension and binding liquid viscosity and γ the interfacial tension between suspension and binding liquid. θ is the apparent or measured contact angle between the solid surface and the water/glycerol mixture whereby carbon tetrachloride was the third phase; this angle is one of the most widely used indices of wettability.

2.3 *Equipment for batch-wise experiments*

Details of the geometry of the experimental 1.1 liter stirred vessel are shown in Figure 2.1. The vessel has a top and bottom flange, provided with in- and outlets, and a jacketed wall. The wall is easily interchangeable and was made either of perspex, steel or glass; the glass walls being used only in the experiments with calcium carbonate particles.
The impeller was a 6-bladed flat disc turbine, situated at 1/7 of the height of the vessel from the bottom, to ensure both good dispersion (binding liquid) and suspension properties [43]. The binding liquid was added by means of a micro-precision buret (Metrohm) ensuring an accuracy of ± 0.02 ml.

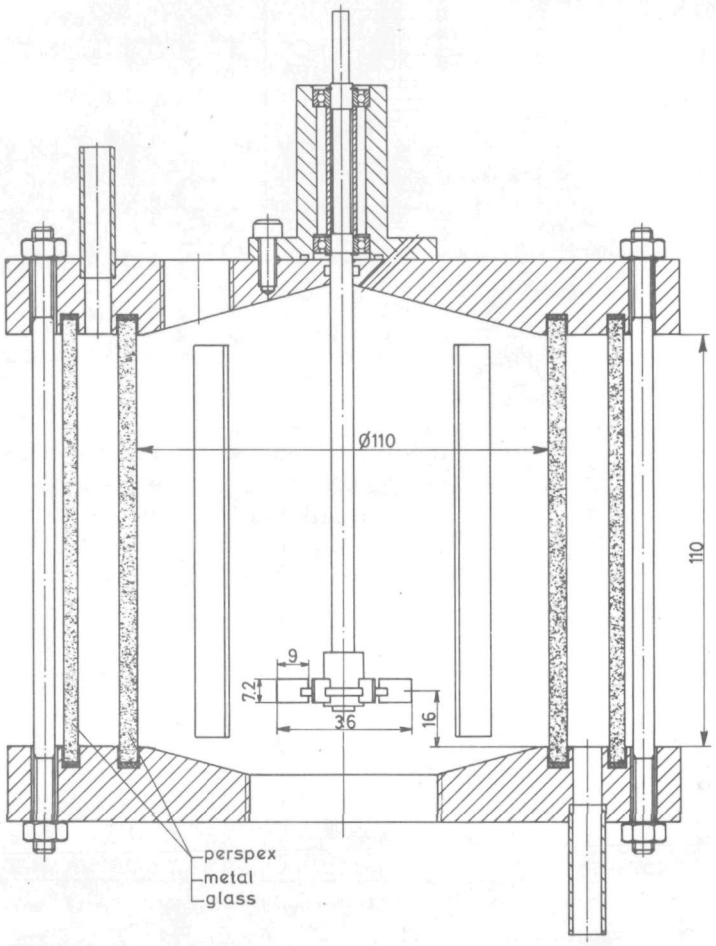

Fig. 2.1 Experimental one liter stirred vessel used for batch experiments (dimensions given in mm).

2.4 *Equipment for continuous experiments*

Zuiderweg [13] indicated the advantages of a staged apparatus to the agglomeration process. The configuration of three CSTR's was further chosen for the relative simplicity from hydrodynamic point of view. In each vessel the hydrodynamics can be considered similar to those in the batch system because the configuration is identical and because the action of the stirrer dominates the effect of the feed. Due to the low feed flow rate, pumps were not adequate and therefore slurry and binding liquid were fed from overhead vessels and controlled by precision valves. A line diagram of the experimental 3 liter continuously operated pelletizer is shown in Fig. 2.2.

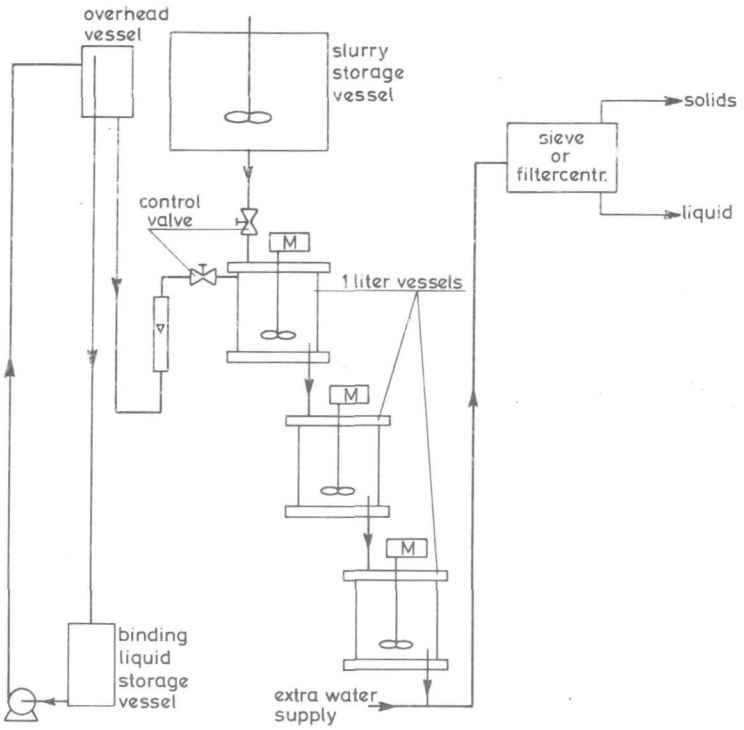

Fig. 2.2 Schematic diagram of the continuously operated pelletizer.

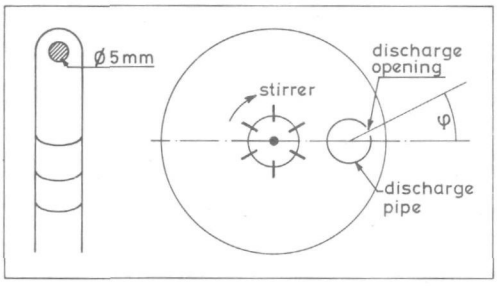

Each of the three stirred vessels features a discharge pipe to remove the solid-liquid suspension from the vessel. By adjusting this pipe near the bottom of the vessel the solid residence time can be made markedly higher than the liquid residence time. Stable pellet hold-up of about 10 vol % could be ensured by a discharge geometry as shown in Fig. 2.3

Fig. 2.3 Discharge geometry used in continuously operated pelletizer.

2.5 *Light backscatter as a method of determining growth kinetics*

2.5.1 Introduction

This on-line method was specially developed [44, 45] to determine the average particle size in a suspension without interfering with the course of the agglomeration process. It was found that an increase in particle size from 1 μm up to about 5000 μm can be monitored and that in this way useful information concerning the growth kinetics can be obtained.

The necessity of using an on-line method is obvious, because for some materials and at suitable operating conditions, a size enlargement of a factor 1000 is reached in a few minutes. In such a short period, sampling is very difficult. Apart from this, obtaining a representative sample from a stirred slurry system is almost impossible. Reviews of on-line methods are given by a number of authors [46, 49]. Many methods are, however, only applicable in diluted suspensions (e.g. light transmission techniques [50-53] and in the small particle range [52-53]. Moreover, they are often very expensive [54]. For these reasons, the possibility of using a backscatter light technique was investigated. In recent publications

[55, 56], the use of a backscatter method based on ultrasonics was suggested. We did not apply this method because it seems only applicable for particles smaller than 80 μm; moreover the very turbulent character of the liquid in a stirred vessel will also influence the ultrasonic responses.

2.5.2 *Initial equipment*

Figure 2.4 shows a schematic diagram of an initial experimental apparatus which was build with the aim of testing the possibilities of light backscatter for determining average particle size in suspensions. A 1 liter stirred vessel, as is described in par. 2.3, was operated in such a way that the particles were homogeneously suspended. Transmittance of light across the vessel occurs when the particles have agglomerated to a size of 500 - 800 μm. At this stage backscatter of the vessel wall starts to interfere with the particle backscatter, and for this reason the stirrer and the inner wall are painted black. The source of light and the light intensity detector are built in one tube, which is mounted on the vessel wall. The source of light is an ordinary microscope bulb and the light detector is a Si-pin diode (Philips type BPY 11/111) with a linear relation between incident light intensity and electrical current. This signal is amplified and recorded in millivolts. An additional light diode is installed to measure and control the light intensity of the bulb.

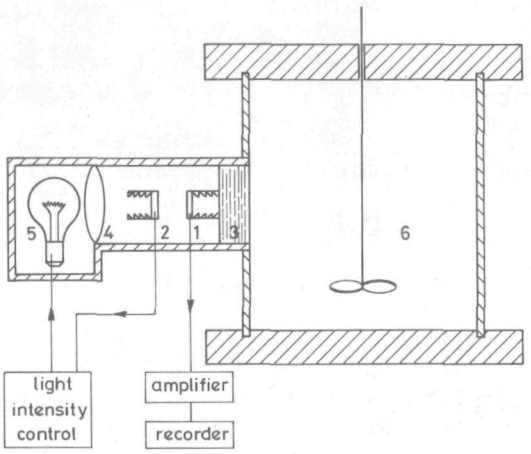

Fig. 2.4 Schematic diagram of the one-channel backscatter meter. 1. light detector, 2. reference light detector, 3. perspex block, 4. lens, 5. bulb, 6. vessel

2.5.3 *Dependence of backscatter intensity on particle size and concentration*

For the development of a relationship between the backscatter intensity and the slurry properties it is assumed that, in every section of the light beam, the intensity of the backscattered light is a constant fraction of the decrease of the transmitted intensity:

$$dI_b = -\alpha dI_x \qquad (2.1)$$

It is further assumed that:

1. the particles are non-transparent, spherical and equally sized;
2. the backscattered intensity that is reaching the light detector is the same for all particles independent of the distance from the detector;
3. the decrease in light intensity due to the liquid can be neglected.

Considering a cross-section of the light beam with area 0 and thickness Δx, the decrease of the transmitted intensity can be calculated.

$$I_{x+\Delta x} = I_x - \frac{A}{0} I_x \qquad (2.2)$$

where A ($= c_p(\pi/4)d^2 0\Delta x$) is the projected area of the particles present in the volume $0\Delta x$ and c_p the particle concentration.

Defining c_v as the volume concentration, then:

$$\frac{dI_x}{dx} = -\frac{3}{2}\frac{c_v}{d} I_x = -KI_x \qquad (2.3)$$

Integrating this equation with the boundary condition $I_x = I_o$ at $x = 0$.

$$I_x = I_o \exp\left[-Kx\right] \qquad (2.4)$$

This equation is analogous to that used in turbidity measurements [50].

So: $$dI_x = -KI_o \exp\left[-Kx\right] dx \qquad (2.5)$$

Substitution of equation (2.1) gives:

$$dI_b = \alpha KI_o \exp\left[-Kx\right] dx \qquad (2.6)$$

Integration of this equation from $x = 0$ to $x = L$, where L is the length of the light path, gives the total backscatter intensity:

$$I_{bt} = -\alpha I_o \left[\exp(-KL) - 1\right] \quad \text{when } L < D_{vessel} \qquad (2.7)$$

and $$I_{bt} = -\alpha I_o \left[\exp(-KD) - 1\right] + I_{bw} \quad \text{when } L \geq D_{vessel} \qquad (2.8)$$

I_{bw} = the backscatter intensity of the wall of the vessel when $K \to 0$.

For $K \to \infty$, I_{bt} becomes the maximum possible backscatter intensity, I_{bm}.

$$I_{bt} = (I_{bm} - I_{bw})\left[1 - \exp(-KL)\right] + I_{bw} \qquad (2.9)$$

However, the length of the light path is not a constant factor, but depends on both particle size and concentration. It is assumed that:

$$L = K_1 c_v^{\,p} d^q \qquad (2.10)$$

Substituting eqn. (2.10) and $K = (3/2)(c_v/d)$ in eqn. 2.9 finally gives:

$$\ln\left(\frac{I_{bm} - I_{bw}}{I_{bm} - I_{bt}}\right) = K_2 c_v^{\,p+1} d^{q-1} \qquad (2.11)$$

2.5.4 Experimental program and results obtained with narrow sized fractions of glass beads and Al-silicate powder

The derived expression for the intensity of the backscattered light (eqn. 2.11) was tested with aqueous suspensions of narrow sized ($c_v < 15\%$) fractions of Al-silicate particles and glass beads. These were obtained by wet sieving and their mean size was derived from Coulter Counter measurements. The mean size of particles larger than 400 µm was evaluated as the arithmetic mean of two adjacent sieve apertures. In the experiments the mean size was varied from 40 to 550 µm and the volume concentration from 0.3 to 2.5%.

The particles were found to be homogeneously suspended at stirrer speeds above 1700 r.p.m. The backscatter intensity of the wall (I_{bw}) was measured when only liquid was present in the vessel. The maximum backscatter intensity (I_{bm}) was measured in a separate cell completely filled with particles of a certain size fraction with the space between the particles filled with liquid. The maximum backscatter intensity I_{bm} appears to be slightly dependent on the size, as is shown in Figure 2.5. The results for Al-silicate particles and glass beads

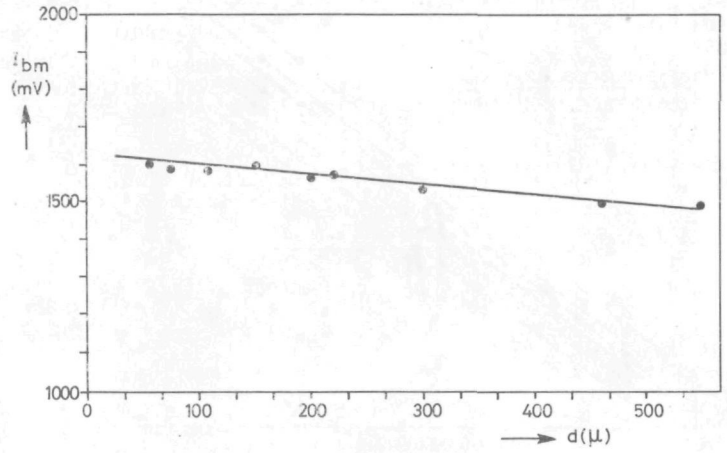

Fig. 2.5 The maximum backscatter intensity as a function of particle size.

are presented in Fig. 2.6 and 2.7, where the dependence of the backscatter factor, written as $\ln (I_{bm} - I_{bw}/I_{bm} - I_{bt})$ on the volume concentration and mean particle size is given.

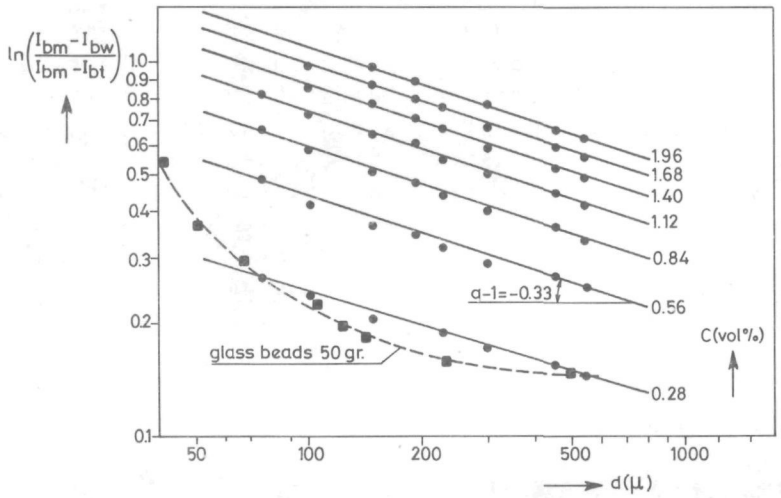

Fig. 2.6 Calibration curves for the mean particle size at different concentrations. —— Al-silicate particles, --- glass beads.

The experiments for Al silicate particles appear to be in good agreement with equation (2.11), for the values of p = -0,23, q = +0,67 and K_2 = 0,2. For other materials, different values of these three parameters will be found.

The dotted line in Fig. 2.6 represents typical values for the experiments with glass beads. These values cannot be described by equation (2.11). This can be explained by the translucency of glass particles, which becomes higher with larger particles sizes.

The apparatus described, however, can not be used for particles of a larger size than indicated in this paragraph. This is due to the non-homogeneous distribution of larger particles over the height of the vessel, at stirrer speeds that we are allowed to use in the agglomeration process. However, this can be overcome by taking measurements at different heights of the vessel.

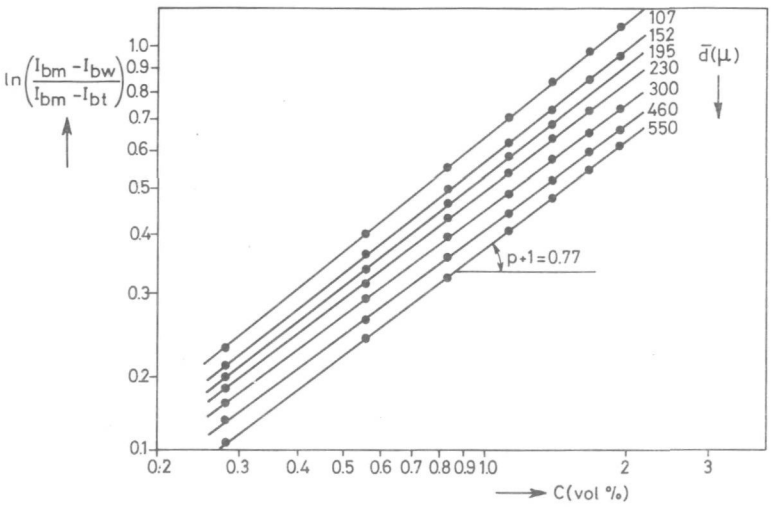

Fig. 2.7 Calibration curves for the concentration at different particle sizes Al-silicate powder.

2.5.5 *Light backscattering to determine large particle sizes at high slurry concentrations*

In this paragraph it will be shown that light backscattering can also be applied at particle sizes upto 5 millimeter and at high volume concentrations (22% was used). As stated in the previous paragraph, the distribution over the height of these relative large particles in the stirred vessel is far from homogeneous. To account for this non-homogeneous distribution, glass fibre optics (Schott) were applied to measure simultaneously at five different heights of the one liter vessel (see Figure 2.8). In Figure 2.9 a line diagram of the equipment is shown.

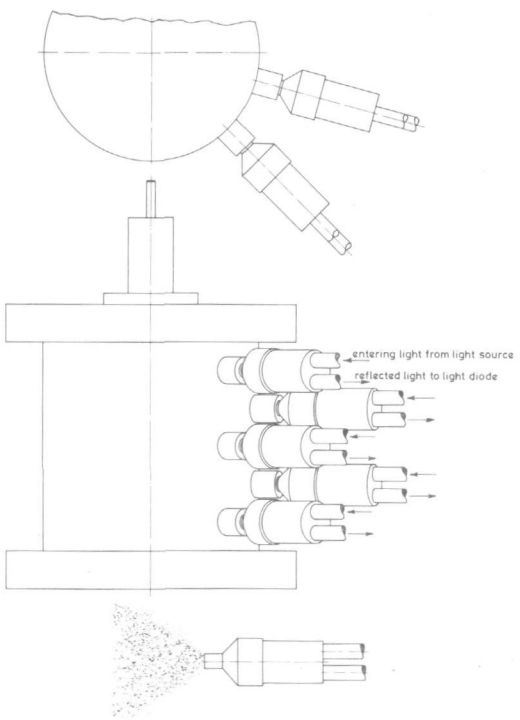

Fig. 2.8 Arrangement of glass fibre optics to measure the backscatter intensity simultaneously at five different heights.

For the mean value throughout the vessel, the arithmetical mean of the five signals was used. However, because the diameter of the light guide was 6 mm, relatively large particles are causing the back scattered light to pulsate. The resulting frequency of the signal depends on particle size and concentration. Integrating the signal therefore becomes necessary. In most experiments, an integration time of fifty seconds was found to be adequate. Readings were taken every 50 seconds, recorded on paper tape and fed into a IBM 370/158 computer for further calculations.
In Fig. 2.10 the backscatter factor is plotted as a function of the mean size for agglomerates of Al-silicate and glass powder. The slope of the obtained curves is almost identical for the two systems and is used for evaluating growth kinetics. A growth curve, in terms of the average pellet size as a function of agglomeration time, can be obtained as follows. Firstly, at the end of the experiment, e.g. at 180 minutes, the mean pellet size $\bar{D}$, obtained from size distribution measurements (see par. 2.7) is taken as the average pellet size

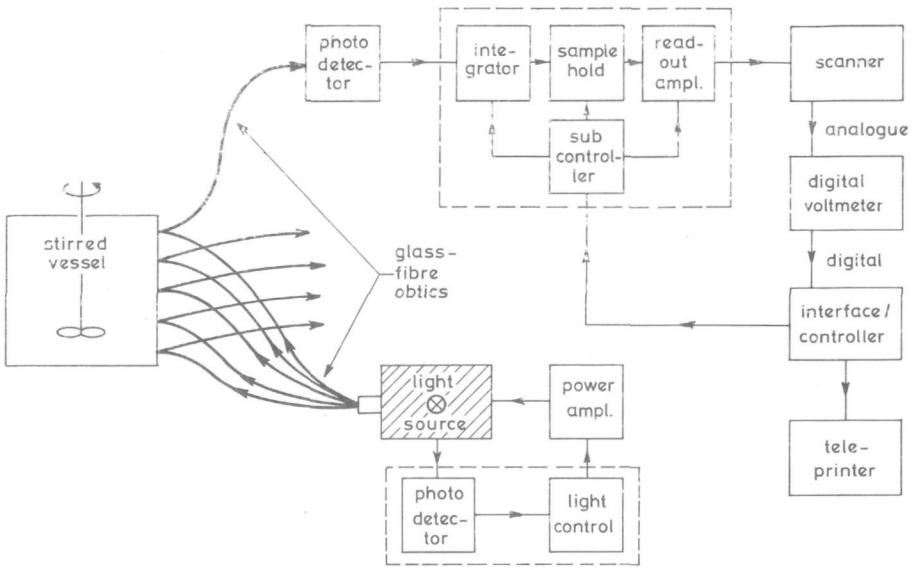

Fig. 2.9 Schematic diagram of 5-channel backscatter meter.

corresponding with the backscatter factor at that moment. Then, using the slope of the calibration curve in Fig. 2.10 the backscatter factor as a function of time is interpreted as the development of the average pellet size in time.

Also the possible application of this method to determine slurry concentration was explored since other methods, as for instance the x-ray absorption technique, are unsuitable in a number of cases. Tests were performed with three different solids and the results are presented in Fig. 2.12

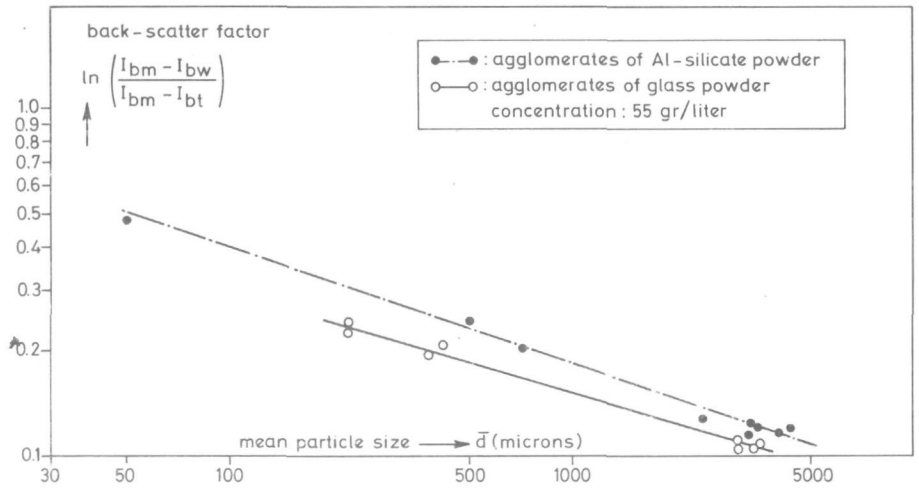

Fig. 2.10 Light backscatter factor as a function of mean particle size.

It is interesting to note that this method holds for high slurry concentrations and although the calibration curve is less steep, even the concentration of black coal particles can be measured.
Further, the possible use in crystallization technology and research (crystal mass concentration with an accuracy of $\pm$ 1 gr/l) is illustrated with the calibration curve for potash alum crystals.
As a conclusion one might say that the method developed can be used to determine slurry concentration or mean particle size over a large range of concentrations and/or particle sizes, for a wide variety of solids.

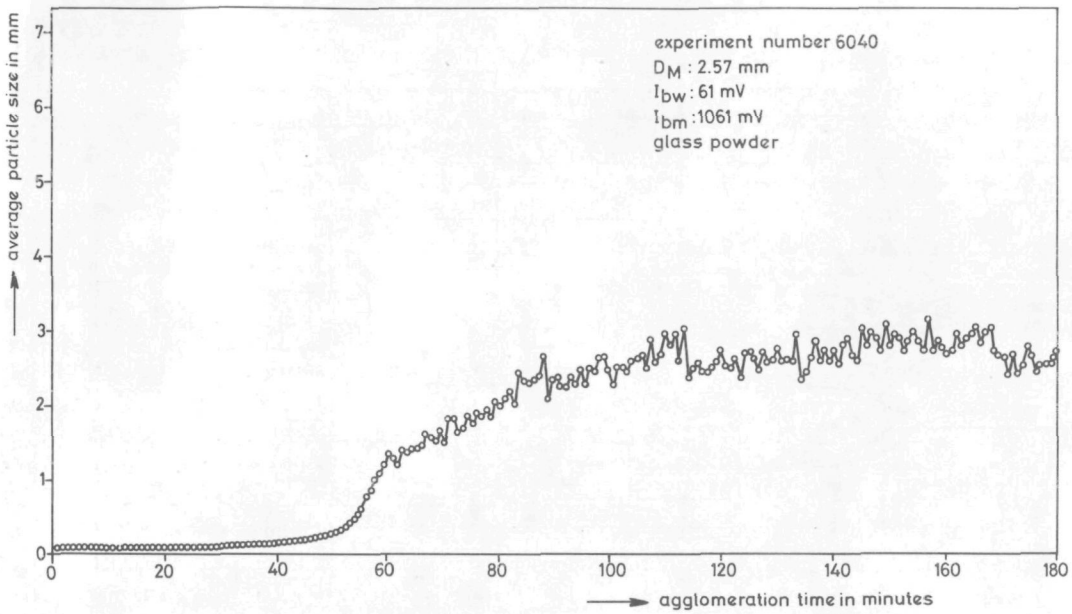

Fig. 2.11 Computer plot of an experimentally determined growth curve (mean particle size as a function of agglomeration time).

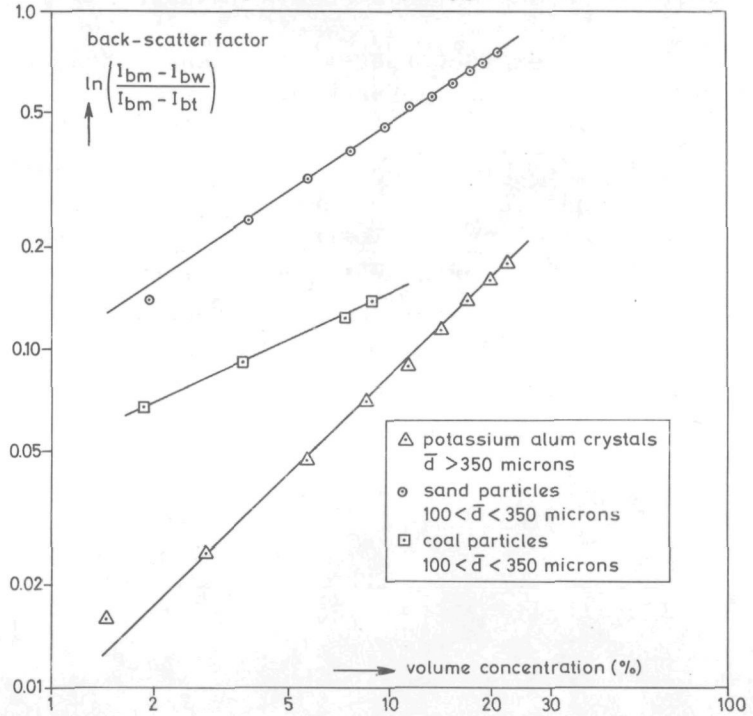

Fig. 2.12 Light backscatter factor as a function of particle concentration for different solids.

2.6 A methods of determining particle-impeller impact forces and collision frequencies

2.6.1 Introduction

Particle-impeller collisions often play a significant role in different areas of chemical engineering where stirred systems are being used. For instance in crystallization technology where secondary nuclei can be produced by contacts between stirrer and crystals. Secondary nucleation appears to be the most important means by which nuclei are produced in industrial crystallizers [57-61]. Breakage of agglomerates is an important parameter in the kinetics of agglomeration in suspension [61]. Most likely this is caused by particle-impeller collisions.

It is almost impossible to calculate these impact forces, even if only an order of magnitude answer is required. Especially, the velocity at the moment of impact and the variation of the elastic modulus of an agglomerate during its growth are highly uncertain factors.
Therefore, a method was developed to determine in situ the impact forces that are exerted on agglomerates when hitting the impeller blade [62]. This method also enables to evaluate the collision frequency that together with the impact force determines the breakage or nucleation rate.

2.6.2 Experimental equipment

In order to determine collision forces occuring as a result of agglomerate-impeller collisions, a measuring device should be built into one of the impeller blades. Requiring high sensitivity and a high response frequency, piezo ceramic elements were considered to be suitable as a force transducer. As diagrammatically shown in Fig. 2.13, two piezo ceramic discs (Philips type PXE-5, sensitivity 12.10^{-6} V.m^2/N;resp. freq. 0,1 μs) were built into one of the blades of a 6-bladed disc turbine impeller. The area thus obtained to registrate the collision impact force had a diameter of 6 millimeters. The signals were first amplified, then transmitted by means of slip-contacts and finally recorded on a digital memory oscilloscope or a puls height analyser.

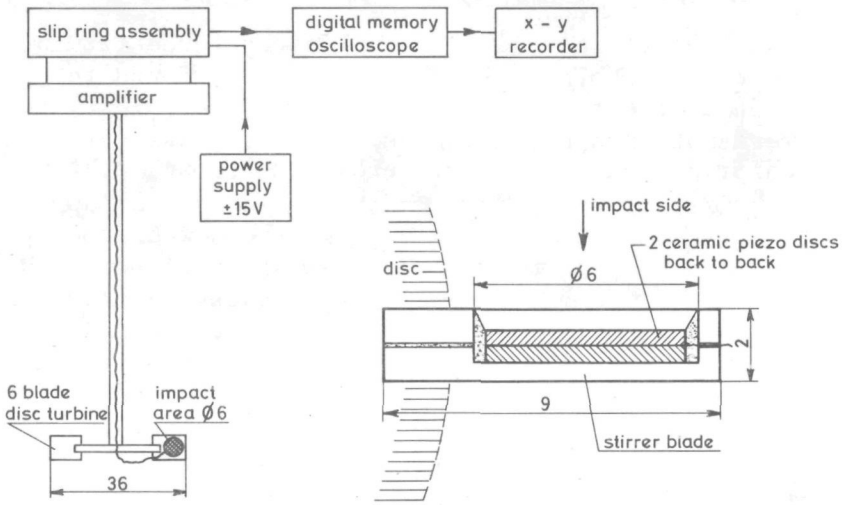

Fig. 2.13 Collision impact meter built into a stirrer blade (dimensions given in mm).

2.6.3 Calibration and results

Small steel beads (1, 2 and 3 mm) were used for calibration purposes. Falling from a known height, their velocity can be calculated using the equations for non-stationary fall of spherical particles [63] or approximated by the law for conservation of energy. The velocities calculated both ways will not differ more than 0.4% and are also in agreement with experimentally determined velocities within 1,5%. The latter were obtained by applying light diodes located along the trajectory of the particles at an exact known distance from each other.
The relation between maximum collision force, velocity and physical properties of the materials is given in [64], being:

$$\frac{(F_i)_m}{R^2 E_p} = -3.0295 \left(\frac{M_p}{M_i} + 1\right)^{-3/5} \cdot (1+K)^{-2/5} \left[\frac{1-\upsilon_p}{(1+\upsilon_p)^5 (1-2\upsilon_p)^3}\right]^{1/5} \left(\frac{u}{C_l}\right)^{6/5} \quad (2.12)$$

whereby the constants C_1 and K are expressed as:

$$C_1 = \left[\frac{E_p}{\rho_p} \cdot \frac{1 - \upsilon_p}{(1+\upsilon_p)(1-2\upsilon_p)}\right] \qquad (2.13)$$

$$K = \frac{E_p}{E_i} \cdot \frac{1 - \upsilon_i^2}{1 - \upsilon_p^2} \qquad (2.14)$$

$(F_i)_m$ being the maximum collision force;

M the mass and R the radius of the particle;

u the velocity;

υ the Poisson constant being for steel $\upsilon_p = \upsilon_i = 0.286$

E the elastic modulus, being for steel $E_p = E_i = 20.10^{10}$ (N/m^2)

ρ the density being for steel 7801 kg/m^3 and

p and i indicating the particle and impeller respectively

The above equation was used to calculate the collision force for the experiments with the different steel balls. The calculated force was found to be related to the observed voltage as plotted in Fig. 2.14. Some preliminary results in the stirred vessel were obtained using agglomerates of glass particles suspended in carbon tetrachloride and a water-glycerol mixture acting as the binding liquid. The applied stirrer speed was 1250 rpm. At this stirrer speed, the output resulting from liquid turbulence was 0,07 volts, while agglomerates with a size of 3 mm give signals of about 1,5 volts. A typical example of a recorded reponse curve of a particle-impeller collision is shown in Fig. 2.15. As long as the particles are larger than 0,7 → 1 mm the response curve can be recorded directly. In this way e.g. the particle-stirrer collisions of sodium choride crystals with a mean size of 800 µm were recorded.

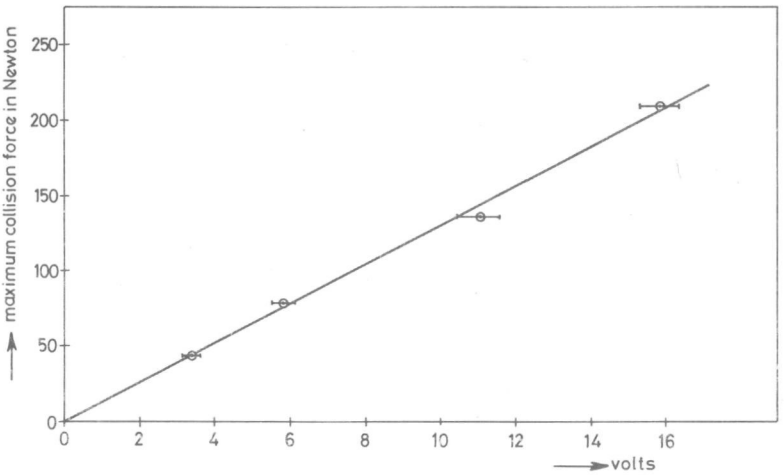

Fig. 2.14 Calibration curve: the maximum collision force as a function of the output in volts.

However, in order to registrate the collisions of the impeller with smaller particles, signal correlation techniques should be used, because signals originating from these collisions have about the same intensity as the signal induced by the liquid motion.

Further, Fig. 2.15 shows that the collision time was about 150 µs. The length of the collision time contains information concerning the elastic properties of an agglomerate. When there is a considerable change of these properties during the process, as indeed is exhibited in the agglomeration process, in-situ information can be valuable.

The encouraging results obtained so far lend support to further research concerning particle-impeller collisions by the use of the proposed method.

- *porosity and degree of saturation of the agglomerates*

The porosity was determined by means of a simple gravimetric procedure. The pellet porosity is:

$$\varepsilon = \frac{V_{pellet} - V_{solid}}{V_{pellet}} ,$$

whereby the pellet volume (V_{pellet}) and the volume of the solid particles within the pellet (V_{solid}) can easily be measured. Batches of 20 pellets were used for this purpose.
The evaluation of the degree of saturation (S) i.e. fraction of ε occupied by binding liquid raises more problems. Since it was difficult to use the usual distillation method due to the presence of relatively non-volatile glycerol, other methods (gravimetric, Fischer) were attempted. No reliable method could however be found, so that we will use the theoretical S value defined as:

$$S = \frac{1 - \varepsilon}{\varepsilon} \cdot BSR$$

where BSR is the binder solid ratio =

$$\frac{\text{vol of binding liquid}}{\text{vol. of solid particles}}$$

CHAPTER 3

Agglomeration kinetics in a batch system

3.1 *Introduction*

As mentioned in chapter 1, one of the main objectives of this study is to assess mechanisms that are responsible for the rate of agglomeration in batch systems. We describe the dynamic part of the kinetics in this chapter, while the results of the growth process, characterised by the equilibrium mean pellet size and Agglomerate Size Distribution (ASD), will be outlined in Chapter 4.

The existing literature concerning the kinetics of agglomeration in suspension is very limited. Kawashima and Capes [19, 20] developed an empirical correlation for the kinetics of the process. But, the derived equations are of limited applicability. As the authors state "Accurate equations to predict the course of the agglomeration process, especially with finer particles, must await a better understanding of the mechanisms involved". Nevertheless, the induction period of slow growth exhibited by their experiments is in accordance with our observations.

Some fundamental aspects of the agglomeration of coal powder were studied by Swanson et al [36]. In particular, they paid attention to the influence of some input variables, like amount of binding liquid, solid concentration, agitation rate and particle size of the feed, on agglomerate size and kinetics. Kinetic data were presented, rather macroscopicly in terms of "inversion time". At the moment of inversion, the viscosity of the coal slurry changes quite suddenly, indicating that the system rapidly achieves a state of maximum flocculation. It is not yet clear however, whether this inversion time is identical to the induction period of slow growth, reported by Kawashima and Capes [19, 29]. Further, the ASD's obtained [20, 36] are similar in form to size distributions obtained in granulation.
Indeed, it seems useful to consider the similarity between agglomeration in suspension and the classic size enlargement operation - granulation - where agitated powder masses are agglomerated in air as the environment. Concerning this process, extensive information is available in literature as will be described in par. 3.2. Another similarity that should be considered is coalescence in liquid-liquid dispersions.

In our study, growth kinetics were experimentally determined in terms of the increase of average pellet size in time, for different model systems as a function of a number of operating variables. From this work three regimes were identified that can occur during a batch growth cycle, i.e. an initial regime of almost zero growth rate, a regime of fast growth and an equilibrium regime. Further, it is tried to develop physical- (mathematical) models to describe these three regimes. In the mathematical developments the growth process is described in terms of population balance equations, because the population balance has been found to be a powerful tool in generating growth rate, equilibrium ASD and the development of the ASD in time.

3.2 *Kinetics and growth mechanisms in granulation*

The production of agglomerates by granulation is generally carried out in balling drums, discs or cones. In this rotating equipment, moist powder masses are tumbled until the granules have grown to the required size. It is likely that there are similarities between this granulation process and agglomeration in suspension, but one has to keep in mind that there are distinct differences, as for instance:
- the distribution in space of the pellets;
- mode of agitation;
- the third fase being air instead of liquid.

The existing literature on the kinetic analysis of granulation [36, 75-96] is extensive; however, the "quantative understanding of the microscopic occurance of the governing forces in pellet growth is far from complete", as stated recently [95].

The adhesion between particles is the basis for the formation of agglomerates. Calculations concerning the strength of agglomerates have indicated [97] that amongst the different possible attraction forces, for instance van der Waals, electrostatic, liquid and solid bridges, the capillary pressure in the pore space of the agglomerate filled with liquid is the major adhesion mechanism. On the basis of the latter mechanism an equation for the maximum strength exhibited by granules composed of as single powder was proposed [75] and later confirmed in more extensive studies [98-100] concerning the behaviour of agglomerates under tensile stress. Analysis of the relevant physical parameters showed that strength and deformation are dependent on the following variables

$$\sigma = f(S, \gamma, \varepsilon, \bar{d}, \theta, p_1, p_2, p_3) \qquad (3.1)$$

where σ is the tensile stress

S the degree of saturation (volume of liquid divided by the volume of voids)

γ the interfacial tension

ε the porosity

$\bar{d}$ mean particle size

θ contact angle

p_1 parameter representing particle size distribution

p_2 parameter representing particle shape

p_3 parameter representing packing structure

Only the influence of S, γ, $\bar{d}$ and ε has been assessed so that the ability to predict the strength of pellets of different materials is still doubtful. In particular, the size distribution of the initial particles is a factor that has significant effect on the strength of the pellets and through this on the agglomeration mechanism and growth rate [87].

The driving force behind the formation of granules is the reduction of surface free energy through reduction of the effective air-water interfacial area. The motion induced on the particles enables the contacting as well as the further compaction of the pellets.

The different mechanisms which can cause changes in granule size were studied by a number of authors [75, 78, 87, 88]. During the early stages of growth in batch systems, coalescence of two pellets, preceded by the rapid formation of nuclei granules, was recognised to be the prevailing mechanism. However, during the later stages the growth mode is more complex, involving preferential coalescence, abrasion and crushing and layering. The size distribution of the initial particles was identified as the cause for the occurence of one or more of these mechanisms. Relatively strong pellets (wide size distribution) showed only slight growth due to abrasion, while with relatively weak pellets (small size distribution) growth occured almost unlimited by crushing of some pellets into the initial particles followed by layering on the other pellets. In continuously operated systems, layering of the added feed is of course important. This aspect will be discussed further in chapter 5. The different possible mechanisms are depicted in Fig. 3.1 [95].

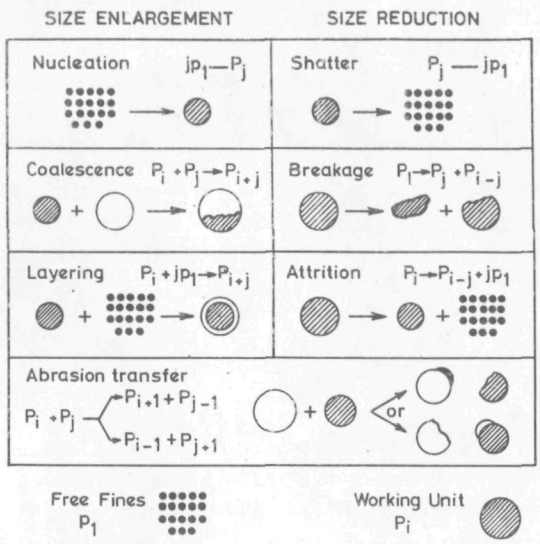

Fig. 3.1 Different growth mechanisms as identified for the granulation process [95].

The increase in pellet size with the number of drum revolutions is illustrated in Fig. 3.2a and 3.2b [87, 95] for different materials and moisture contents (or binding liquid). The S-shape of the curves is considered by many authors to be characteristic for granulation. Apparently, for some materials there is a tendency towards a steady-state size. This flattening of the growth cruve is attributed to the increase of pellet strength.
The sensitivity for the amount of added binding liquid is typical for the process. Successful operation is ensured when the binding liquid fills up more than about 60 percent of the pore volume, at minimum pellet porosity, while maximum growth rate is obtained at 90-100 percent. At this degree of saturation the pellets have a wet appearence and are easily

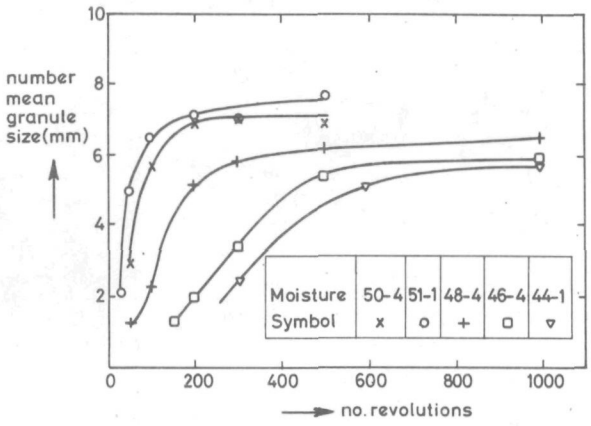

Fig. 3.2 a [87]

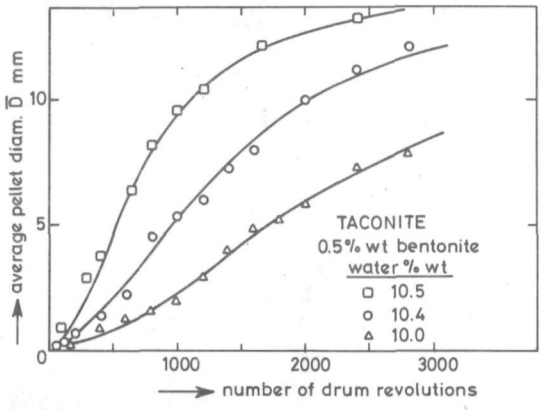

Fig. 3.2 b [95]

The increase of mean particle size with the number of drum revolutions as a function of moisture content.

deformable so that coalescence frequency can be high. Generalised equations for the binding liquid requirement were derived [94] by which the weight fraction of binding liquid in the agglomerate can be calculated on basis of particle- and binding liquid densities.
Other variables, like drum load and speed of rotation, have received less attention because their range is limited by the required easy tumbling of the granules.

The evolution in time of the ASD has received considerable attention. In general the ASD appears to be relatively narrow. Capes and Danckwerts [78] have shown an interesting feature of the ASD's: when plotted as a function of reduced size D/D_M (where D_M is the median pellet size), only one curve was obtained irrespectively of material properties or operating conditions (self preserving size spectrum).
In order to predict this behaviour, mathematical equations were developed in terms of population balance equations [80, 82, 83, 86, 89-93]. Assuming that

coalescence or coalescence in combination with crushing and layering are the prevailing mechanisms, it could be proved that the ASD's predicted by these models exhibited the 'selfpreserving' character with respect to time. However, as will be outlined in the next chapter (par 4.3.2), in which the population balance method is dealt with in more detail, this is not entirely in agreement with our experiments.

The prediction of growth rate was also attempted on basis of the same population balance equations as used for the prediction of the ASD and the following expression was obtained by Ouchiyama and Tanaka [89]:

$$\frac{d\bar{D}}{dt} \sim (\bar{D})^{3i-2a} \tag{3.2}$$

where a and i are factors that represent respectively the preference of the coalescence with respect to pellet size and the spacial distribution of the pellets. This equation can be fitted to experimental results if one accepts different factors a (or i) for three different stages of growth. It was experimentally observed that:

$$\begin{aligned} &\text{in the initial state } \frac{d\bar{D}}{dt} \sim \bar{D} \\ &\text{in the middle state } \frac{d\bar{D}}{dt} \sim (\bar{D})^{-1} \\ &\text{in the later state } \frac{d\bar{D}}{dt} \sim (\bar{D})^{-3} \end{aligned} \tag{3.3}$$

which can be accounted for by a constant value of i = 1 and a = 1, a = 2 and a = 3 respectively. The proposed growth equations are unsatisfactorily insofar that they do not predict a steady-state at the end of the agglomeration process, but a continuous increase of granule size.

3.3 Experimental results

3.3.1 Experimental procedure

Kinetic information concerning batch agglomeration in suspension was obtained by using methods and materials which were described in chapter 2. The standard 1.1 liter vessel was filled completely with a suspension of in general 55 gr solid particles (for glass powder: 1,72 vol %) in carbon tetrachloride. After stirring the suspension for 15 minutes the binding liquid was injected in the liquid stream leaving the impeller. The amount of binding liquid is expressed in terms of the Binder Solid Ratio defined as:

$$BSR = \frac{\text{volume binding liquid}}{\text{volume of solid particles}}$$

To ensure proper emulsification of the binding liquid and to obtain a reproducible starting situation uniform throughout the vessel, the power-imput was kept for 3 minutes at a high level (for glass powder N^{*} = 1750 rpm; P=4,5 W/kg). During this period the agglomeration rate was approximately zero. Then the stirrer speed was lowered to the required value (in general N = 1250 rpm; P = 1,5 W/kg) and this moment was chosen to be t = 0 min. in the growth curves.

3.3.2 Growth regimes in agglomeration in suspension

The reproducibility of the experimental system was assessed by six experiments, carried out under identical conditions. Glass powder no. 3 was used as this system appeared to be the most sensitive to operating variables. Fig. 3.3 shows that the maximum average pellet size and the slope of the steep part of the growth curve are fairly reproducible. The reproducibility of the moment at which the fast growth starts (t_z) is less satisfactory, for most of the curves t_z ranges between 30 and 38 minutes, with as an exception experiment no. 6021 (45 minutes).

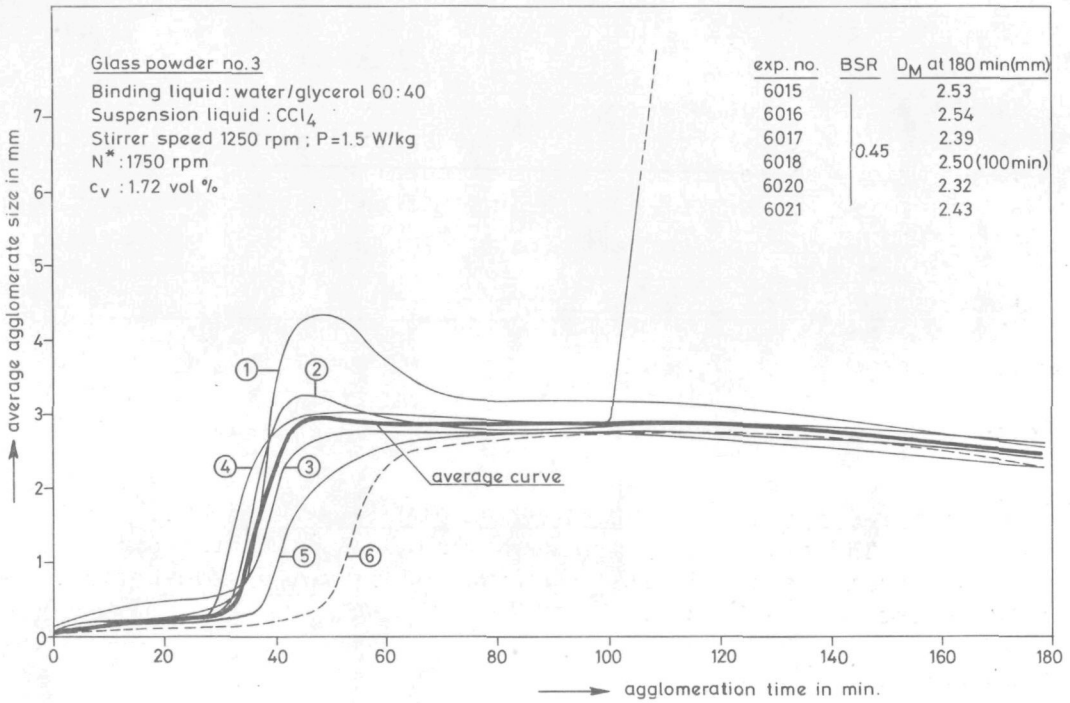

Fig. 3.3 The increase of agglomerate size with agglomeration time. Reproducibility of the system.

In this particular experiment probably the preparation procedure of the powder has not been carefully carried out.
Nevertheless, we proceeded to use the described experimental system since it showed that even small variations of the various experimental parameters caused much larger shifts in the growth curves (Fig. 3.4 and Fig. 3.5) than the spread shown in the data on Fig. 3.3. Moreover, we will restrict ourselves mainly to qualitative interpretation of the differences in growth behaviour; for this purpose the obtained accuracy is sufficient.

Fig. 3.4 shows that large differences in shape of the curves result from small variation in shape and size distribution of the primary particles. Fig. 3.5 shows a similar impact of a small variation of the BSR on the growth rate. From this, it appears that a variety of complex phenomena and interactions determines the way and rate of which pellets are formed.
Some features of the different growth curves leap to the eye:

- period of zero growth

  The curves (2) and (4) in Fig. 3.4 show, after an immediate flocculation step where flocs of 100-300 μm in size are formed, an extended period of zero growth (which even can last for 100 minutes or more), followed by a period of very fast growth. This in contrast with the curves (1) and (3), in the same figure, where the growth rate changes more smoothly.

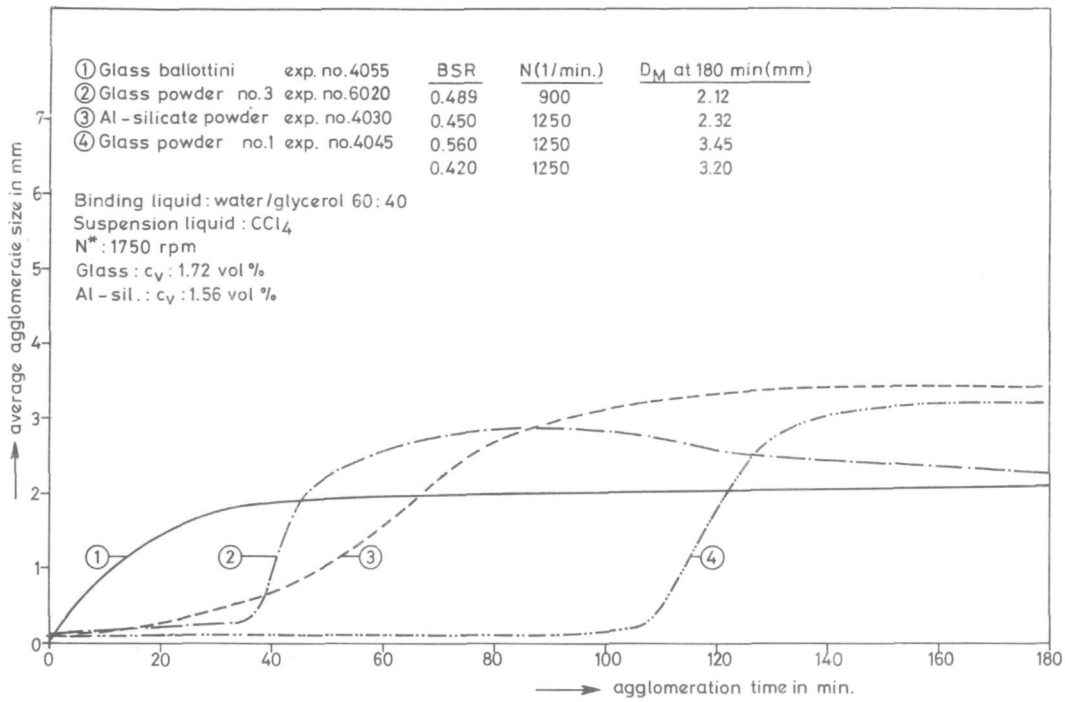

Fig. 3.4 Experimental growth curves for various particle systems.

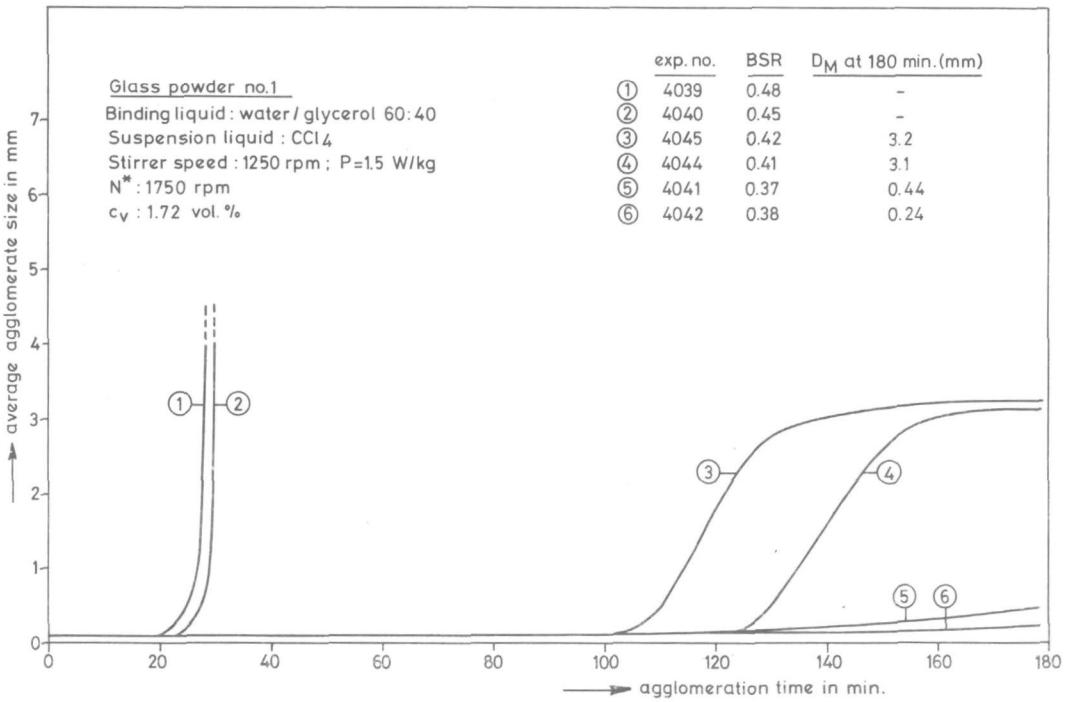

Fig. 3.5 Effect of BSR on growth rate.

- steady state

  In most experiments a steady state is reached within the observation period of 180 minutes; the average size of the agglomerates does not change anymore.

- decrease in size

  Agglomerates grown from glass powder no. 3 (curve (2) in Fig. 3.4) show a slow decrease in average size after a maximum was reached at t ≈ 50 minutes.

For a further discussion of these last two features we refer to Chapter 4.

Considering the differences in growth behaviour between the different solids, four growth regimes can be recognized (Fig. 3.6):

a. flocculation regime;
b. zero growth regime;
c. fast growth regime;
d. equilibrium regime, which can include a slow decrease in agglomerate size.

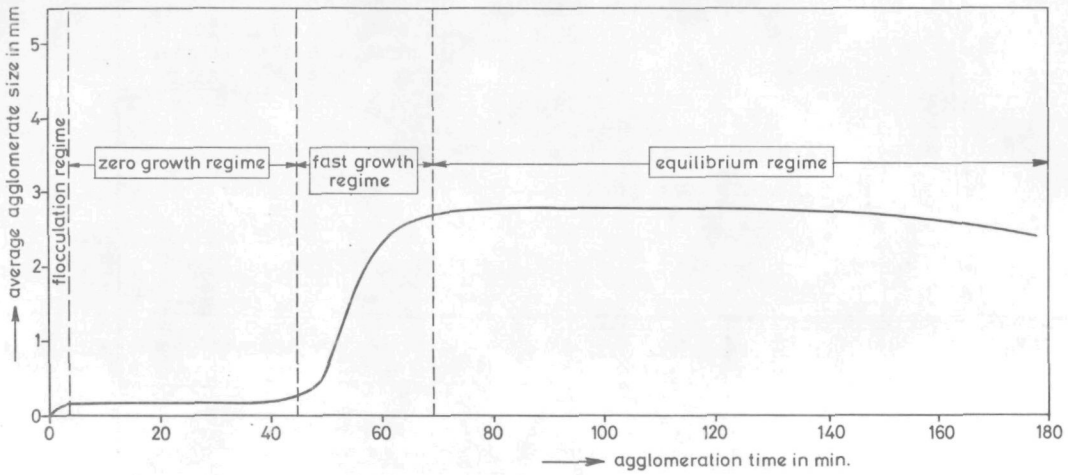

Fig 3.6 Growth regimes for batch agglomeration in suspension.

The occurence and length of these regimes can differ, depending on the particles to be agglomerated and the operating conditions. In the flocculation regime we observed that in all our experiments flocs with a size of 200-300 µm were formed. Larger liquid droplets (30 µm) were found to pick up or coalesce with relatively smaller (10 µm) solid particles. This is contradictory to the common view that small liquid droplets are supposed to adhere to the surface of the solid particles. The total flocculation period took less than 2 minutes. Therefore, in this study, the flocculation step is of minor importance in growth kinetics and is merely defined for the sake of completeness [101].

3.3.3 Growth rate as a function of operating variables

Growth curves were determined whereby the following parameters were varied: the binding-liquid/solid ratio (BSR), stirrer speed (N), binding liquid viscosity (µ), particle volume concentration (c_v) and the stirrer speed at which the binding liquid was emulsified (N^*). The effect of the different variables and particle systems on growth rate is shown in Figs. 3.7, 3.8 and 3.9. It can readily be readily that the zero-growth regime often dominates agglomeration kinetics. Its duration (t_z) ranges from almost zero minutes (Fig. 3.9c) to 180 minutes and more (Fig.3.7a). Moreover, t_z appears to be quite sensitive to most operating variables. Decreasing the BSR from 0.45 to 0.38 increases t_z from 25 to at least 200 minutes (Fig.3.7a). The other variables have a less pronounced influence. But in general one can observe that t_z decreases with increasing BSR, N, N^* and solid concentration, while t_z shows probably a minimum when the viscosity of the binding liquid varies. Considering the extreme influence of the BSR as well as the differences in degree of saturation (glass powder $\pm$ 1.0, Al-silicate powder $\pm$ 0.75) it is considered not useful to deduce a generalized equation for the binding liquid requirement as was done for granulation (see page 23)

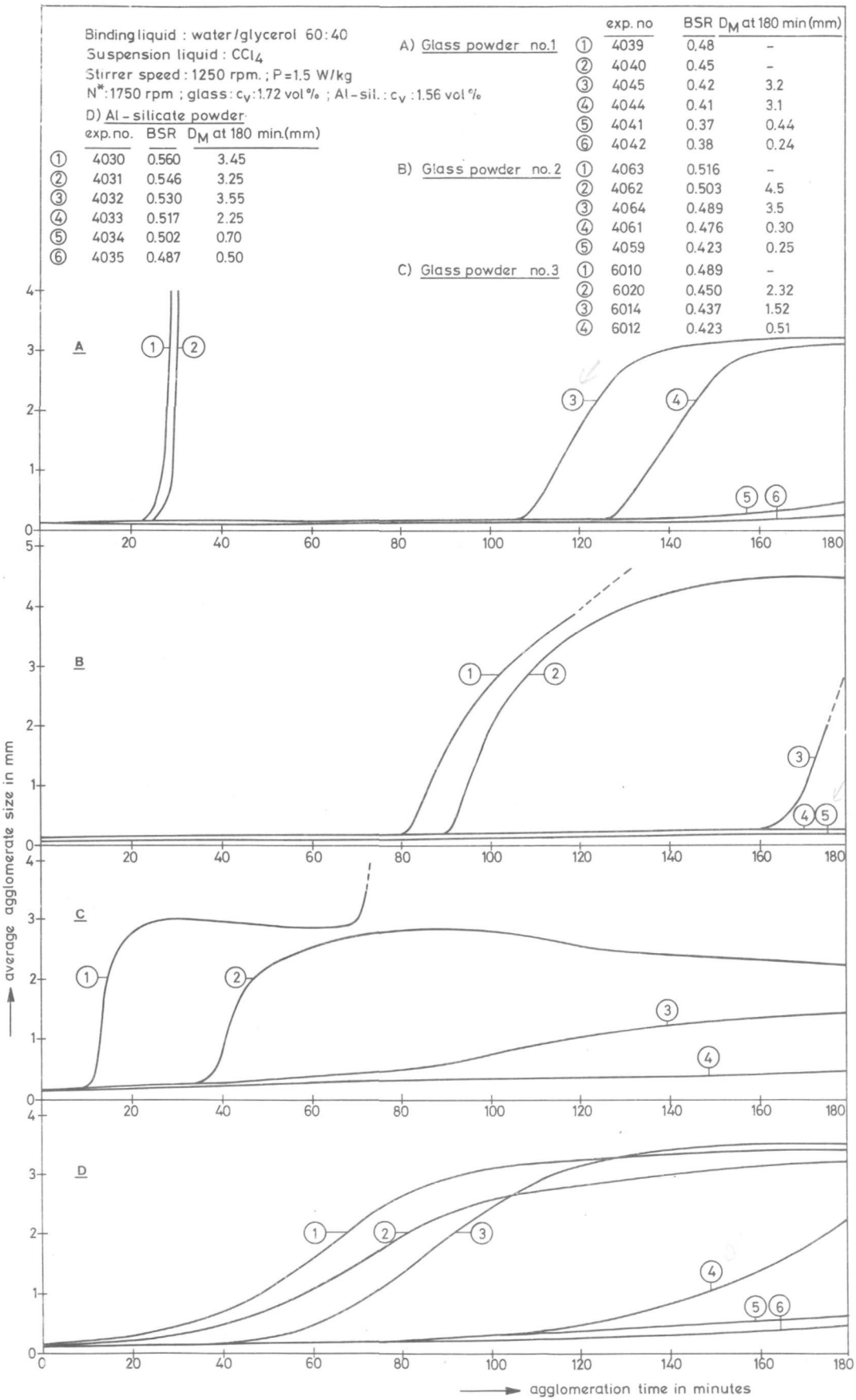

Fig. 3.7 Experimental growth curves as a function of BSR for various powders.

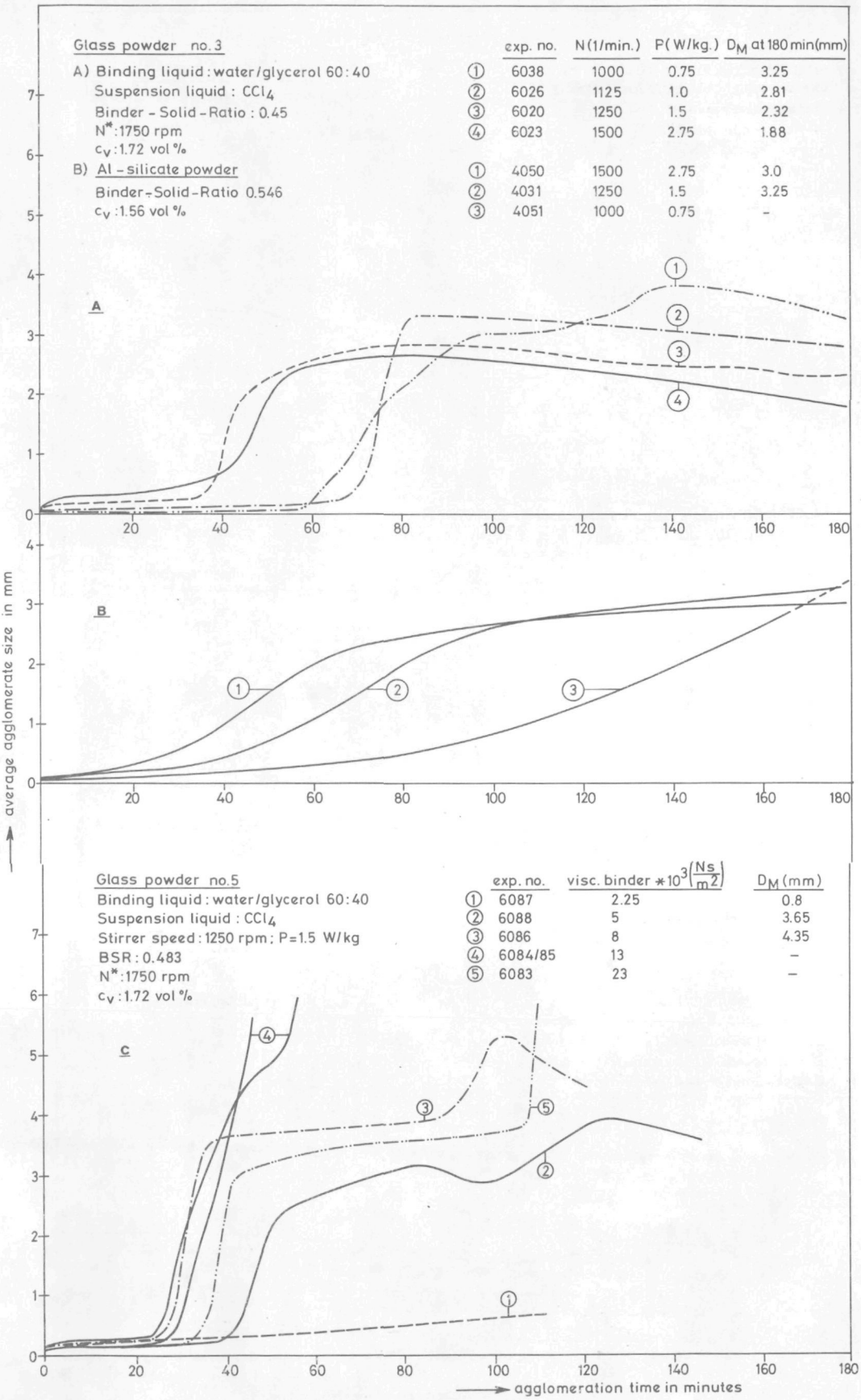

Fig. 3.8 Experimental growth curves as a function of stirrer speed and binding liquid viscosity.

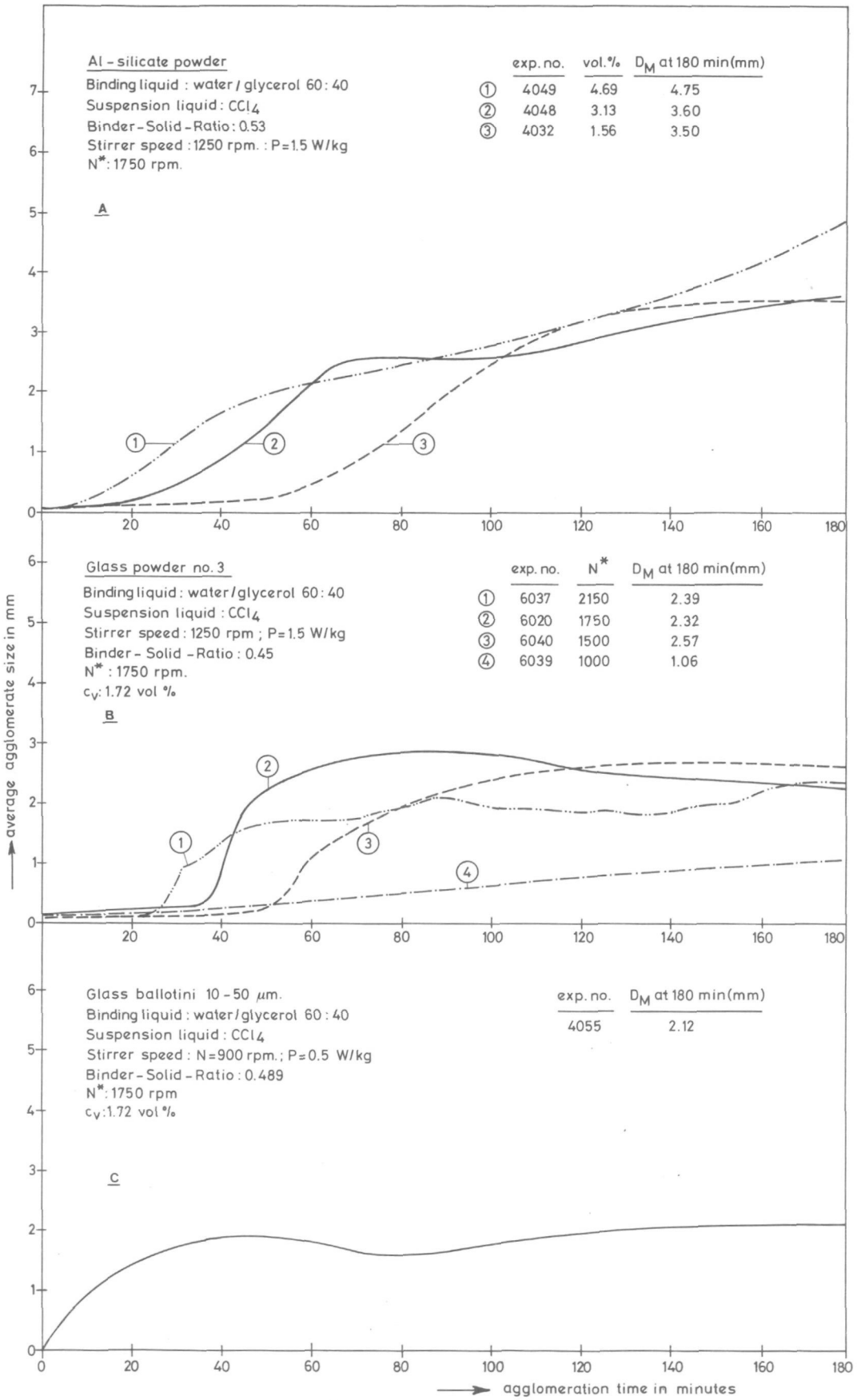

Fig. 3.9 Experimental growth curves as a function of particle concentration and the stirrer speed at which the binding liquid was injected.

By comparison of Figs.3.7, 3.8 and 3.9 we see that the maximum growth rate (i.e. the slope) in the fast growth regime, for one single type of particles shows little variation and is independent of BSR, N, concentration etc. Particle properties however have a marked influence.
For respectively glass powder 3, 2, 1 and Al-silicate powder, maximum growth rate decreases successively: 0.24, 0.19, 0.13 and 0.06 mm/min. Some interesting experiments in this respect are depicted in Fig. 3.10. The experiment represented by curve (2) was performed with a relatively low BSR until 90 minutes; then, additional binding liquid was injected so that the BSR was equal to the BSR applied in the experiment represented by curve (1). By comparison of these curves, one can clearly see that growth rate is not affected by the "history" of the pellets. This can also be observed in exp. no. 6080 (curve 3), where an excess of binding liquid was injected at t = 90 min.

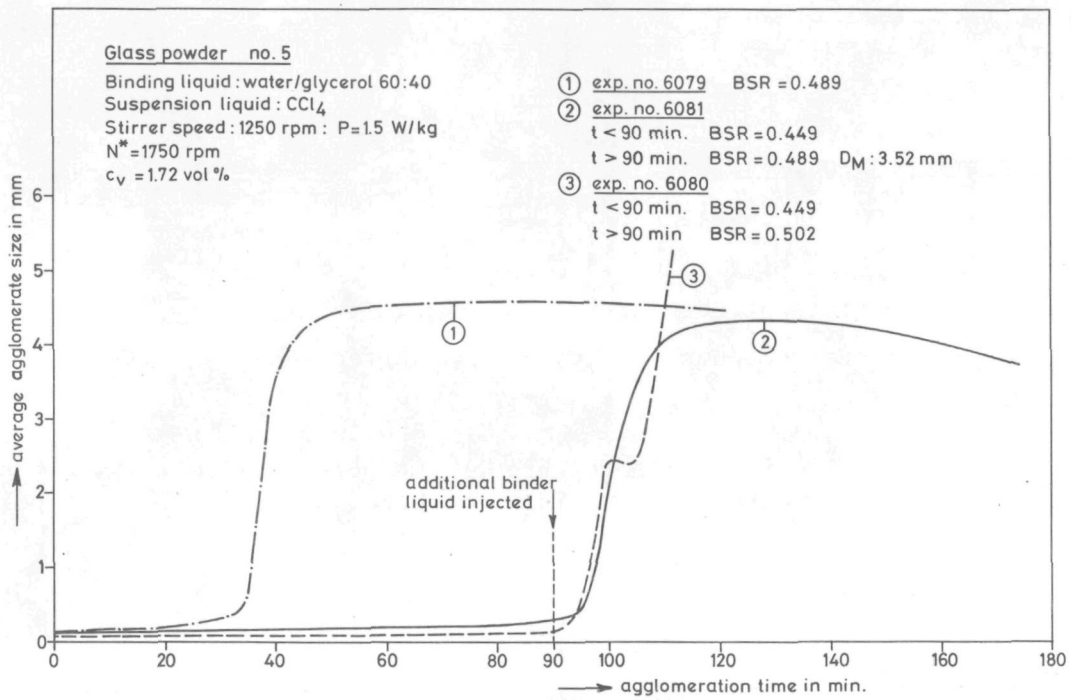

Fig. 3.10 Effect of the 'history' of the pellets on the growth rate in the fast growth regime.

3.4 *Discussion of the "zero-growth-rate" regime*

In the flocculation regime, quite loose flocs are formed being a few hundred μm in size. As already shown, the mean size of these flocs will hardly change during time t_z. Because the loose flocs are transformed during the growth process into closely packed pellets, it is evident that porosity of the flocs/pellets will decrease. As a result, floc strength will increase and the entrapped suspension liquid will be squeezed out. The binding liquid will gradually fill up the pore space in the floc until it appears at the surface of the floc. Then growth by pellet coalescence can start again, marking the beginning of the fast growth regime.
Thus, in order to explain the zero growth regime, it is assumed that the amount of binding liquid present at the floc/pellet surface is not sufficient for pellet coalescence. The hypothesis that under certain conditions the pellet surface is relatively dry, could be proved by the following experiment: a batch of 10 gr glass powder was added to a batch of growing pellets without adding extra binding liquid. It was observed that when the powder was added during

the z-regime (exp. no. 4035 after 60 minutes and exp. no. 4056 after 420 minutes), it was not wetted by binding liquid and was not taken up by the flocs. When in contrary the powder is added during the fast growth regime, it is completely taken up by the existing pellets (exp. no. 4057, 4058).
The rate controlling step is therefore thought to be the sqeezing of the binding liquid out of the pores onto the pellet surface. The length of the z-regime t_z will then be inversly proportional to the liquid velocity in the pores:

$$t_z \sim \frac{1}{u} \tag{3.4}$$

An extensive number of different pore space models exist but for the sake of simplicity we will use the Kozeny-relationship:

$$u = c_1 \frac{1}{\mu} \frac{\varepsilon^3}{(1-\varepsilon)^2 A_v^2} \cdot \frac{\Delta p}{R} \tag{3.5}$$

where

u = superfical liquid velocity

μ = viscosity of the liquid

ε = porosity

A_v = specific surface of the particles per unit volume

Δp = pressure difference between centre and surface of the pellet

R = pellet radius

The driving force for liquid transport through the pores will mainly be the external pressure brought about by liquid turbulence, pellet-pellet and pellet-stirrer collisions.
Stirrer speed N and the solid concentration c_v both have a positive effect on $p_{external}$, so that following eqns.3.4 and 3.5, t_z will decrease with N as well as with solid concentration. This is indeed confirmed by the experimental results. Further, t_z should decrease with pore size.
One might suppose that the initial packing of the flocs is already more dense when the binding liquid is emulsified more finely. This would explain the effect of the initial stirrer speed N^*. The above simplified model does not describe adequately the influence of binding liquid viscosity. Factors like the initial floc geometry and the distribution of the binding liquid within the floc were assumed to be similar for all operating conditions. Apparently, this is not valid for different liquid viscosities.

3.5 *Mechanisms with respect to the 'fast growth' regime*

The observation of double and triple sets of pellets, shown on the photographs 3.1a, b and c strongly indicates the existence of a coalescence growth mode.

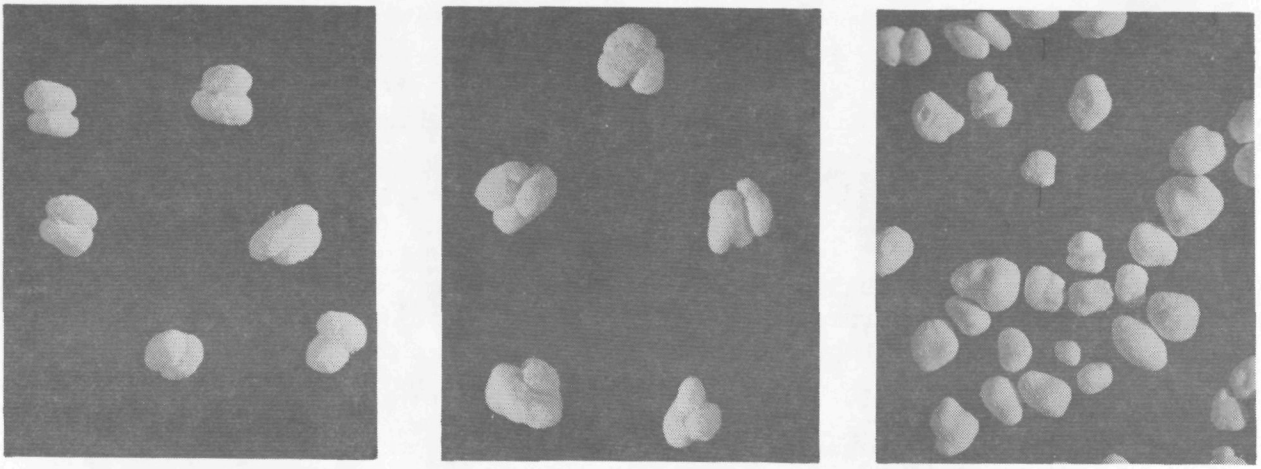

(a) *(b)* *(c)*

Photograph 3.1 (a)(b)(c) Al-silicate powder pellets.

These photographs were taken from Al-silicate pellets that were growing at a relatively low power input of P = 0,75 W/kg (N = 1000 rpm) so that the process of coalescence was sufficiently retarded to make the observation of pairs of pellets possible. The photographs 3.2a, b and c, showing the progress of pellet growth, further indicate that floc-floc and/or pellet-pellet coalescence is the prevailing mechanism in the fast growth regime for batchwise operated pelletizers.

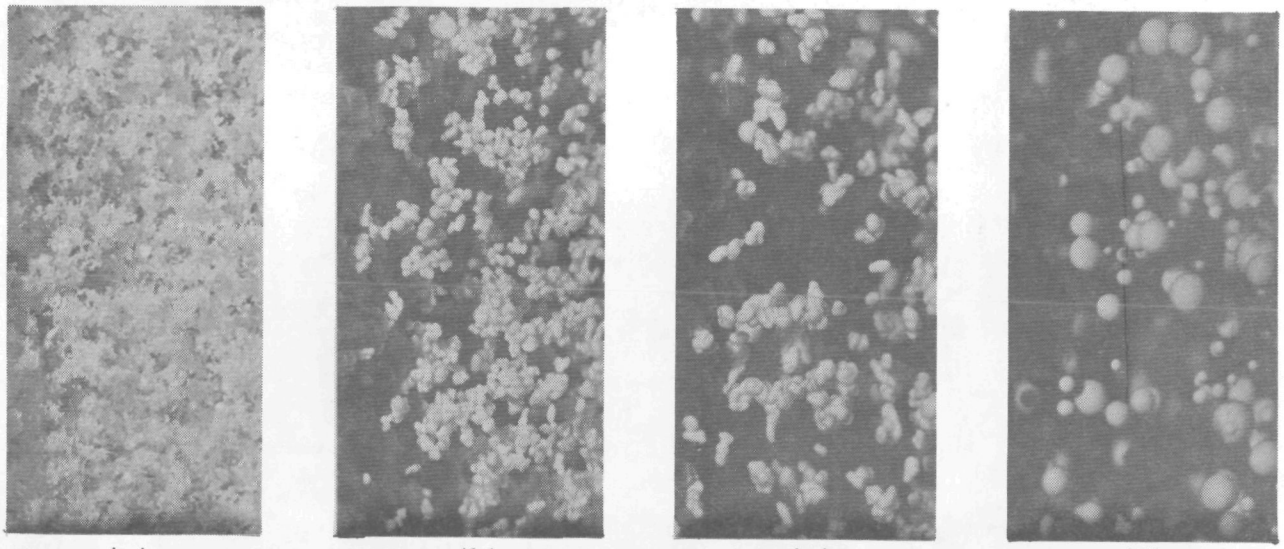

(a) *(b)* *(c)* *(d)*

Photograph 3.2 (a) (b) (c) (d) Glass powder pellets at different agglomeration times.

However, besides coalescence another phenomenon plays an important role in agglomeration kinetics: i.e. breakage of pellets. As shown in Fig. 3.4, in some experiments a slow decrease in average size of the pellets is observed after a maximum had been reached. This can be accounted for by postulating a breakage mechanism of pellets. Carefully designed experiments, described and discussed in chapter 4, show that pellets can break indeed into a discrete number of parts

(most likely in two parts) under growth conditions; moreover the breakage frequency appears to increase with pellet size.
Possibly this is only valid for low viscosity binding liquids. For binding liquids with higher viscosities than applied in this study, quite different mechanisms may be involved.
On the basis of the above mentioned mechanisms, coalescence and breakage, a mathematical formulation to predict agglomeration rate has been set up which is described in the next paragraph.

3.6 A coalescence-breakage model for the fast growth regime

3.6.1 Introduction

Models to describe particle-particle interactions whereby coalescence can be identified as one of the basic underlying mechanisms can be found in literature for a variety of processes. Mathematical equations, in terms of population balances were developed for instance in the fields of aerosol science [102-105], colloid science [106-110], granulation technology [80, 82, 83, 86, 89-93, 111] and liquid-liquid dispersions [112-116]. Also the more general behaviour of particle populations was studied for small as well as for large populations [120-122]. Large populations of small particles, subjected to coalescence are in fact also present in the agglomeration in suspension process.
A population balance equation can be used for the following purposes:

- the growth function, e.g. in terms of $\bar{D} = f(t)$, can be derived by integrating the population balance equation over all particle sizes and solving the resulting equation.
- prediction of the ASD development in time, whereby the equation has to be solved with respect to both time and size.

Therefore, when assessing the validity of a proposed model both the above aspects have to match with experimental results.

3.6.2 Models used for granulation

The basic equation describing the kinetics of granulation is:

$$\frac{\partial n(x,t)}{\partial t} = \tfrac{1}{2} \int_0^x R(x-\bar{x},\bar{x}) \frac{n(x-\bar{x},t)n(\bar{x},t)}{N^i(t)} d\bar{x} - \int_0^\infty R(x,\bar{x}) \frac{n(x,t)n(\bar{x},t)}{N^i(t)} d\bar{x} \qquad (3.6)$$

where $n(x,t)dx$ is the number of agglomerates with volume between x and x + dx, at time t;

$N(t) = \int_0^\infty n(x,t)dx$ is the total number of agglomerates at time t;

$R(x,\bar{x})$ is the collision-coalescence rate function or coalescence frequency for a pair of particles with volume x and $\bar{x}$.

The first term on the right-hand side represents the number of particles n(x,t) growing into the volume interval x + dx by coalescence of smaller particles, while the second term represents the number of particles leaving the interval x + dx by coalescence with larger particles. This equation is valid for a "restricted in space" system when i = 1, which implies that a particle can only collide with particles in its immediate surroundings [82]. Adopting a "free in space" concept, where a particle can collide with every other particle available,

would change the power i of N(t) from 1 to 0, but would not change the approach and results of the numerical analysis of eqn. (3.6).
As mentioned in par. 3.6.1 $\bar{D} = f(t)$ as well as the ASD can be obtained from the population balance equation. Firstly, we will discuss the ASD. Eqn. (3.6) is a non-linear partial integro-differential equation and analytical solutions are only available for simple expressions of the coalescence frequency factor [120]. For frequency factors of physical significance no analytical solutions seem to be possible as for instance when

$$R(x,\bar{x}) = \frac{C}{(x\bar{x})^a} \qquad (3.7)$$

which is frequently used in describing granulation kinetics.
Solutions of eqn. (3.6) combined with (3.7) were obtained [92] following a method based on similarity transformation. By a particular grouping of the independent variables, a similarity transformation can reduce the number of independent variables from two to one. Eqn. (3.6) is then transformed into an ordinary integro-differential equation that can be solved numerically (see chapter 4). We made a number of example calculations on basis of eqn. (3.6). The resulting size distribution curves are presented in Fig. 3.11. Curve (1) represents the solution for random non-preferential coalescence ($R(x,\bar{x})$ = constant) while curve (2) shows a solution for non-random or preferential coalescence

$$\left(R(x,x) \sim \frac{1}{(x\bar{x})^a} \; ; \; a = 0{,}6 \right)$$

It was found that experimental ASD's obtained for granulation can be fitted rather well for values of a = 0.6.

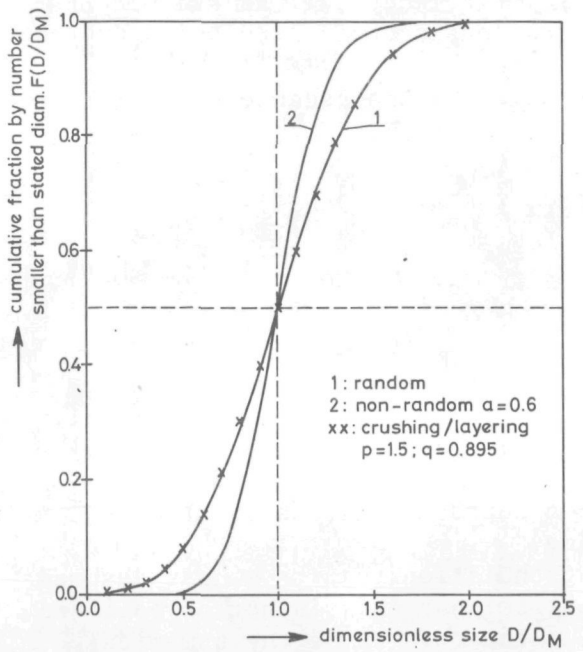

Fig. 3.11 ASD's predicted by the random and non-random coalescence models.

When apart from coalescence also crushing and layering is adopted as growth mechanism, the kinetic equation becomes:

$$\frac{\partial n(x,t)}{\partial t} = -C(x,t)n(x,t) - \frac{\partial}{\partial x}\left[G(x,V(t))n(x,t)\right] + \tfrac{1}{2}\int_0^x R(x-\bar{x},\bar{x}) \cdot \frac{n(x-\bar{x},t)n(\bar{x},t)}{N(t)}\, d\bar{x} - \int_0^\infty R(x,\bar{x}) \frac{n(x,t)n(\bar{x},t)}{N(t)} d\bar{x} \qquad (3.8)$$

C(x,t) being the crushing function and G(x, V(t)) the growth function representing the rate at which granules are growing larger than size x by picking up the crushed material with volume V(t). For this model, approximated analytical solutions were presented [91] for $R(x,\bar{x})$ = constant, $R(x,\bar{x}) = x + \bar{x}$ and several forms of the crushing function. The solution contains parameters that can be chosen in such a way that the effect of crushing and layering is maximalised. Using the most extreme values for these parameters, we calculated the size distribution curve. It appeared then that the solution was almost identical to the solution obtained for coalescence, without crushing and layering (Fig. 3.11).

To obtain an expression for the growth kinetics, eqn. (3.6) has to be integrated over all particle sizes. Applying the similarity transformation technique, expressions for the growth rate, expressed here in terms of mean pellet size, can be obtained (see Appendix I).

preferential coalescence : $$\frac{d\bar{D}}{dt} = C_1 D^{1-6a} \qquad (3.9)$$

coalescence/crushing layering: $$\frac{d\bar{D}}{dt} = C_2 D^{1+3b} + C_3 D^{1-6a} \qquad (3.10)$$

where C_1, C_2, C_3 and $\underline{a}$ have positive values, $C(x,t)$ in eqn. (3.8) $\sim x^b$ where b can take negative as well as positive values.
Eqn. (3.9) and (3.10) both predict a continuous increase of pellet size, which is in contradiction with experimental results we obtained for the agglomeration in suspension process. For this reason another model will be described that predicts a steady state solution for the average size as well as a correct ASD.

3.6.3 The population balance approach to agglomeration in suspension

A breakage mechanism of pellets is postulated and, for the convenience of mathematical computation, it is assumed that an agglomerate breaks into r equal parts. In difference with the crushing and layering model, it is assumed that the broken parts equally participate in the coalescence process like the non-broken particles.
The population balance equation for agglomeration by coalescence and breakage can be formulated as follows:

$$\frac{\partial n(x,t)}{\partial t} = - B(x)n(x,t) + r^2 B(rx)n(rx,t) + \tfrac{1}{2}\int_0^x R(x-\bar{x},\bar{x})\,\frac{n(x-\bar{x},t)n(\bar{x},t)}{N(t)}\,d\bar{x} - \int_0^\infty R(x,\bar{x})\,\frac{n(x,t)n(\bar{x},t)}{N(t)}\,d\bar{x} \qquad (3.11)$$

where B(x) is the breakage frequency function representing the fraction of agglomerates of volume x broken per unit time.
In first instance, and for comparison with granulation results, i was assumed to be 1 (restricted-in-space system). We realise that this is not a realistic situation for agglomeration in suspension but the results of the numerical analysis are in principle not influenced by the power i. The influence of pellet hold-up, however, can not be assessed for this case (see [44] for liquid-liquid systems).
It is not possible to use the similarity transformation technique as was discussed in par. 3.6.2 independently of the functional forms chosen for $R(x,\bar{x})$ and B(x). This is explained in Appendix I.
Before giving some results of the numerical analysis of eqn. (3.11), we will try to deduce functional forms for $R(x,\bar{x})$ and B(x).

3.6.4 The functional form for the coalescence frequency

In a recent publication, Pulvermacher and Ruckenstein [92] expressed their opinion with respect to the development of a coalescence model in agglomeration as follows:
"Due to the complex influence which air (or suspension liquid), water and solid phases have on the mechanical and rheological properties of the ensemble, no expression was yet derived for the coalescence frequency factor between granules".

Nevertheless, it seems reasonable that a general expression for the coalescence frequency is written as:

$$R(d_1,d_2) = \alpha(d_1,d_2) \cdot \beta(d_1,d_2) \qquad (3.12)$$

where $\alpha(d_1,d_2)$ is the collision frequency between particles of size d_1 and d_2 and $\beta(d_1,d_2)$ is the coalescence efficiency of particles having size d_1, d_2. We will consider coalescence of a pair of pellets to be established when a bridge consisting of binding liquid and solid particles is formed. The possible subsequent rupture of the bridge, will be considered as breakage and thus incorporated in the breakage frequency.
For particles larger than 100 μm and suspended in a turbulent liquid, Abrahamson [123] derived the following expression for the collision frequency:

$$\alpha(d_1,d_2) = 5.0\,(d_1 + d_2)^2 \sqrt{\overline{U_{p1}^2} + \overline{U_{p2}^2}} \qquad (3.13)$$

where $\overline{U_{p1}^2}$ is the variance of the velocity distribution of a particle with size 1. Since $\overline{U_p^2}$ is known as a function of the specific power input p and particle size d, [129] eqn. (3.13) can be written as follows:

$$\alpha(d) = 198 \left(\frac{\mu}{\rho_d}\right)^{\frac{1}{2}} \cdot P^{1/6}\, d^{5/3} \qquad (3.14)$$

This equation is valid for equally sized particles falling within the size range of inertial subrange eddies. For the coalescence efficiency it will be assumed as a first approximation that pellet coalescence proceeds in a similar way as droplet coalescence in turbulent liquid-liquid dispersions. For the latter system, the basic assumption is that coalescence takes place if the contact time of the drops exceeds the coalescence time. It is further assumed that the time required to drain the film between the drops is rate controlling and that subsequent coalescence takes place instantaneously.
Following the work of Tavlarides et al [115, 116, 124, 125] the following equation can be obtained for the coalescence efficiency:

$$\beta(d_1,d_2) \sim \exp\left[-c_1 \nu_c P^{-1/3} (d_1 + d_2)^{-4/3}\right] \qquad (3.15)$$

where ν_c is the kinematic viscosity of the continuous phase and c_1 is a constant. Eqn. (3.15) is again only valid for particles with size $d >> \eta'$; η' being the order of the viscous subrange eddies ($\simeq$ 30 μm).
Substituting eqn. (3.14) and (3.15) into (3.12), the following equation for the coalescence frequency is reached:

$$R(d) = c_2 P^{1/6} d^{5/2} \exp\left(-c_3 P^{-1/3} d^{-4/3}\right) \qquad (3.16)$$

Whether R(d) increases or decreases with d, depends on the values of c_2 and c_3. Tavlarides evaluated these constants from experiments and found that R(d) decreased with d.
But still, one has to bear in mind that to describe coalescence between pellets, other factors, additional to those responsible for droplet coalescence should be considered. In particular, one might assume that filmdrainage is not the rate controlling step in the coalescence mechanism. After the initial contact has been established, the subsequent coalescence will not proceed instantaneously but will depend on the rate of formation of the solid-liquid bridge connecting the pellets. This could be visually observed: particles were 'flowing' from the bulk of the pellet towards the connecting point (Fig. 3.12).

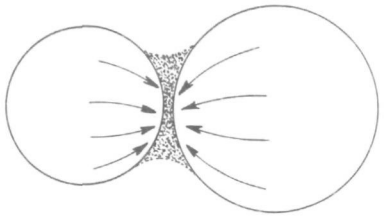

Fig 3.12 Formation of a solid-liquid bridge between two coalescing pellets.

So eqn. (3.12) has to be extended with a third factor as follows:

$$R(d_1,d_2) = \frac{\alpha(d_1,d_2)\,\beta(d_1,d_2)}{\gamma(d_1,d_2)} \qquad (3.17)$$

where $\gamma(d_1,d_2)$ represents the resistence factor for the transport of particles from the bulk of the pellet towards the connecting bridge.
The resistence factor $\gamma(d_1,d_2)$ will strongly depend on the amount of binding liquid present on or near the surface of the pellet.
Similar experiments as were described in par. 3.4 were carried out, whereby this time additional powder was added at various stages of growth after the beginning of the fast growth regime. It was found that the rate at which the powder was taken up by the existing pellets decreased with increasing average pellet size and finally almost stopped when the equilibrium size was reached. This means that the amount of binding liquid on the pellet surface decreases as a function of time (and pellet size). Therefore it seems reasonable as to assume that γ increases with pellet size, e.g. $\gamma(d) \sim d^k$, where k is positive.
So, finally we may conclude that:

$$R(d_1,d_2) \sim \frac{1}{(d_1,d_2)^{a'}} \qquad (3.18)$$

or, in terms of particale volume x:

$$R(x,\bar{x}) \sim \frac{1}{(x\bar{x})^a} \qquad (3.19)$$

This is the same expression as the one that is used in granulation (eq. 3.7).

3.6.5 The functional form for the breakage frequency

The breakage frequency of a pellet of size d is:

$$B(d) = \frac{1}{t_b} \cdot \frac{\Delta N(d)}{N(d)} \qquad (3.20)$$

where t_b is a characteristic breakage time and $\Delta N(d)/N(d)$ is the fraction of pellets breaking.

On the basis of experimental observations, breakage mechanisms are discussed in chapter 4. It is subsequently shown that pellet-impeller collisions or the pressure differences near the impeller are the major factors responsible for single pellet breakage or the break-up of a pair of pellets connected by a bridge.
If we deal here with pellet-impeller collisions, it is assumed that the fraction of pellets breaking is proportional to the fraction of collisions that have an impact force greater than the cohesive forces of the pellet or of the bridge between a pair of pellets.

Considering pellets with constant physical properties one can assume that:

$$\frac{\Delta N(d)}{N(d)} \sim P(d) \cdot \frac{F_i(d)}{F_c(d)} \tag{3.21}$$

where P(d) is the probability of a pellet hitting the impeller blade; this is taken proportional to the inertia force acting on the pellet

$$P(d) \sim d^3 \tag{3.22}$$

$F_i(d)$ is the impeller-pellet impact force (see par. 2.6.3), being for a pellet with constant elastic modulus and Poisson constant

$$F_i(d) \sim d^2 \, u_{tip}^{6/5} \tag{3.23}$$

u_{tip} = tip velocity of stirrer $\sim N.D_T$

whereby N = impeller speed and D_T = impeller diameter (3.24)

$F_c(d)$ is the cohesive force, being

$F_c(d) \sim d^2$ for a single pellet (3.25a)

$F_c(d) \sim d$ for a pair of pellets (3.25b)

From eqns. (3.21), (3.22), 3.23) and (3.25) the fraction of pellets breaking can be written as:

$$\frac{\Delta N(d)}{N(d)} \sim d^3 \, u_{tip}^{6/5} \quad \text{for a single pellet} \tag{3.26a}$$

$$\frac{\Delta N(d)}{N(d)} \sim d^4 \, u_{tip}^{6/5} \quad \text{for a pair of pellets} \tag{3.26b}$$

The characteristic breakage time t_b is taken to be inversely proportional to the circulation frequency of the liquid in the vessel (the terminal velocity of the pellet is small compared to the liquid velocity);

$$\frac{1}{t_b} \sim N D_T^3 \tag{3.27}$$

One finally obtains for the breakage frequency:

$$B(d) \sim d^3 \, N^{2\frac{1}{5}} \, D_T^{4\frac{1}{5}} \quad \text{for a single pellet} \tag{3.28a}$$

$$B(d) \sim d^4 \, N^{2\frac{1}{5}} \, D_T^{4\frac{1}{5}} \quad \text{for a pair of pellets} \tag{3.28b}$$

So that one might conclude that a functional form for the breakage frequency in terms of particle volume x is:

$$B(x) = B \cdot x^b$$

where b is of the order 1.

3.6.6 Numerical analysis and results

An expression for the growth rate is obtained by integrating the population balance, eqn. (3.11) which yields in terms of the total number of pellets:

$$\frac{dN(t)}{dt} = \underbrace{(r-1)\int_0^{\infty} B(x).n(x,t)\,dx}_{\text{breakage part}} - \underbrace{\tfrac{1}{2}\int_0^{\infty}\int_0^{\infty} R(x,\bar{x})\,\frac{n(x,t)n(\bar{x},t)}{N(t)}\,dx\,d\bar{x}}_{\text{coalescence part}} \qquad (3.30)$$

An analytical expression for dN(t)/dt can not be deduced since the similarity transformation technique can not be applied in this case (see Appendix I). Attempts to formulate approximated solutions of eqn. (3.30) failed, because no expression could be found that simultaneously predicted for constant numerical values of the variables a and b, in respectively eqn. (3.19) and eqn. (3.29), correct ASD's and an adequate form of the growth curve. Therefore, the population balance equation (3.11) has to be solved with respect to both x and t. In this way the evolution of the ASD (see chapter 4) can be obtained and thus also $\bar{D} = f(t)$. Sonneveld and Bemer [134] developed a numerical method , shortly outlined in Appendix II, that is able to solve eqn. (3.11) in the time-space, using the expressions for $R(x,\bar{x})$ and $B(x)$ derived in par. 3.6.4/3.6.5.

Numerical calculations were carried out, whereby a and b were varied while the parameters C and B were kept constant (= 1). Then, for comparison with experiments, the D and t axes of the computed curves can be scaled by inserting different values for C and B (see Appendix II[b]). For the examples shown in Fig. 3.13 such values for C and B were chosen that:

- average pellet size at steady state is 3.3 mm
- the duration of the fast growth regime was about 60 minutes which is representative for the experiments with Al-silicate powder.

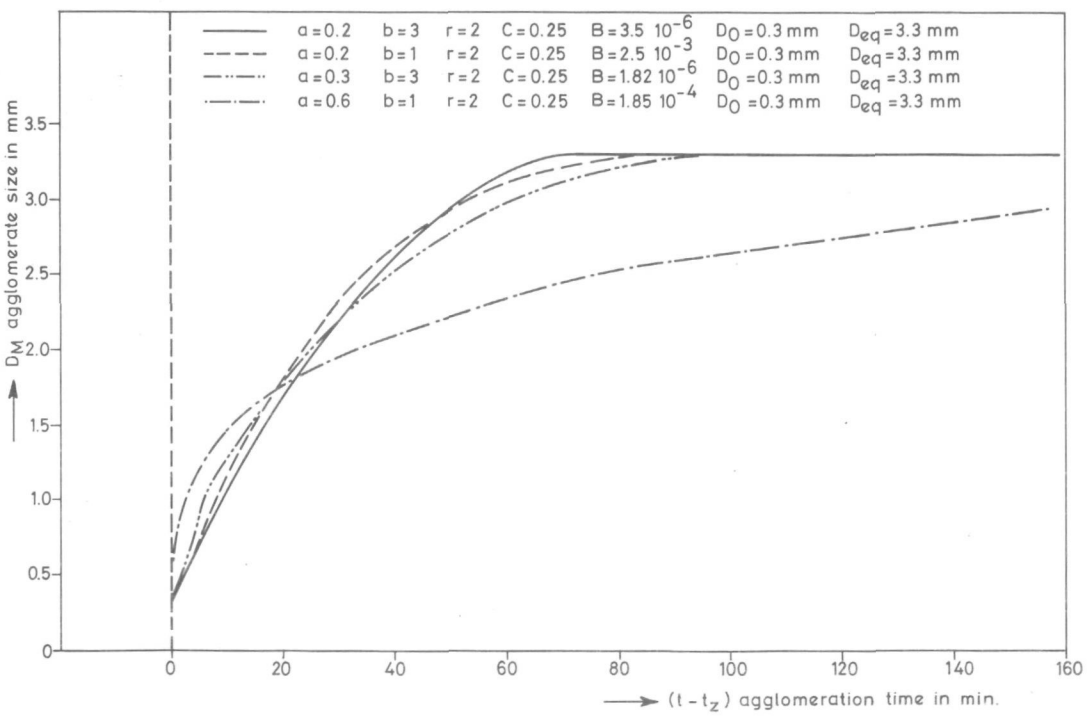

Fig. 3.13 Increase of mean agglomerate size with agglomeration time as predicted by the coalescence-breakage model for some values of the parameters a and b.

Fig. 3.13 shows that a steady state solution is predicted. The shape of the growth curve agrees rather well with experimentally determined growth curves for a value of a in the order of 0.2. When a = 0.6 is tried, the predicted shape does not correspond with the experimental shape. For the latter a value the slope of the curve at $t-t_z = 0$ is too steep compared with the long time needed to reach steady state size. It is further shown that the shape of the curve is not sensitive to the value of b. Changing b from 1 to 3 (For a discussion on b = 3 we refer to chapter 4), hardly effects the growth curve.

In order to explain the observed differences in maximum growth rate between Al-silicate and glass powder pellets, we made some example calculations, showing the effect of the C and B values on the duration of the fast growth regime (t_F). The values of C and B (see Table 3.1) were chosen in such a way that the predicted t_F values were 60, 20 and 10 minutes. These are typical values for respectively Al-silicate pellets and pellets grown from glass powder no. 1 and no. 3.

Table 3.1 Comparison of the length of the fast growth regime and C, B, $R(x,\bar{x})$ and $B(x)$.

C *)	B *)	$R(x,\bar{x})$ **)	$B(x)$ **)	t fast growth (min)
$2.5\ 10^{-1}$	$3.5\ 10^{-6}$	$1.5\ 10^{-1}$	$2.25\ 10^{-4}$	60
$7.5\ 10^{-1}$	$10.5\ 10^{-6}$	$4.5\ 10^{-1}$	$6.75\ 10^{-4}$	20
$15.0\ 10^{-1}$	$21.0\ 10^{-6}$	$9.0\ 10^{-1}$	$13.5\ 10^{-4}$	10

*) $\bar{D}$ at steady state = 3.3 mm **) $x = \bar{x} = 4\ mm^3$

a = 0.2 b = 3

The values in the table for $R(x,\bar{x})$ (growth rate) and B(x) (breakage rate) were calculated at about half way the fast growth regime (average size of pellets about 2 mm). Of course when the steady state is reached, growth and breakage rate are about equal.
By comparing the values of $R(x,\bar{x})$ and B(x) in Table 3.1 we see that the slope of the growth curve in the fast growth regime is mainly controlled by $R(x,\bar{x})$. Moreover we see that:

$$\frac{1}{t_F} \sim C \sim B$$

when $\bar{D}$ at steady state is kept constant (which seems reasonable when comparing the Figs. 3.7, 3.8 and 3.9). In fact, we reach the conclusion that the fast growth regime can be described by only two parameters: i.e. a for shape and C for rate. However, the correlation of these parameters with, in particular, pellet properties has to await for a more fundamental understanding of the pellet-pellet coalescence process.

3.7 *Discussion of the fast growth regime*

From the results that are presented in par. 3.6.6, we tentatively conclude that the population balance equation (3.11), which is based on the hypothesis that coalescence and breakage are the relevant mechanisms, is suitable to describe growth rate in the fast growth regime. The shape of the growth curve is predicted correctly (for a = 0.2) and moreover also a steady state solution is reached.
We may add here, already, that in chapter 4 it shows that for a = 0.2 combined with b = 3 also the best fit of the predicted ASD to experimental results is reached. It is further shown that growth rate in the fast growth regime can described by using only two parameters i.e. a and C .

In par. 3.3.3 it is conclusively shown that growth rate only depends on the properties of the particle system. The observed differences in growth rate can be explained by assuming that the resistence factor $\gamma(x,\bar{x})$ in eqn. (3.17) is the rate controlling factor in the coalescence process.
For respectively glass powder 3, 2, 1 and Al-silicate powder, maximum growth rate decreases successively: 0.24, 0.19, 0.13 and 0.06 mm/min. The resistence factor $\gamma(x,\bar{x})$ will be smaller when the deformability of the pellets is higher, implying in that case a higher coalescence rate. Indeed, deformability of the pellets decreased successively when glass powder 3, 2 or 1 was used. The deformability of Al-silicate pellets was even lower*) than for glass-powder pellets; Al-silicate pellets were more irregular and clusters of incompletely coalesced pellets could easily be observed. In this way, the differences in growth rate are mainly to be attributed to differences in deformability of the pellets, and it becomes evident that only particle properties and not operating variables, e.g. BSR and power input,control the maximum growth rate.
The size desitribution of the initial particles as well as their shape do influence pellet growth.
Considering, however, the characteristics of the particles, see table 2.1, no clear correlation with growth behaviour can be deduced. Apparently, the particle properties have to be determined in more detail before a quantitative understanding of the effect of particle properties on growth behaviour is reached.

*) In general, the degree of saturation S for Al-silicate pellets was about 0,75 which is relatively low compared with S ≈ 1 for glass powder pellets.

CHAPTER 4

Steady state pellet size and size distribution

4.1 *Introduction*

Agglomerates or pellets obtained from batch agglomeration, can be characterized by for instance their mean size, size distribution, strength, porosity and degree of saturation of their pores. These factors are of great concern to product quality and to the ease of dewatering and separation of the product [36]. Another factor that is important in practice is the agglomeration efficiency, i.e. the fraction of fine particles transformed into pellets. However, since in all our experiments an efficiency close to 100% was reached, it will not be discussed further. Thus far, the most striking property, the average pellet size at steady state, received hardly any attention in literature. Swanson et al [36] quite speculatively state that "agglomerate size is controlled by the balance between agglomerate strength determined by capillary forces and the destructive forces determined by the shear regime". In this chapter we will first investigate factors that determine maximum pellet size, i.e. pellet strength and pellet breakage. It will also be attempted to identify which of the forces in the stirred system may cause destruction of pellets. Secondly, the pellet size distribution will be discussed.

4.2 *Mechanisms responsible for the development of the steady state regime*

4.2.1 *Introduction*

The existance of a steady state in growth kinetics was shown by the experiments described in chapter 3. It was also shown that by adopting pellet breakage, a steady state size is predicted when $R(x,\bar{x}) \simeq B(x)$. Here, we will experimentally show that, at least for most experimental systems used in this study, breakage of pellets occurs.
Hence, before discussing other mechanisms responsible for limiting the pellet size, we will first deal with the assumption that in a stirred vessel the conditions are such that:

- a pellet can be broken into parts;
- a liquid bridge connecting two pellets can be ruptured.

4.2.2 *Pellet strength*

The degree of saturation (S) is in our experiments in general well above 0,7 and therefor capillary pressure in the voids of the pellet is the major adhesion mechanism, at least for the low viscosity binding liquids as were used in this study.

For the capillary state (S > 0,7), Newitt and Conway-Jones [75] found for sand particles with a narrow size distribution:

$$k = \frac{F_b}{D^2} = 0{,}7 \cdot S \cdot p_c \qquad (4.1)$$

where k = strength factor (N/m^2)
F_b = pellet breaking load (N)
D = pellet diameter (m)
S = degree of saturation
p_c = capillary pressure (N/m^2)

Maximum pellet strength was experimentally found to occur when the pellets are almost completely saturated. The capillary pressure for $S \rightarrow 1$, the "entry-suction", may be calculated as follows:

$$(p_c)_{S \rightarrow 1} = K \frac{(1-\varepsilon)}{\varepsilon} \cdot \frac{\gamma}{d} \qquad (4.2)$$

where γ = interfacial tension (N/m^2)
ε = porosity
d = particle surface mean diameter (m)
K = constant

Eqn. (4.2) is valid for a bed of randomly packed, irregular particles with a narrow size distribution.
We will assume that p_c is more or less independent of S and equals the value at $S \rightarrow 1$.

$$p_c \simeq (p_c)_{S \rightarrow 1} = \text{constant} \qquad (4.3)$$

When combining eqns. (4.1) and (4.2) we obtain for the strength factor:

$$k = K' \cdot \frac{(1-\varepsilon)}{\varepsilon} \cdot \frac{\gamma}{d} \qquad (4.4)$$

For sand particles a value of the constant K' of 5,6 was found [75]. Rumpf [97] evaluated for limestone particles 6,1 as the constant.

Further, it can be shown that the strength factor in eqn. (4.4) is approximately equal to the tensile strength. In the capillary pressure regime is

$$k = \frac{F_b}{D^2} = \sigma_D \cdot \frac{\pi}{4} = 0{,}78\, \sigma_D \qquad (4.5)$$

Rumpf [97] could relate the pressure strength σ_D and the tensile strength as follows:

$$\sigma_t = 0{,}77\, \sigma_D \qquad (4.6)$$

so that

$$k \simeq \sigma_t \qquad (4.7)$$

Subsequently, the solid and dotted lines in Fig. 4.1 can be constructed, taking into account that the strength-factor k is of course zero for completely saturated pellets (S = 1). The solid lines give the dependence of k on S for a particle size d of respectively 5, 10 and 20 μm, while the dotted lines illustrate the effect of pellet porosity ε. Experimentally determined ε-values are:

glass powders : $\varepsilon \simeq 0{,}30 - 0{,}32$
Al-silicate : $\varepsilon \simeq 0{,}40 - 0{,}42$

The degree of saturation that can be calculated from the BSR and the measured ε-values are:

glass powders : $S \simeq 0{,}95 - 1{,}06$
Al-silicate : $S \simeq 0{,}72 - 0{,}78$

We have determined experimental k-values by crushing a pellet between two parallel flat plates and the maximum load before breakage was recorded (method described by Vervoorn [128]). The shaded area's represent the range of measured k-values; for S also a range was adopted in consequence of the difficulties mentioned in par. 2.7 with respect to determining accurate S-values.

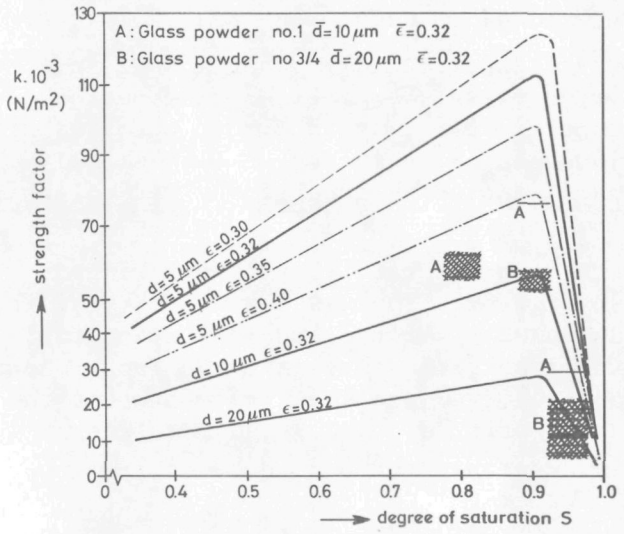

Fig. 4.1 Comparison of experimentally determined and by the capillary pressure model predicted strength factors.

The experimentally determined k-values agree fairly well with the values predicted by the capillary pressure-model*). However, the existing theoretical models as well as the experimental k-values have limited importance for predicting breakage phenomena quantitatively. First of all, one has to realise that forces induced on the pellet in a stirred vessel last only in the order of magnitude of micro or milli-seconds, while in the crushing test the breakage load was slowly increased during minutes. (For the much larger iron-ore pellets the resistance to fracture by impact is generally assessed by the "drop test"). Further, Schubert [100] showed that the ability of a pellet to deform increases considerably when S increases from S = 0,7 to S = 0.9. We can expect therefore that pellets with a S-value of 0,7-0,8 will tend to brittle fracture while pellets with S → 1 will tend to break by deformation. Hence, the k-value can only be used for sake of comparison for one breakage mechanism and at the same S-value.

The cohesive force resulting from a liquid bridge was studied extensively by e.g. Schubert [100] for various geometrical systems. For two equally sized spheres, a binding-liquid/solid ratio of 0,4 → 0,5 and complete wetting, the dimensionless cohesive force is:

$$\frac{F}{\gamma.D} \simeq 3 \qquad (4.8)$$

and when one sphere is small compared with the other:

$$\frac{F}{\gamma.D} \simeq 6 \qquad (4.9)$$

where D is the diameter of the smaller sphere.
For two pellets of 2 mm in size or e.g. a 1 mm pellet attached to a 4 mm pellet, we obtain for the cohesive force:

$$F \simeq 2{,}7\ 10^{-4}.N$$

or in terms of tensile strength (eqns. 4.5, 4.7):

$$\sigma_t \simeq 10^2\ N/m^2$$

Hence, it shows that the cohesive force of a liquid bridge is 100 times smaller than the strength of a pellet.

*) When using binding liquids of higher viscosity the model of Wada and Tsuchiga [127] might be used. They extended the capillary model, taking into account both capillary pressure and visco-capillary forces. The effect of binding liquid viscosity was qualitatively confirmed by Roorda et al [6].

4.2.3 Pellet breakage

The breakage rate of pellets can be observed experimentally when a small number (e.g. 20) of pellets is put into the stirred vessel for a fixed time period. The coalescence frequency of a pellet is reduced in this way to almost zero and also breakage caused by pellet-pellet collisions can be neglected. The breakage frequency observed under these conditions is caused by impeller-pellet collisions or liquid-pellet interactions only.

In order to study the liquid-pellet interaction separately, also experiments were carried out in a flow model,(depicted in Fig. 4.2).The issuing velocity of the liquid jets was taken equally to the mean velocity of the liquid leaving the impeller blades (in the stirred vessel experiments).In this way, the local shear rate in the jet (Hinze [129] pag. 432) approximated the shear rate present in the vortex behind the impeller blades in the stirred vessel. The mean energy dissipation however was, as a consequence, only 0,3 (W/kg).

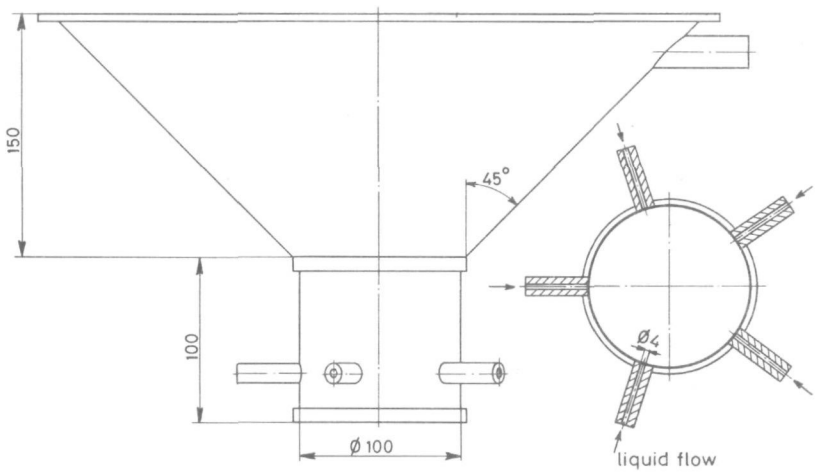

Fig. 4.2 Flow model for breakage experiments.

The increase of the number of particles was observed in the flow model as well as in the stirred vessel whereby in the latter case stirrer speed, stirring time and pellet size were varied. Also pellets grown from different glass powders (1, 3, 4) and ballotini beads were used. It was considered to be not necessary to study experimentally the rupture of a liquid bridge connecting two pellets, since the cohesive force resulting from the liquid bridge is about 10^2 smaller than the strength of a pellet.

A first inspection of the results (compiled in appendix no. III[a]) reveals that pellets grown from glass powder no. 1, do not break even at a stirrer speed of 1650 r.p.m. (normal growth condition was 1250 r.p.m.). Only when the degree of pellet saturation S is significantly lowered, from about 1 to 0,8, brittle breakage occurs (see photograph 4.1). Pellets made of glass powder 3, 4 or ballotini beads did break in the stirred vessel at 1250 r.p.m. Besides parts of pellets that are the results of brittle breakage, also elongated pellets were found (photograph 4.2).
Experiments performed in the flowmodel, also showed an increase of the number of particles with time. Only elongated pellets could be observed,so that here the only mode of breakage is: deformation.

The breakage rates in the stirred vessel and the flow model are compared in Fig. 4.3(a) and 4.3(b). For pellets grown from ballotoni beads (which possess the lowest strength), the breakage rate in the flow model is much smaller than the

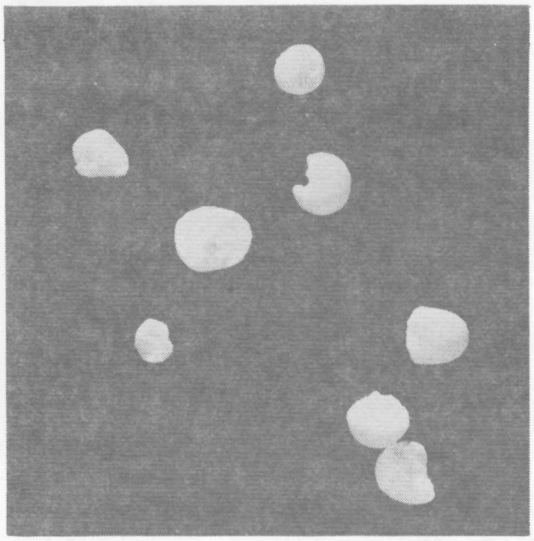

Photograph 4.1 Parts of glass powder pellets: brittle breakage.

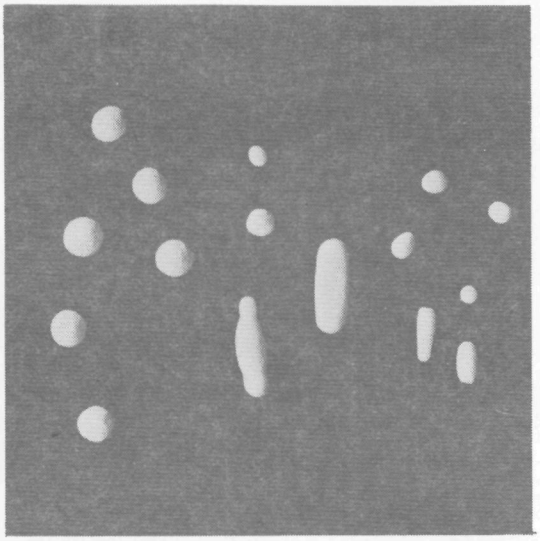

Photograph 4.2 Elongated pellets.

breakage rate in the stirred vessel. For glass powder pellets no. 4 this is only true for the first 5 minutes of the experiments; afterwards the breakage rates are similar. In both cases, no original pellets could be found after 15 minutes. But on the contrary, repeating the experiment with glass powder pellets 3, only 2 or 3 pellets out of 20 appeared to break independently of the applied stirrer speed (Fig. 4.3(d)) and stirring time. A similar result was found in the flow model (exp. no. B6038; $\bar{D}$ = 3.2 mm): also at higher liquid velocities, the total number of particles increased with time while the number of unbroken pellets remained the same again. Apparently, not all pellets are equally strong.

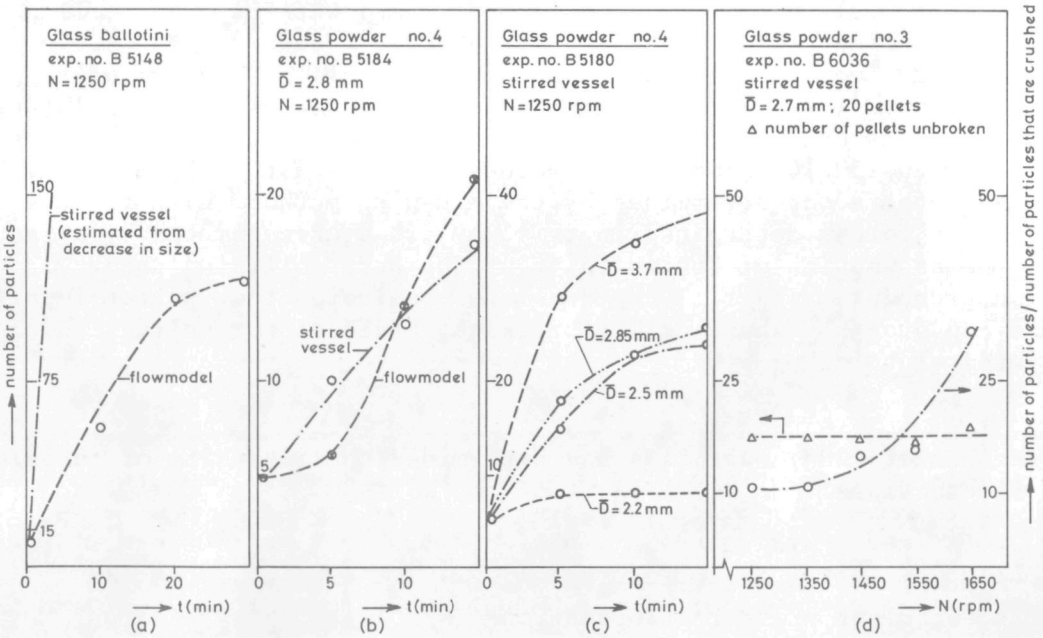

Fig. 4.3 The increase of the number of particles with time for different powders:
(a)+(b) Comparison of the stirred vessel and the flow model;
(c) Effect of pellet size;
(d) Effect of the stirrer speed on the number of unbroken particles and on the ratio of the initial number of particles/number of crushed particles.

The effect of pellet size on the breakage rate is shown in Fig. 4.3(c). It is seen that for pellets larger than 2 mm, the breakage rate increases strongly with pellet size*). In general one can observed that pellets, which are at the beginning of the experiment smaller than 2 mm, do not break at all. This was indeed predicted by the coalescence breakage model on page 41.

Although insufficient data have been collected to quantify the breakage rate in terms of operating variables and pellet properties, we can draw the conclusion that, at least pellets with an initial size larger than 2 mm, break at a power input of 1,5 W/kg. Both brittle breakage and breakage by deformation were observed. In the following paragraph we will investigate which mechanisms can be responsible for the observed phenomena.

4.2.4 Forces acting on agglomerates in a stirred vessel

The force acting on agglomerates in a stirred vessel consists of many different contributions. In general the most relevant ones are:

a. forces as a result of collisions with the impeller, vessel wall or other pellets;
b. forces due to pressure differences across the pellet;
c. shear-rate forces;
d. other forces due to e.g. rotation of the pellet, pellet velocity relative to the fluid, gravity.

ad a:

As already stated in par 2.6 it is rather impossible to evaluate theoretically the impeller-pellet impact force, even if only an order of magnitude answer is required. In particular, the velocity at the moment of impact as well as the variation of the elastic modulus of an agglomerate during its growth, are highly uncertain factors. Therefore, we attempted to measure the impact force of pellet-impeller collisions, using the method described in par. 2.6. Both pellets grown from glass powder 1 and 4 ($D_M \simeq 3$ mm) were used and collision response curves were recorded. The applied stirrer speed was 1250 r.p.m. The determined maximum collision force, i.e. the value of the maximum of the collision response curve (Fig. 2.15), ranged from 8,5 → 22 N. If we translate these values in terms of the strength factor, we obtain the following corresponding values: 95.10^4 to 250.10^4 N/m^2. These values are at least a factor 10 higher than the strength factor determined by the crushing method. Even if we assume that the impact forces determined in this way are over-estimated by a factor 2 (due to the assumption of the validity of the Herz collision theory in the calibration procedure) we still can draw the conclusion that pellet-impeller collisions can probably cause pellet breakage, at least for pellets which may be considered elastic.

ad b:

Uberoi (see Hinze [120], page 243) has determined the intensity of turbulent pressure fluctuations:

$$p' = 0{,}7 \cdot \rho \cdot U'^2 \qquad (4.10)$$

where p' = turbulent pressure fluctuations (N/m^2)

ρ = density (kg/m^3)

$U' = \sqrt{\overline{U}^2}$ = root mean square value of turbulent velocity fluctuations (m/s)

*) Close inspection shows that $B \sim D^3$, which agrees surprisingly well with the derived eqn. 3.28[a].

For pellets of a size within the inertial subrange of an isotropic turbulent flow $(2.10^{-5}\text{m} < D < 7.10^{-3}\text{ m})$

$$U'^2(d) = 1.88\,\varepsilon^{2/3}\,d^{2/3} \qquad (4.11)$$

where

d = scale of energy dissipation (m)

ε = energy dissipation per unit mass (W/kg)

When we consider an agglomerate of $\bar{D} = 4.10^{-3}$ m, suspended in carbontetrachloride, at an energy dissipation level of $\varepsilon = 1{,}5$ W/kg, the turbulent pressure fluctuations are estimated to be:

$$p' \simeq 55\ \text{N/m}^2$$

This value is small when compared with pressure differences in the impeller vortex*) or with the related centrifugal acceleration, which are in the order of magnitude of 5.10^4 N/m^2 acting over a distance of about 3 mm, i.e. the average pellet size [130]. Since the pellet strength factor, measured by means of the crushing test, is $5.10^3 \rightarrow 60\ 10^3$ N/m^2, it is quite well possible that pressure differences in the vortex behind the impeller blades contribute to pellet breakage.
Moreover, a pair of pellets connected by a liquid bridge can be separated easily by the pressure differences over the agglomerate, since the force which tends to hold the two-pellets together is of the order of 50 N/m^2 (eqn. 4.8) for 3 mm pellets).

ad c:

The size of the shear stress is given [130] as:

$$\tau = \mu.s \qquad (4.12)$$

τ = shear stress (N/m^2)

μ = dynamic viscosity (Ns/m^2)

s = shear rate (1/s)

The shear rate s is again relatively high in the vortex behind the stirrer blades when compared with the shear rate in the bulk of the liquid. The average shear rate in the vortex at:

$$Re = \frac{\rho\ N\ D_T^2}{\mu} \simeq 2.10^4 \qquad (4.13)$$

where

N = stirrer speed (1/s)

D_T = impeller diameter (m)

as is valid for our experimental conditions, was

$$s \simeq 90\ .\ N \qquad (4.14)$$

*) This presents interesting consequences for scale-up, since the pressure difference relevant for a pellet depends strongly on the distance in which the pressure difference is realised and therefore on the impeller size. Hence, for larger impellers the pressure differences relevant for the pellets can be much smaller, so that the steady state size can be larger.

Therefore the shear stress, calculated from eq. 4.12 and 4.14 for N = 20 1/s and $\mu = 1.6\ 10^{-3}$ (Ns/m^2), is quite small: $\tau \simeq 3$ N/m^2.

Also the maximum force exerted on a pair of pellets as a result of shear or elongational flow can be derived [131]

$$F = c_1 \mu \cdot s \cdot D_1 \cdot D_2 \qquad (4.15)$$

where $D_1 D_2$ are the diameters of the single pellets (m) and

c_1 can range from $\frac{3\pi}{4}$ for shear flow to $\frac{3\pi}{2}$ for elongational flow.

From this $\frac{F}{D^2} = 6{,}8$ N/m^2 is again smaller than the force which hold the pellets together so that we have to assume that in the stirred vessel, pressure differences and not shear forces cause pellet breakage by deformation.
When we consider the deformation of pellets that occurred in the flow model, it will be clear that also this is not due to shear forces. But it is also difficult to explain the breakage phenomena in the flow model as a result of pressure differences. Comparison of the work of Hinze [129] (page 429) and van 't Riet [130] shows that the static pressure differences in a free jet are a factor 50 less than those observed in the impeller vortex (at corresponding liquid velocities). Therefore the pressure differences in the flow model are in the order of 10^3 N/m^2 which is smaller than the pellet strength factor of $5.10^3 - 60.10^3$ N/m^2.

ad d:

In general we may assume that these factors can be neglected in comparison with pellet strength.

4.2.5 Other mechanisms responsible for steady state size

Besides pellet breakage, two other observations are relevant in this respect:

- when steady state is reached, pellets removed from the vessel either have a dry appearance or they are still coated with a layer of binding liquid, so that in the latter case coalescence is still possible.
- in some experiments pairs or triplets of pellets exist, even if steady state is reached.

In consequence of the above observations we consider it reasonable that the following mechanisms may also be responsible for limiting the pellet size:

a. insufficient binding liquid is available at the surface of the pellet to establish pellet-pellet contact so that in eqn. (3.17) $\beta(x,x) \simeq 0$ and therefore $R(x,\bar{x}) \to 0$.
   or
b. $\gamma(x,\bar{x})$ (see eqn. 3.17) is large, so that the bridge between two pellets is not filled up with solid particles. Hence the force that tends to hold the pellets together is not sufficient to withstand destructive forces near the impeller; coalescence is then prevented, so that again $R(x,\bar{x}) \to 0$.

In both cases also B(x) should be small.

4.2.6 Discussion

Resuming, we find that two mechanisms are responsible for the development of a steady state regime i.e.

(1) $R(x,\bar{x}) \to 0$
    with either a) $\beta(x,\bar{x}) \simeq 0$
                b) $\gamma(x,\bar{x}) \simeq 0$
(2) $R(x,\bar{x}) \simeq B(x)$

The latter mechanism (2) can clearly be observed for glass powder no. 3. Pellet breakage is proved to occur and the growth curves in general show a slow decrease in size when the steady state regime is reached. Moreover, Fig. 3.8a shows that the average pellet size at steady state increases with decreasing stirrer speed. For the other powders that were used, it is more difficult to indicate the responsible mechanism, since no independent experiments were carried out. But since for Al-silicate, relatively low values for the degree of saturation were measured ($S \simeq 0{,}75$) and in addition the pellet appearence was always dry, probably mechanism (1a) $[\beta(x,\bar{x}) \rightarrow 0]$ will be involved. On the other hand, pellets grown from glass powder 1 or 2 often had a wet appearence while S-values of 1,0 to 1,1 are typical for this system. Hence, in these systems mechanism (1b) may cause the steady state.

The introduction of a breakage term in the population balance equation (3.11) shows to be valid when mechanism (2) occurs. But, even when mechanism 1b is more likely to limit pellet size, one can still use the same mathematical formulation as used in eqn. (3.11). The separation of a pair of pellets, which have not completely coalesced, can be described, in mathematical terms, as the breakage of one pellet into two parts.

4.3 *Agglomerate size distribution*

4.3.1 *ASD at steady state*

Agglomerate size distributions were determined for all experiments, using the image analysing method, described in par. 2.7. For those experiments for which growth curves were presented in chapter 3, the ASD's at steady state are compiled in Figs. 4.4, 4.5 and 4.6. Figure 4.4 shows ASD's of 5 experiments carried out under identical conditions. Figs. 4.5 and 4.6 give ASD's for Al-silicate powder, $CaCO_3$ powder as well as for the glass powders 1, 2 and 3. Different operating variables are included such as binder-solid ratio , stirrer speed, solid concentration and the stirrer speed at which the binding liquid was emulsified.

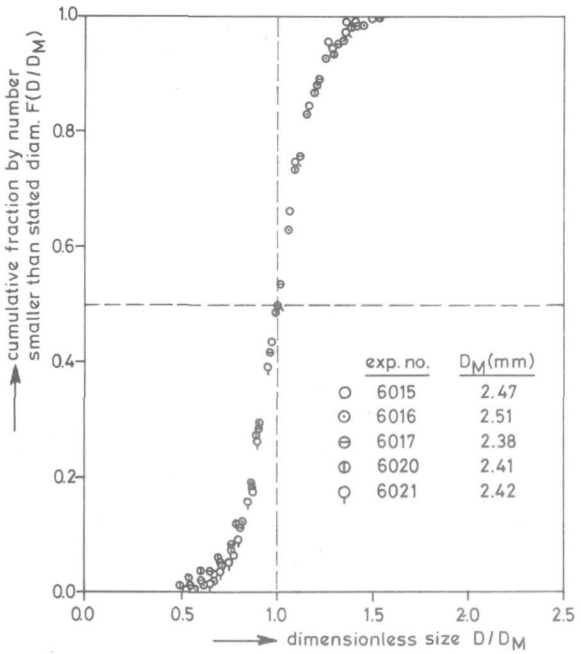

Fig. 4.4 ASD at steady state for 5 experiments carried out under identical conditions.

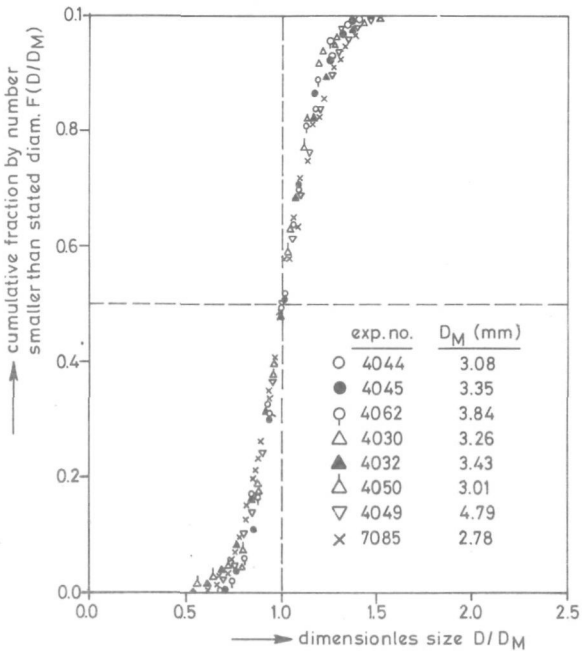

Fig. 4.5 Effect of different operating conditions and model systems on ASD at steady state.

Since the scatter of the data in all three plots is similar, it may be concluded that when a batch experiment has reached its steady state, the resulting dimensionless ASD is identical for all operating conditions as well as independent of system properties. So, from the results presented above, we may expect that the ASD for steady state pellets can be represented with sufficient accuracy by the solid curve in Fig. 4.7. It shows that the dimensionless pellet size D/D_M in general ranges between 0,6 and 1.4.
Experiments carried out in rotating granulation drums, showed the same phenomenon, except that the measured granule size distributions were somewhat wider: $0.5 < D/D_m < 1,5$ [86].
The ASD at steady state also follows from the coalescence-breakage model developed in chapter 3. At steady state,

$$\frac{\partial n(x,t)}{\partial t} = 0$$

so that eqn. (3.11) can be rewritten as follows:

$$n(x) = \frac{1}{r^2 B(x)} \left[B\left(\frac{x}{r}\right) n\left(\frac{x}{r}\right) - \tfrac{1}{2} \int_0^{\frac{x}{r}} R\left(\frac{x}{r} - \bar{x}, \bar{x}\right) n\left(\frac{x}{r} - \bar{x}\right) n(\bar{x})\, d\bar{x} + \int_0^{\infty} R\left(\frac{x}{r}, \bar{x}\right) n\left(\frac{x}{r}\right) n(\bar{x})\, d\bar{x} \right] \quad (4.16)$$

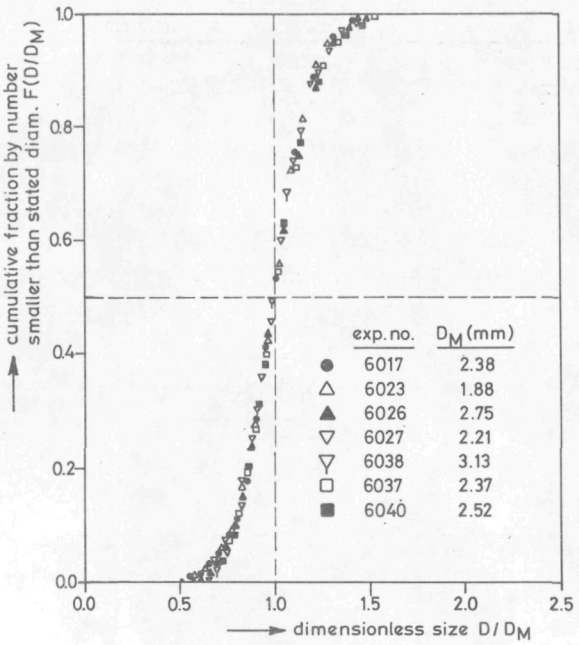

Fig. 4.6 Effect of different operating conditions on ASD at steady state.

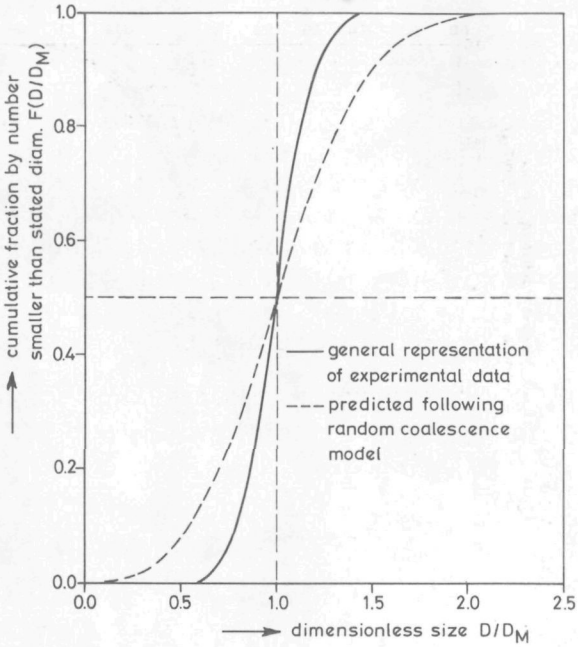

Fig. 4.7 Comparison of experimental ASD at steady state with ASD predicted by random coalescence model.

A numerical technique was used that employed an adaptive integration method and a piecewise cubic interpolation routine on a logarithmic equi-distant mesh. Starting with a reasonable value for n(x) at $x << 1$, this value was iteratively improved in order to satisfy the constraint of conservation of mass:

$$\int_0^\infty x^k \cdot n(x)\, dx = 1 \qquad (4.17)$$

with $k = +1$ and $k = -a$.

The results of the computation are presented in Fig. 4.8, showing the influence of the parameters a and b, that were defined in respectively eqn. (3.19) and (3.29):

$$\text{coalescence frequency } R(x,\bar{x}) \sim \frac{1}{(x\bar{x})^a}$$

$$\text{breakage frequency } B(x) \sim (x)^b$$

The parameter r was defined in eqn. 3.11 as the number of parts into which a pellet breaks. The computed ASD's tend to get narrower with increasing a and/or b or with decreasing r.
From the comparison of the model solutions with representative experimental data (Fig. 4.9) it follows that when b = 1, an acceptable fit can only be obtained for a value of a as high as 2.5. In par. 3.6.6 it was, however, already concluded that a should be about 0.2. If we also adapt this value here, then, as shown in Fig. 4.9, the combination of a = 0,2, b = 3 and r = 2 provides an excellent fit of the predicted ASD with experimental data. We should remark that for a value of b = 3, the influence of a on the predicted ASD becomes less significant, as shown in Fig. 4.8 (compare b = 3, a = 0,2 and b = 3, a = 0,6).

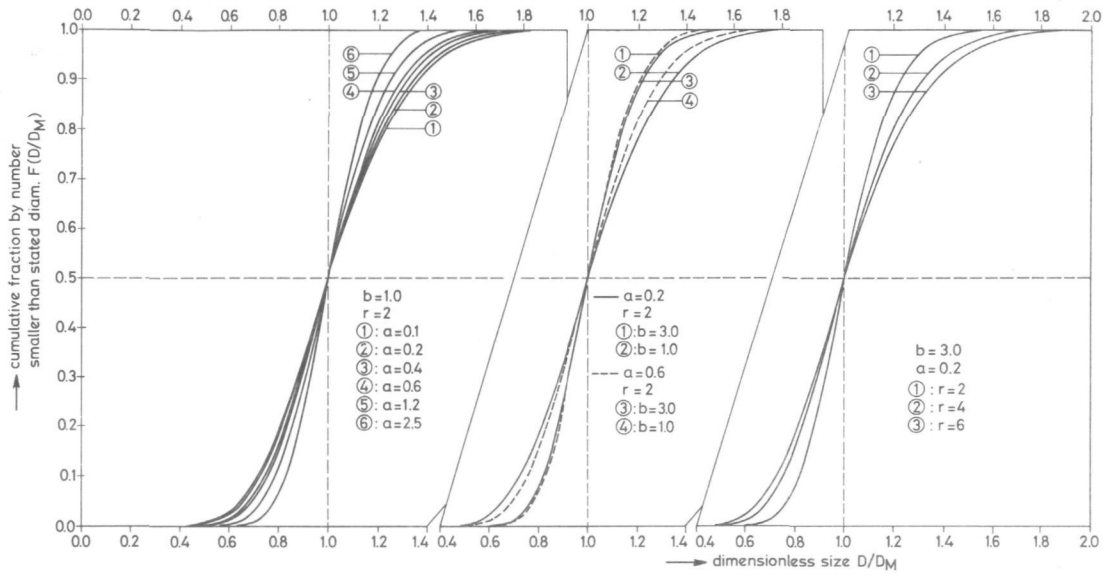

Fig. 4.8 ASD's at steady state predicted by coalescence breakage model.

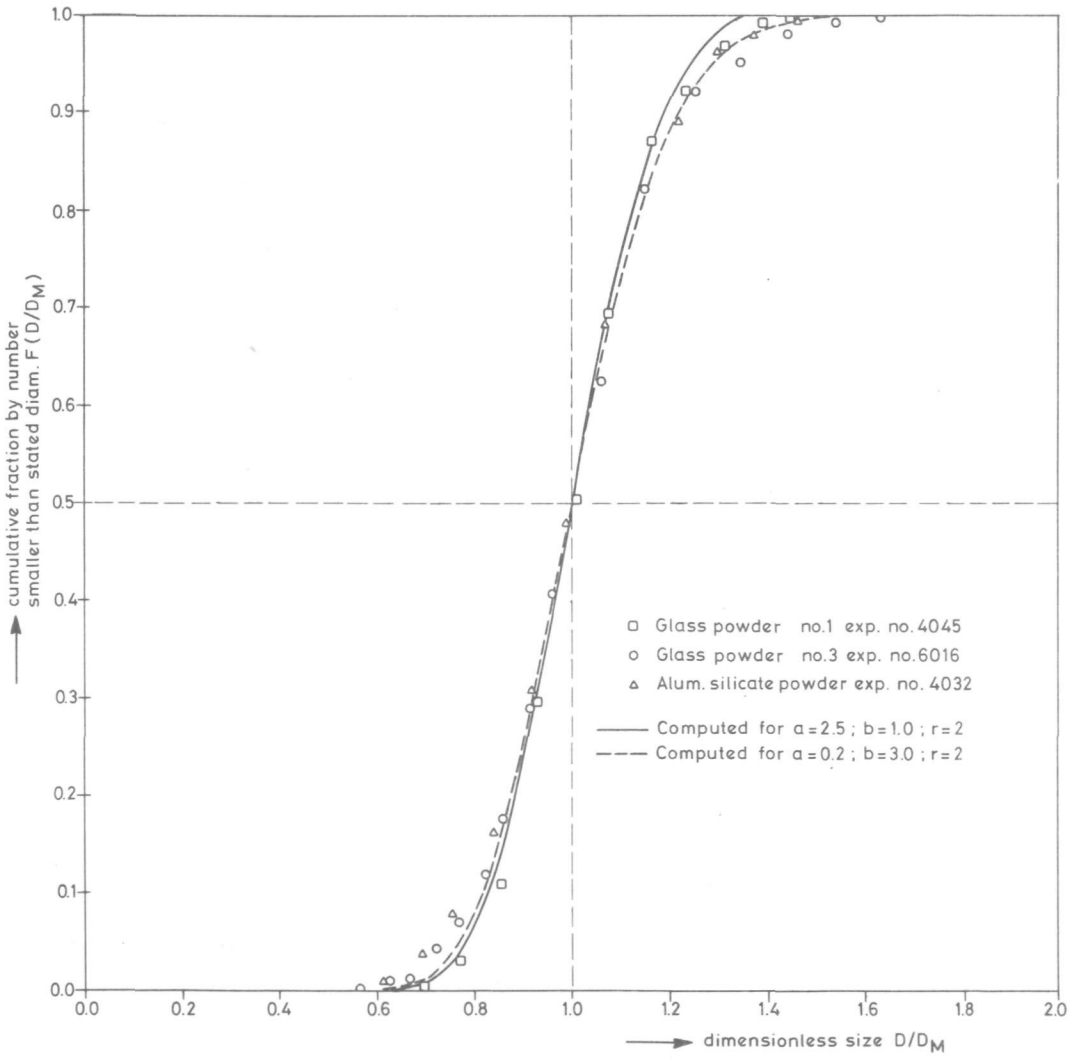

Fig. 4.9 Comparison of experimental ASD's at steady state with ASD's predicted by coalescence-breakage model.

Assuming that pellet-impeller collisions in the main breakage mechanism, it is shown in par. 3.6.5 that b should be about 1. This was more or less confirmed in par. 4.2.3. However, from the above presented simulations we find that $b \simeq 3$*). We further assumed that $r \simeq 2$, since for $r > 2$ the required value for b becomes even higher than 3. Apparently the assumptions made, mainly with respect to a simple functional form for the coalescence frequency and the pellet breaking into r equal parts, need further consideration.
Nevertheless, even this simplified model can explain the relative insensitivity of the ASD with respect to system properties and operating conditions. The predicted form of the ASD is only dependent on r and the parameters a and b in eqn. (3.19) and (3.29) and not on the absolute values of $R(x,\bar{x})$ or $B(x)$. From the evaluations made in par. 3.6.4 and par. 3.6.5 it is not to be expected that the parameters a and b will strongly depend on operating variables and system properties. In this way one solution for the ASD at steady state is predicted, in general irrespectively of the used system or variations in operating variables.

4.3.2 Time evolution of ASD

As mentioned in par. 3.2, most of the literature on the time evolution of size distributions is concerned with the concept of "self-preserving size spectra". If a size distribution is self-preserving, it implies that there exists only one unique curve for the size distribution, if plotted in terms of an appropriate dimensionless size (e.g. D/D_M). The obtained distribution will be independent of the size distribution of the initial particles and time. To account for experimental observations of the particle size distribution of stratospheric aerosols, that tended to show a self-preserving behaviour, a similarity theory was developed [132], which was further used to predict size distributions of hydrosols [106], coagulating colloids [107], metal catalysts [133] and granulation [92].
The basic assumption is that the size-distribution function can be expressed as follows:

$$n(x,t) = \mu(t) \cdot \psi(x,\xi(t)) \qquad (4.18)$$

$$= \mu(t) \cdot \psi(\eta) \qquad (4.19)$$

where $\mu(t)$ and $\xi(t)$ are functions only depending on time t.
It is shown that for some simple functions of the coalescence frequency $R(x,\bar{x})$ the dependence of the size distribution can be represented by only two variables:

$$\eta = \frac{N.x}{\phi} \qquad (4.20)$$

and

$$\psi(\eta) = \frac{n(x,t).\phi}{N^2} \qquad (4.21)$$

where

$$N = \int_0^\infty n(x,t)\, dx \qquad (4.22)$$

and

$$\phi = \int_0^\infty x\, n(x,t)\, dx \qquad (4.23)$$

*) In a recent publication [139] on agitated liquid-liquid dispersions a breakage model for droplets is proposed. It is assumed that the droplets break due to their oscillations that result from relative velocity fluctuations. The breakage probability is predicted as $\sim (x/x_s)^{8/3}$, where x_s is the maximum stable drop volume.

If we use equation (3.8) as an example, it may be reduced to:

$$M\left[\eta\frac{d\psi(\eta)}{d\eta} + 2\psi(\eta)\right] + \int_0^\infty R(\bar{\eta},\eta-\bar{\eta})\psi(\bar{\eta})\psi(\eta-\bar{\eta})\,d\bar{\eta}$$

$$- 2\int_0^\infty R(\eta,\bar{\eta})\,\psi(\eta)\psi(\bar{\eta})d\bar{\eta} = 0 \qquad (4.24)$$

where

$$M = \int_0^\infty\int_0^\infty R(\eta,\bar{\eta})\psi(\eta)\psi(\bar{\eta})\,d\eta d\bar{\eta} \qquad (4.25)$$

The solution of eqn. (4.24), being an ordinary integro-differential equation, is semi-invariant with time and only depending on $R(\eta,\bar{\eta})$.

In the field of granulation it has been tried to prove the hypothesis of self-preserving size spectra experimentally. Although superficially seen the ASD, in terms of D/D_M, is not depending on operating conditions, it should be pointed out that with respect to the time evolution this is questionable. A closer inspection of the data presented by Kapur [86] and further evaluated by Ruckenstein [21], consistently shows a systematic narrowing of the size distribution as granulation time proceeds. Therefore, we may consider the experimental proof of the self-preserving concept as insufficient.

The time evolution of the agglomerate size distribution in this work was evaluated by solving the complete population balance equation 3.11 with respect to both particle volume x and time t. The computation of eqn. 3.11 was performed following a for this purpose developed numerical method. This method is described by Sonneveld and Bemer [134] and shortly summarized in appendix II. An experimentally determined size distribution of pellets in the zero-growth regime (D_M = 0,4 mm) was taken as the initial size distribution at t = 0. Some preliminary calculations were carried out of which an example is given in Fig. 4.10 This figure shows that when the agglomeration process proceeds, the ratio of largest to smallest pellet diameter decreases. The coalescence-breakage model, therefore, does not predict self-preserving growth, but a narrowing of the dimensionless size distribution with time.

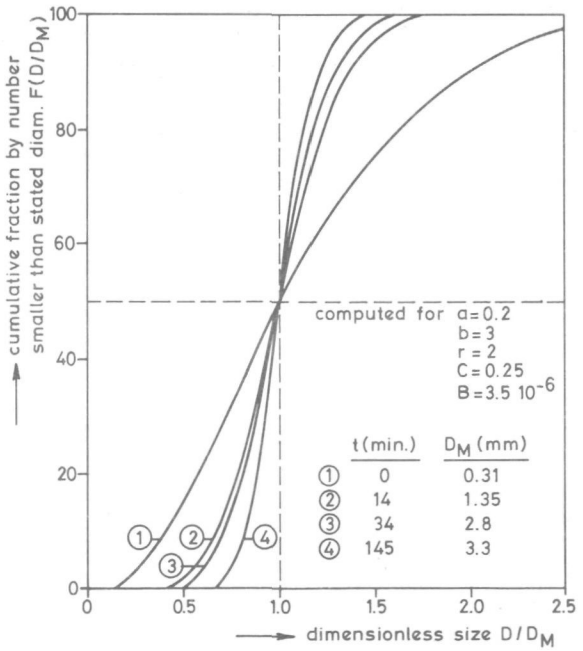

Fig. 4.10 Evolution of ASD in time as predicted by coalescence-breakage model.

The described method of solving the population balance eqn. 3.11 with respect to time, eventually also produces a steady state solution. For a fixed set of the parameters a, b and r, it could be established that the in this way obtained steady state solution was identical to the solution calculated with the steady state method described in par. 4.3.1.

In order to obtain experimental data for the time evolution of the ASD, two different methods were followed:

a. During a batch growth experiment the stirrer was switched off so that the growth process was interrupted. Subsequently, about 1/3 of the pellets were removed from the vessel and photographed.

After putting these pellets back again into the vessel and starting the stirrer, the growth process was continued. By repeating this procedure after certain time intervals, an impression of the time evolution of the ASD was obtained.
Some typical results are plotted in Fig. 4.11 and 4.12. It was checked that the in this way obtained growth curves were identical to those where the experiment was not interrupted.

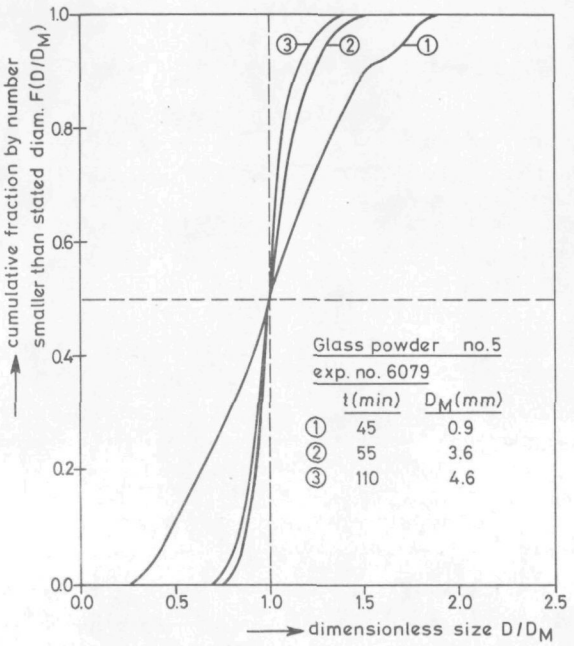

Fig. 4.11 Evolution of ASD in time: experimentally determined following method a).

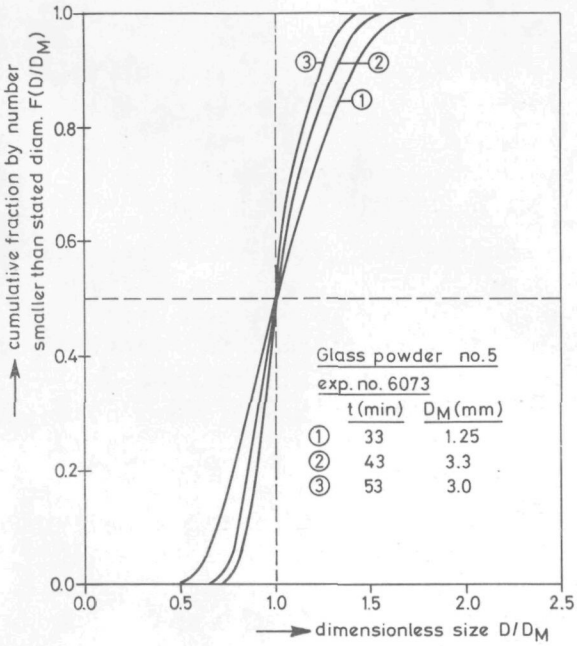

Fig. 4.12 Evolution of ASD in time: experimentally determined following method a).

b. Another method is based upon the conclusion reached in Chapter 3 (and clearly illustrated in Fig. 3.7), that the amount of binding liquid has an effect merely on the duration of the zero-growth regime. Increasing the amount of binding liquid, reduces the time after which the fast growth regime starts, but within the fast growth regime the form of the growth curve seems to remain unchanged.Therefore, we consider e.g. the ASD's of the experiments no. 4034, 4033 and 4031 (Fig. 3.7d), determined at t = 180 minutes as representative for the ASD's at respectively 45,90 and 180 minutes of the single experiment 4031 (see Fig. 4.13). A similar procedure can also be followed with respect to the experiments 4061, 4064 and 4062 (Fig. 3.7b) and to a lesser extent with 6012, 6014 and 6020 (Fig. 3.7c).
Two examples hereof are presented in Fig. 4.14 and 4.15. These data, together with those presented in Fig. 4.11 and 4.12 show that the ASD gets narrower when the agglomeration process proceeds. This phenomenon is indeed predicted by the coalescence-breakage model.

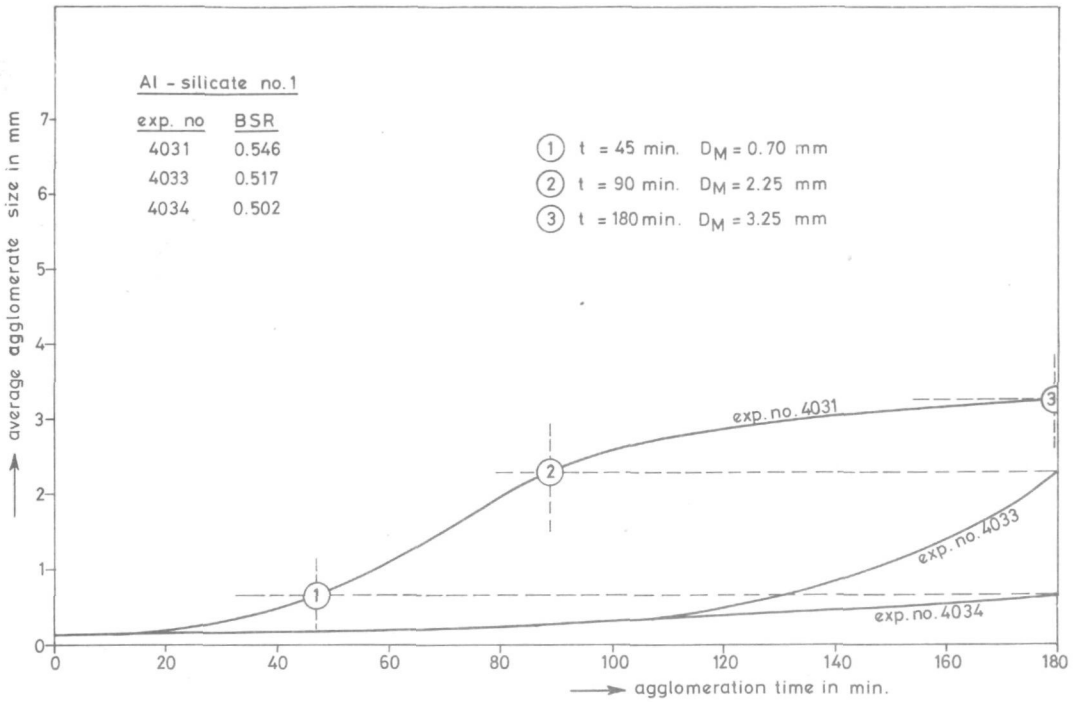

Fig. 4.13 Comparison of the experiments 4031, 4033 and 4034.

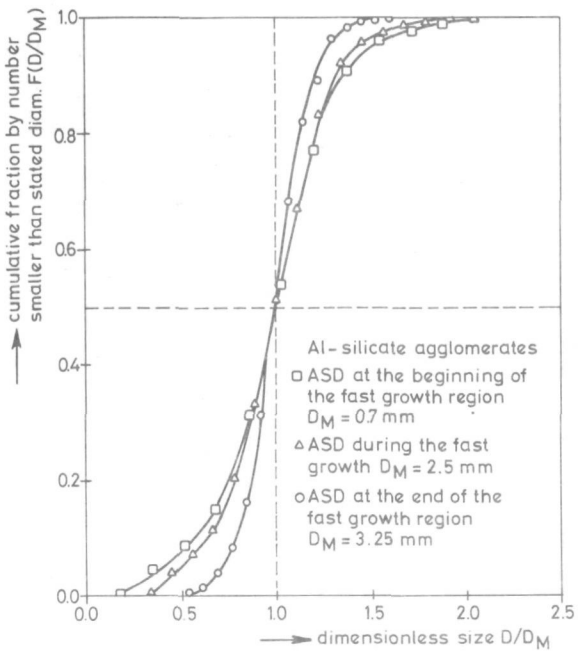

Fig. 4.14 Evolution of ASD in time: experimentally determined following method b).

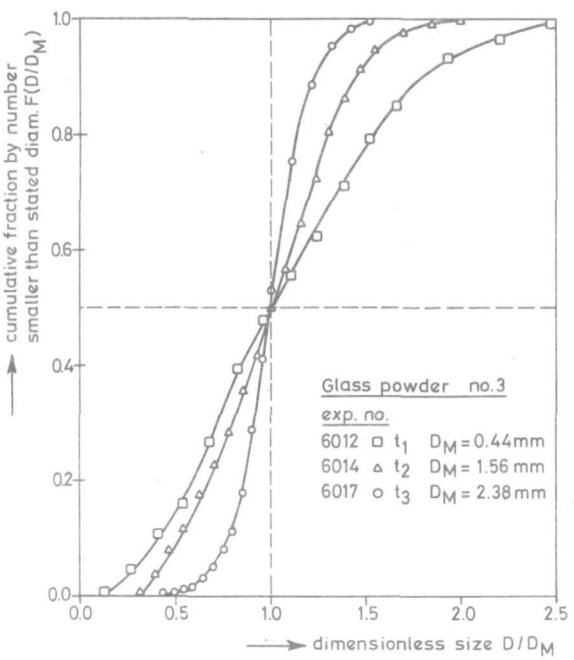

Fig. 4.15 Evolution of ASD in time: experimentally determined following method b).

CHAPTER 5

A preliminary study on a continuously operating pelletizer

5.1 *Introduction*

Previous chapters were concerned with mechanisms and kinetics in batch operated pelletizers. It was found that agglomerate growth takes place by the mechanisms of coalescence and breakage. During the growth process three distinct regimes are subsequently passed through i.e. the zero-growth regime, the fast growth regime and the equilibrium regime. In particular the first regime, where the increase of the mean pellet size is almost zero, can extent the required agglomeration time to several hours. Of course, this will be hardly acceptable when large-scale, commercial operation is considered. But, in this case continuously operating equipment will be used and kinetics hereof may be different. It is important therefore to establish to what extent the zero-growth regime, as identified for batch agglomeration, determines residence time in continuous agglomeration.

In case the slurry proceeds through the pelletizer in plug flow, the required residence time for the continuous systems equals of course the batch agglomeration time. But, when the solid residence time is higher than the liquid residence time ($\tau_s/\tau_l > 1$, high pellet hold-up) the situation becomes much more complicated (advantages of a high pellet hold-up will be outlined in the following). When $\tau_s/\tau_l > 1$, the feed particles will follow the liquid trajectories, whereas the established pellets will be held back. In this way the feed particles and the pellets will have different residence times. Consequently, they are present together at one place. One may consider this to be the main difference with batch pelletizing. Since feed particles come into contact with established pellets, layering of the feed particles onto the pellets becomes possible and this may contribute, next to coalescence, to agglomerate growth. The conditions whereby the mechanism of layering occurs are identified by the experiments described in par. 3.4, p. 31. To a batch of growing pellets, an additional amount of powder was added (20 wt.%) without adding extra binding liquid. It was conclusively shown that layering only occurs when the surface of the pellet contains sufficient binding liquid; the feed particles are most easily absorbed during the fast growth regime.

A consideration of the layering growth mode suggests that the rate of layering is simply proportional to the exposed surface area of the agglomerates and thus also to the pellet hold-up [135]. But there are more arguments in favour of a high pellet hold-up. In general, it was shown in chapter 3 that the required agglomeration time decreases considerably at higher pellet hold-up (h). In fact, the duration of the z-regime decreases when h increases (see Figure 3.9). Moreover, since a part of the feed particles may layer further on in the apparatus, not all the particles have to coalesce into nuclei pellets. The amount of nuclei to be generated by coalescence should equal the number of pellets in the product stream. We may expect therefore, that the BSR, available for the generation of nuclei, is relatively high. Hence, coalescence will proceed much quicker (see Figure 3.7). Another way to generate the required nuclei pellets is by breakage of the established agglomerates (see chapter 4). Subsequently, growth of pellets only takes place by the layering mechanism. Which of the two methods will result in a lower overall residence time is difficult to predict. The latter described method will probably be favourable when a long period of zero-growth is exhibited in batch experiments.

In this chapter, some existing ideas concerning the design of continuously operating equipment are given. They follow mainly from the work described in

the previous chapters. Nevertheless, it is inevitable that more experimental work has to be undertaken. For this reason a preliminary experimental study was set up, whereby the obtained results encourage further research in the proposed direction.

5.2 *Experimental system and procedure*

System:

Due to their hydrophilic character, the silica particles that were used in batch experiments, had to be suspended in a non-polar liquid. But, the use of such liquids in larger quantities involves special safety precautions. Therefore, in order to restrict the experimental efforts, a system is favoured that can be agglomerated in water. Some further preconditions are set. The ability of the powder to reflect light has to be sufficiently high so that the light-back-scatter method can be used for determining batch growth kinetics. The in this way determined agglomeration time has to be less than 60 minutes. After an elaborate search, it finally proved that $CaCO_3$ powder is suitable as a model system. It can be agglomerated in water when kerosine, mixed with 5 vol % oleic acid*) is used as the binding liquid.

The $CaCO_3$-system was firstly tested batch-wise, following the same methods as were used for the silica systems. It readily showed that the $CaCO_3$-system exhibits a markedly different growth behaviour. For the silica system it was observed that all the primary particles were taken up by the binding liquid and readily transformed into flocs: no primary particles were left in suspension. However, in case of the $CaCO_3$-system not all the particles are readily flocculated. A number of them is left in the suspension. And as the growth process proceeds, these 'free' particles are slowly taken up by the established pellets. Apparently the preferential wetting of the binding liquid is insufficient.

It is further observed that the amount of unflocculated particles increases with decreasing B.S.R. In this way, the increasing growth rate, in the fast growth regime, with increasing B.S.R. is explained (see Figure 5.1). (For the silica system, the B.S.R. did not influence growth rate significantly). Apparently, the layering of the primary particles retards the overall growth in the fast growth regime.

Another difference with most silica systems is the relatively short zero-growth regime. This $CaCO_3$ system is therefore, at least for the studied conditions, not suitable to ascertain the influence of a long z-regime on the kinetics of continuously operating systems.

As a first approximation for the operating conditions of the continuous system, B.S.R. and power-input values were used that ensured successful batch operation:

B.S.R : 0,35
N (1° vessel) 1750 rpm
N (2° + 3° vessel) 1500 rpm (P = 3,2 W/kg)
Feedconcentration 1.8 vol %

From Figure 5.1 we see that the required residence time, to grow pellets of a few millimeters, is about 15 minutes. The feed rate was therefore tentatively fixed on 0.2 l/min.

*) The detergent, oleic acid, is used to reverse the wettability of the $CaCO_3$ particles from hydrophilic to hydrophobic. In literature, the detergent is always added to the suspension liquid phase. The conditioning of the binding liquid, as is done here, has not been applied yet. This has the advantage that the suspension liquid is not contaminated,which is of great importance, e.g. for waste water treatment.

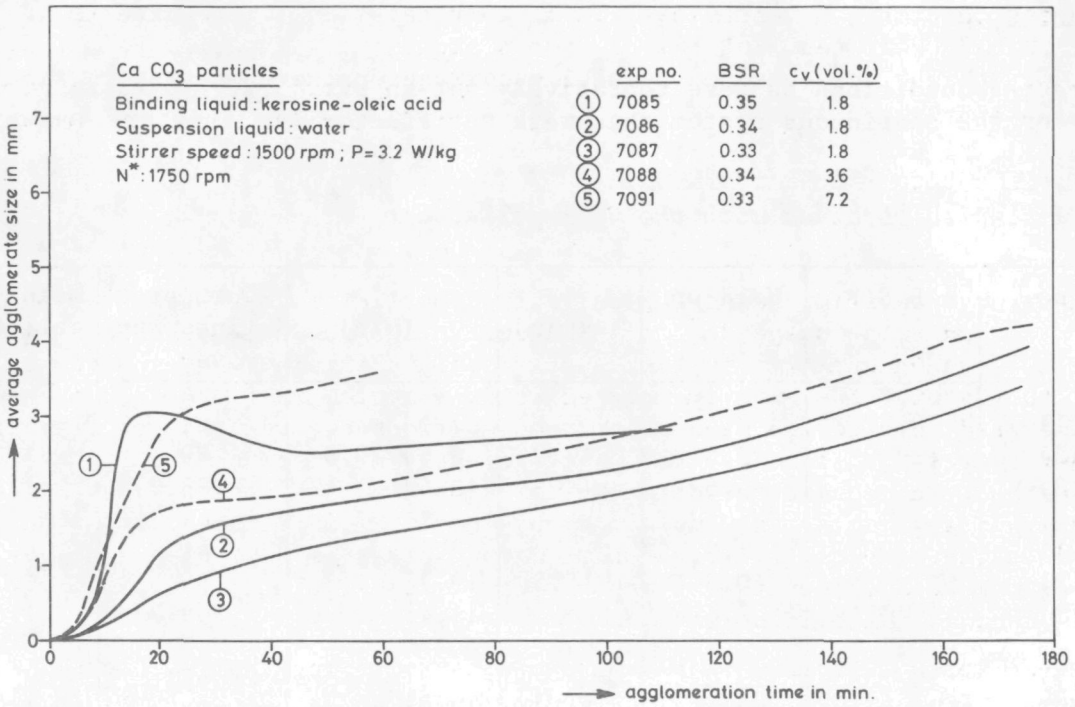

Figure 5.1 Growth curves for the CaCO3-system as a function of B.S.R. and solids concentration.

Equipment:

The reasons for chosing an CSTR arrangement were already outlined in par. 2.4. We may add here that the main problem in operating the described equipment was to maintain a stable pellet hold-up. Above the fact that the pellet hold-up had to be constant, it also should be markedly higher than the solid hold-up in the feed. The desirability of a high hold-up was indicated in the introduction of this chapter.
Different discharge geometries were tried, but most of them proved to be unsuccessful : they caused inherently instable conditions, e.g. only a small pellet hold-up was maintained or the small, not full grown, pellets were removed preferentially. Finally, the discharge geometry described in par. 2.4 proved to work fairly satisfactory. It is capable of maintaining a fairly stable pellet hold-up up to 4-5 times the feed hold-up during 6-8 residence times. It showed not possible to apply a hold-up higher than 10 vol % since otherwise the pellets were not adequately suspended anymore.
It is believed that still existing problems with the present discharge geometry can be largely overcome when the volume of the vessels is increased. Longer runs are than possible.

Procedure:

The start-up procedure showed to be easy: slurry and binding liquid feed were started whereby the B.S.R. was at first maintained at a relatively high level. The discharge opening was located in the upper end of the vessel so that larger pellets were not allowed to leave the first section. After about 20 minutes the pellet hold-up in the first vessel had reached approximately the required hold-up value at steady state. Then, the B.S.R. was reduced to the required test value and also the discharge pipe of the first vessel was relocated in its correct position. This procedure was followed through for the three sections of the CSTR.

5.3 Results

The operating conditions as were tentatively set in par. 5.2, proved to give results for the continuous system that were satisfactorily. They are summarized in Table 5.1

TABLE 5.1 Results obtained with the CSTR-pelletizer

exp. no.	B.S.R.	Hold-up vol %	τ_L (min)	τ_s (min)	Cum.perc fines removed	Mean (mm) pellet size
7516(1)	0,37	2.4		7.5	61	
(2)		3.6	19.9	9.4 29.9	89	1.67
(3)		5.6		13.4	98.9	1.85
7517(1)	0,30	1.2		5.2	41	
(2)		10.3	15.5	19.7 41.3	99.5	1.76
(3)		8.6		16.4	99.7	1.66
7518(1)	0,35	3.2		7.3	62	
(2)		8.4	14.8	17.0 43.0	92	1.92
(3)		9.5		18.7	97.4	2.04
7519(1)	0,35	4.4		8.8	93	
(2)		9.5	16.8	21.4 51.6	99.4	2.12
(3)		9.5		21.4	99.8	1.94

(1), (2), (3) refer to respectively the first, second and third vessel.

5.4 Discussion

a. Efficiency

The feed particles are removed from the liquid stream with a very good overall efficiency of 99-99.8 %. In two experiments (7517 and 7519) the maximum efficiency is more or less reached already in the second vessel. Thus, two stages are sufficient to obtain a fairly good clean up of the liquid stream. But, on the other hand it also shows that in the third vessel only little fine material layers onto the pellets. Apparently these pellets are already too dry to take up a significant amount of feed particles (as indicated by the experiments in par. 3.4). Hence, if a part of the binding liquid was introduced into the second vessel, this would certainly have improved the overall efficiency.

b. Residence time

The required solid residence time shows to be between 30 and 50 minutes. Or when only two vessels are considered (exp. 7517 + 7519): 25 - 30 minutes. The corresponding liquid residence time is 15 - 20 minutes for the three vessels and 10 minutes for the two.
The required residence time appears to be hardly influenced by the B.S.R., which varied between 0,30 and 0,37. This is markedly different from the sensitivity of the batch agglomeration time which ranges from 12 minutes for B.S.R. = 0,35 to 100 minutes for B.S.R. = 0,33. Moreover, the required agglomeration time depends also on the solid concentration as Figure 5.1 clearly shows.
It is therefore not clear yet, whether the solid - or the liquid residence time corresponds with the batch agglomeration time. But, it is established that when the solid residence time drops below 5 minutes, no suitable pellets are

formed. Only loose, dry flocs are generated that are unable to act as receiving pellets for the feed particles in the 2^{Q} and 3^{Q} section. Good results are obtained for $\tau_s \simeq 10$ min.; the pellets are then in the beginning of the fast growth regime so that they contain sufficient binding liquid on the surface for layering. From this we tentatively conclude that for powders that exhibite a long zero-growth regime, a long solid residence time in the first section is required.

c. Pellet hold-up

Pellet hold-up in the first vessel ranged between 1.2 and 4.4 vol %. To use a hold-up above 4.5 vol % is not possible since then the established pellets start to absorb preferentially a major part of the binding liquid. As a consequence, pellet-pellet coalescence increases considerably, so that the production of new pellets is strongly reduced. The pellet hold-up in the second and third vessel has to be kept at about 10 vol %. Then, the exposed surface for the layering mechanism is apparently sufficiently large to ensure a > 99% removal of the $CaCO_3$-particles. Further, comparison of the pellet sizes in the second and third vessel shows that, at least in the third vessel, the layering mechanism is predominant compared with the coalescence of pellets.

From the above, it becomes evident that the influence of the pellet hold-up on the performance of a pelletizer can not only be expressed in terms of exposed surface available for the layering of fines. Its function is more complicated, e.g. the relative occurance of the coalescence and layering mechanism in the first vessel shows to be strongly dependent on the pellet hold-up. This is an important assessment for further studies concerning the mechanisms in continuous pelletizers. Also the stability of the hold-up, in particular in the first vessel, is of crucial importance to the stability of operation. The stability of operation is, next to hydrodynamic factors, mainly controlled by the relative occurance of the growth mechanisms. A sufficient amount of nuclei pellets has to be generated (by coalescence) to create sufficient exposed surface for the feed particles that are bypassed to the second and third section to layer onto. Any disturbance in the balance between the mechanisms inevitably leads to fluctuations in cleaning efficiency and product rate. This phenomenon was indeed observed for large iron-ore balling circuits [136, 137, 138] where similar considerations are valid. From this point of view, also special constraints are put to the hydrodynamics of a continuously operating commercial unit.

The hydrodynamics as well as the assessment of the relative occurance of the different growth mechanisms in continuous operation should be the topic for further research in this field. Additionally, the effect of pellet hold-up should be carefully examined further, since a close relation between hold-up and efficiency as well as stability of operation is suggested by the work done so far.

APPENDIX I

Expression for the growth rate derived from the coalescence model

The population balance equation for the coalescence mechanism is:

$$\frac{\partial n(x,t)}{\partial t} = \tfrac{1}{2}\int_0^x R(x-\bar{x},\bar{x}) \cdot \frac{n(x-\bar{x},t)n(\bar{x},t)}{N^i(t)}\, d\bar{x} - \int_0^\infty R(x,\bar{x})\, \frac{n(x,t)n(\bar{x},t)}{N^i(t)}\, d\bar{x} \qquad (I.1)$$

The growth function, i.e. the total number of particles as a function of time can be obtained by integrating eqn. (I.1) over all particle volumes. For the 'restricted-in-space' system (i = 1) one obtains:

$$\frac{dN(t)}{dt} = -\tfrac{1}{2}\int_0^\infty \int_0^\infty \frac{R(x,\bar{x})n(x,t)n(\bar{x},t)}{N(t)}\, dx d\bar{x} \qquad (I.2)$$

Introduction of the following similarity variables:

$$\psi(\eta) = \frac{\phi}{N^2(t)} \cdot n(x,t) \qquad (I.3)$$

and

$$\eta = \frac{N(t)}{\phi} \cdot x \qquad (I.4)$$

whereby

$$N(t) = \int_0^\infty n(x,t)dx \qquad (I.5)$$

$$\phi = \text{total volume of particles} = \int_0^\infty x\, n(x,t)dx \qquad (I.6)$$

and putting

$$R(x,\bar{x}) = \frac{1}{(x\bar{x})^a} = \left(\frac{\phi}{N}\right)^{-2a} \cdot R(\eta,\bar{\eta}) \qquad (I.7)$$

or written in similarity variables

$$R(x,\bar{x}) = \frac{\phi}{N}^{-2a} (\eta\bar{\eta})^{-a} \qquad (I.8)$$

leads to the following expression:

$$\frac{dN(t)}{dt} = -\tfrac{1}{2}\int_0^\infty \int_0^\infty \left(\frac{\phi}{N(t)}\right)^{-2a} (\eta\bar{\eta})^{-a}\, N(t)\, \psi(\eta)\psi(\bar{\eta}) d\eta d\bar{\eta} \qquad (I.9)$$

Since ϕ as well as $\int_0^\infty \int_0^\infty (\eta\bar{\eta})^{-a}\, \psi(\eta)\psi(\bar{\eta})d\eta d\bar{\eta}$ are independent of t, eqn. (I.9) may be reduced to:

$$\frac{dN(t)}{dt} = - C_1 . N(t)^{1+2a} \tag{I.10}$$

where

$$C_1 = \tfrac{1}{2}\, (\phi)^{-2a} \int_0^\infty \int_0^\infty (\eta\bar{\eta})^{-a}\, \psi(\eta)\psi(\bar{\eta})d\eta d\bar{\eta} \tag{I.11}$$

or in terms of mean size ($\phi = N \frac{\pi}{6}\, \bar{D}^3$)

$$\frac{d\bar{D}(t)}{dt} = C_2 . (\bar{D})^{1-6a} \tag{I.12}$$

Similarity transformation with respect to coalescence-breakage model

The population balance for agglomeration by coalescence and breakage is formulated as follows:

$$\begin{aligned}\frac{\partial n(x,t)}{\partial t} &= -B(x)\, n(x,t) + r^2\, B(rx)\, n(rx,t) \\ &+ \tfrac{1}{2} \int_0^x R(x-\bar{x},\bar{x})\, \frac{n(x-\bar{x},t)\, n(\bar{x},t)}{N(t)}\, d\bar{x} \\ &- \int_0^\infty R(x,\bar{x})\, \frac{n(x,t)\, n(\bar{x},t)}{N(t)}\, d\bar{x}\end{aligned} \tag{I.13}$$

If a simularity transformation is attempted like

$$n(x,t) = \mu(t)\ \ \psi(x.\xi(t))$$

with

$\mu(t) = \xi^2(t)$ for conservation of mass and putting

$x' = x.\xi(t)$ and

$\bar{x} = s.\xi(t)$

and putting again $R(x,\bar{x}) = \frac{1}{(x\bar{x})^a}$ and $B(x) = x^b$ we find for eqn. (I.13):

$$\begin{aligned}\xi(t)\ \frac{d\xi(t)}{dt}\ \left[2\psi + \frac{x'd\psi}{dx'}\right] &= - \xi^{2-b}(t)\ \left[B(x')\psi(x') - r^2 B(rx')\psi(rx')\right] \\ &+ \frac{\xi^{2+2a}(t)}{N(t)}\ \left[\tfrac{1}{2} \int_0^{x'} R(x'-s,s)\psi(x',s)\psi(s)ds\right. \\ &\left. - \int_0^\infty R(x',s)\psi(x')\psi(s)\, ds\right]\end{aligned} \tag{I.14}$$

However, no reasonable function of $\xi(t)$ can split up eqn. (I.14), in order to obtain a time independent equation.

APPENDIX II

Numerical simulation of the coalescence-breakage model

In order to evaluate theoretically the evolution of the agglomerate size distribution and at the same time obtain a prediction for the increase of mean pellet size with time, the following model was simulated [61]:

$$\frac{\partial n(x,t)}{\partial t} = - B(x)\, n(x,t) + r^2\, B(rx)\, n(rx,t) + \tfrac{1}{2}C \int_0^x \frac{n(\bar{x},t)\,n(x-\bar{x},t)}{\left[\bar{x}(x-\bar{x})\right]^a\, N(t)}\, d\bar{x} - C \int_0^\infty \frac{n(x,t)\,n(\bar{x},t)}{(x\bar{x})^a\, N(t)}\, d\bar{x} \qquad \text{(II.1)}$$

where

$n(x,t)$ is the density of particles with volume x at time t

$B(x) = B.x^b$ is the breakage function for breakage into r equal parts

$R(x) = \dfrac{C}{(x\bar{x})^a}$ is the coalescence frequency function

$N(t) = \int_0^\infty n(x,t)dx$

The constants B and C may be chosen 1 without loss of generality.

In the simulation program, developed by Sonneveld [134] with the objective of solving eqn. (II.1) numerically, the unknown function $n(x,t)$ is represented by a suitable chosen function ϕ, depending on a finite number of parameters $Q_1 \ldots Q_N$ and the volume x. The time dependence of n is now represented by the time dependence of the parameters Q_k:

$$n(x,t) \doteq \phi\,(Q_1(t),\, Q_2(t) \ldots Q_N(t), x) \qquad \text{(II.2)}$$

with

$$Q_k(t) = \phi\,(Q_1(t), \ldots Q_N(t), x_k)$$

$$\simeq n\,(x_k,t),\ k = 1(1)N$$

where $x_1, x_2, \ldots x_n$ are suitable chosen reference values on the volume-axis. Or, in a shorter notation:

$n(x,t) \doteq \phi\,(Q(t),x)$, with

$\underline{Q}(t) \in \mathbb{R}_N$ (is a vector in the N-dimensional Euclydian space)

In the work done so far the following expression for the function ϕ was used:

$$\phi = \exp\left\{ \sum_{k=1}^{N} \ln\left[Q_k(t)\right]\, P_k\left[\ln(x)\right] \right\} \qquad \text{(II.3)}$$

where

P_k are cardinal cubic splines with parabolic runout, based on a uniform mesh, i.e. let

$x_1 < x_2 < \ldots < x_N$

be a uniform mesh (in such a way that $x_k - x_{k-1} = h$, h is an increment), then for k = 1(1)N:

a. $P_k(x)$ = third degree polynomial for $x \in [x_i, x_{i+1}]$, i = i = 1(1)N-1

b. P_k, $\frac{dP_k}{dx}$, $\frac{d^2P_k}{dx^2}$ are continuous for $-\infty < x < +\infty$

c. $P_k(x)$ is quadratic, $x < x_1$, $x > x_N$

d. $P_k(x_i) = \begin{cases} 1 & k = 1 \\ 0 & k \neq i \end{cases}$, i = 1(1)N

In fact the distribution function, whereby n is a function of x (Fig. II.1), is transformed into a distribution function whereby ln n is a function of ln x (Fig. II.2).

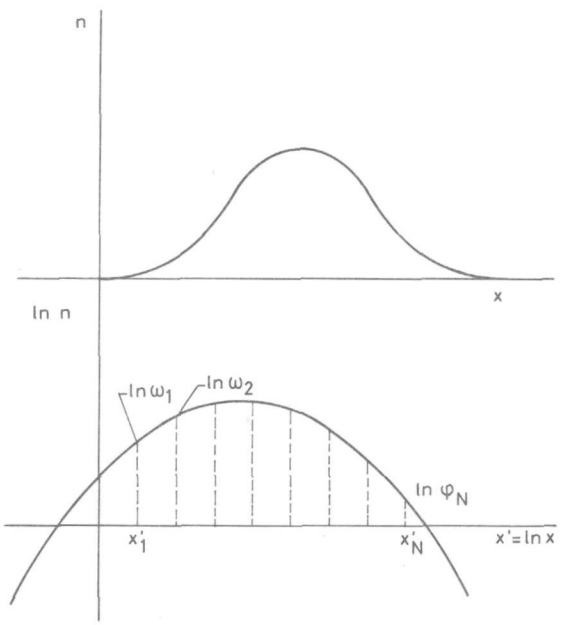

Fig. II.1 Distribution function on n-x scale.
Fig. II.2 Distribution function on ln n-ln x scale.

The choice of making a map of ln x ln n, is motivated by the observation that ln n as a function of ln x behaves very smoothly and shows a suitable asymptotic behaviour for small and large values of x. This justifies the use of low degree (3Ω) spline-functions with parabolic runout, involving only few (say 10 to 20) parameters.
Moreover, when time t proceeds, the relevant interval $[x_1, x_N]$ on the logarithmic scale stays more or less constant. In this way the main problem in the simulation attempts i.e. the fact that the domain on the x-axis where n(x,t)is important is depending strongly on time, is overcome.
When time increases, sometimes the defined mesh points ln (x_k) are updated in such a way that the relevant part of the information is contained in the interval $[x_1, x_N]$.

With eqn. (II.2), eqn. (II.1) is reduced into an ordinary system of N first order differential equations:

$$\frac{\partial' Q_k}{\partial t} = - B(x_k)Q_k(t) + r^2 B(r,x_k)\,\phi[Q(t), r.x_k] + \tfrac{1}{2} C \int_0^{x_k} \frac{\phi[\underline{Q}(t),\bar{x}]\,\phi[\underline{Q}(t), x_k - \bar{x}]}{[x_k - \bar{x}), \bar{x}]^a}\, d\bar{x} - C \int_0^{\infty} \frac{\phi[\underline{Q}(t), x_k]\,\phi[\underline{Q}(t),\bar{x}]}{(x_k,\bar{x})^a\, N(t)}\, d\bar{x} \qquad \text{(II.4)}$$

where

k = 1(1)N

This can be written formally as:

$$\frac{d\underline{Q}}{dt} = \underline{F}(\underline{Q}) \qquad \text{(II.5)}$$

This system can be solved by any initial value procedure like Runga Kutta, since, given $\underline{Q}$, the function $\underline{F}$ can be evaluated straightforwardly, using for instance an adaptive quadrature procedure in order to evaluate the integrals in the coalescence terms.

Remark I

The functions for the coalescence frequency as well as for the breakage frequency may be chosen as complicated as possible, without affecting in principle the possibility of carrying out the above approach.

Remark II

The number of agglomerates n, the time t and the volume x are related to the mathematical values for these three parameters, as they are used in the simulation programme, resp. ν, τ and ξ, by the scale-factors N_o, T and λ as follows:

$$n = N_o.\nu$$
$$t = T.\tau$$
$$x = \lambda.\xi$$

The population balance equation can be written as:

$$\frac{N_o}{T}\left[\frac{\partial \nu}{\partial \tau}\right] = B.N_o\lambda^b \left[-(\xi)^b.\nu(\xi) + r^2\,(r\xi)^b\ \nu(r\xi,\tau)\right]$$

$$+ C.\frac{N_o}{\lambda^{2a}}\left[\int_o^{\xi} \frac{\nu(\bar{\xi},\tau)\quad \nu(\xi-\bar{\xi},\tau)}{\left[\bar{\xi}.(\xi-\bar{\xi})\right]^a \mu_o}\, d\xi\right.$$

$$\left. - \int_o^{\infty} \frac{\nu(\xi,\tau)\ .\ \nu(\bar{\xi},\tau)}{\left[\xi.\bar{\xi}\right]^a \mu_o}\, d\xi\right] \qquad \text{with } \mu_o = \int_o^{\infty} \nu d\xi$$

So that for B and C, we derive at:

$$B = \frac{1}{T.\lambda^b} \qquad \text{and} \qquad \frac{C}{B} = \lambda^{2a+b}$$

APPENDIX III[a] Breakage experiments

Exper. no.	Type powder	N $\left(\frac{1}{min}\right)$	Duration of test (min)	D_M (mm)	Number before test	Number after test	Numer unbroken after test	Breakage occured?
4052		1250	10	3.5	34	34	34	no
4057	Glass powder	1250	10	3.7	10	25	4	yes
4057	no. 1	1250	10	3.0	7	14	3	yes
4058		1250	10	3.0	12	24	2	yes
5136	Glass powder	1250	40	3.0	15	15	15	no
5136	no. 1	1650	40	3.0	15	15	15	no
5181		1250	15	3.3	15	15	15	no
5040		1750	110	2.4	20	20	20	no
5042		1250	10	3.0	20	28	18	yes
5042		1250	10	3.0	20	31	18	yes
6036		1250	10	2.7	20	25	17	yes
6036		1250	20	2.7	20	23	19	yes
6036	Glass powder	1250	30	2.7	20	33	18	yes
6036	no. 3	1350	10	2.7	20	25	17	yes
6036		1450	10	2.7	20	40	17	yes
6036		1550	10	2.7	20	47	17	yes
6036		1650	10	2.7	20	32	19	yes
6043		1250	20	3.0	15	24	13	yes
6044		1250	30	2.8	15	113	6	yes
5179		1250	10	-	5	20	0	yes
5179		1250	10	2.7	5	5	5	no
5180	Glass powder	1250	15		5	8	-	yes
5180	no. 4	1250	15		5	24	-	yes
5180		1250	15		5	27	-	yes
5180		1250	15	3.5	5	38	1	yes
5184		1250	15	3.1	5	17	0	yes
5148	Glass ballotini	900	30	-	10	∞	0	yes

Breakage test in flowmodel

Exper. no.	Type powder	jet velo-city (m/s) Equiv. N	Duration of test (min)	D_M (mm)	Number before test	Number after test	Numer onbroken after test	Breakage occured?
5148	Glass ballotini	1,69/ 900	30	2.8	10	124	0	yes
6038	Glass powder 3	1,89/ 1000	60	3.0	10	16	6	yes
6038	Glass powder 3	3,8/ 2010	10	3.0	10	70	7	yes
5184	Glass powder 4	2,35/ 1250	15	3.3	5	21	0	yes

APPENDIX III[b] Experimental conditions

Experiment no.	Type of powder	Concentr. (kg/m^3)	visc. binder * 10^3 (Ns/m^2)	BSR	N($\frac{1}{min}$)	D_M (mm)
4030	Al-silicate	50	5	0,560	1250	3.45
4031	"	"	"	0,546	"	3.25
4032	"	"	"	0,530	"	3,55
4033	"	"	"	0,517	"	2,25
4034	"	"	"	0,502	"	0,70
4035	"	"	"	0,487	"	0,50
4039	Glasspowder 1	"	"	0,48	"	-
4040	"	"	"	0,45	"	-
4041	"	"	"	0,37	"	0,44
4042	"	"	"	0,38	"	0,24
4044	"	"	"	0,41	"	3,1
4045	"	"	"	0,42	"	3,2
4048	Al-silicate	100	"	0,53	"	3,6
4049	"	150	"	0,53	"	4,75
4050	"	50	"	0,546	1500	3,0
4051	"	"	"	0,546	1000	-
4052	Glass powder 1	"	"	0,436	1250	3,5
4053	"	50+10	"	0,423	1250	0,20
4055	Glass ballotini	50	"	0,489	900	2,12
4056	Glass powder 1	50+10	"	0,436	1250	0,48
4057	"	50+10	"	0,463	"	3,61
4058	"	50+10	"	0,489	"	3,81
4059	Glass powder 2	50	"	0,423	"	0,25
4061	"	"	"	0,476	"	0,30
4062	"	"	"	0,503	"	4,5
4063	"	"	"	0,516	"	-
4064	"	"	"	0,489	"	3,5
5040	Glass powder 3	"	"	0,463	"	-
5042	Glass powder 3	"	"	0,475	"	-
5136	Glass powder 1	"	"	0,500	"	-
5148	Ballotini	"	"	0,500	900	-
5179	Glass powder 4	"	"	0,475	1250	2,27
5180	Glass powder 4	"	"	0,475	"	2,8
5181	Glass powder 1	"	"	0,514	"	2,7
5184	Glass powder 4	"	"	0,475	"	2,1
6010	Glass powder 3	"	"	0,489	"	2,83
6012	"	"	"	0,423	"	0,51
6014	"	"	"	0,450	"	1,52
6015	"	"	"	0,450	"	2,53
6016	"	"	"	0,450	"	2,54
6017	"	"	"	0,450	"	2,39
6018	"	"	"	0,450	"	-
6020	"	"	"	0,450	"	2,32
6021	"	"	"	0,450	"	2,43
6023	"	"	"	0,450	1500	1,88
6026	"	"	"	0,450	1125	2,81
6027	"	"	"	0,450	1375	2,21
6036	"	"	"	0,450	1250	-
6037	"	"	"	0,450	"	2,39
6039	"	"	"	0,450	"	1,06
6040	"	"	"	0,450	"	2,57
6043	"	"	1.3	0,43	"	2,98
6044	"	"	67	0,397	"	2,70
6073	Glass powder 5	"	5	0,489	"	3,09
6079	"	"	"	0,489	1125	4,41
6080	"	"	"	0,503	1250	-
6081	"	"	"	0,489	"	3,52
6083	"	"	23	0,483	"	3,46
6084	"	"	13	0,483	"	-
6085	"	"	"	0,483	"	-
6086	"	"	8	0,483	"	4,35
6087	"	"	2.3	0,483	"	-
6088	"	"	5	0,483	"	3,65
7085	$CaCO_3$	50	1.2	0,35	1500	2,78
7086	"	"	"	0,34	"	3,28
7087	"	"	"	0,33	"	2,90
7088	"	100	"	0,34	"	4,10
7091	"	200	"	0,33	"	3,59
7516	"	53	"	0,37	"	1,70
7517	"	"	"	0,30	"	1,67
7518	"	50	"	0,35	"	1,90
7519	"	"	"	0,35	"	1,85

A	projected area of the particles in measuring volume	(m^2)
ASD	agglomerate size distribution	
A_v	specific surface of the particles per unit volume	(m^2/m^3)
a	parameter representing the preference of coalescence with respect to particle size	
B.S.R.	binding-liquid/solid ratio	
	$= \frac{\text{vol. binding liquid}}{\text{vol. of solid particles}}$	(m^3/m^3)
B(x)	breakage frequency function	(1/s)
B	breakage rate constant	
b	parameter representing the preference of pellet breakage with respect to particle size	
C.V	coefficient of variation	(%)
C	coalescence rate constant	
C(x,t)	crushing frequency function	(1/s)
$C_{1...n}$	constants	
c_p	particle concentration	$(\#/m^3)$
c_v	volume concentration	(m^3/m^3)
D	diameter; pellet size	$(\mu m, mm, m)$
$\bar{D}$	mean pellet size	$(\mu m, mm, m)$
D_M	median pellet size	$(\mu m, mm, m)$
D_T	impellet diameter	(m)
d(p)	mean particle size	$(\mu m, mm, m)$
E	elastic modules	(N/m^2)
$F_i(d)$	impeller-pellet impact force	(N)
F_c	cohesive force	(N)
F_b	breaking load	(N)
F_e	force exerted on a pair of pellets	(N)
G(x,V(t))	growth rate function representing the rate at which granules are growing larger than volume x by picking up the crushed material with volume V(t)	(1/s)
I	light intensity	(mV)
I_{bt}	back scattered intensity	(mV)
I_{bw}	back scattered intensity of the wall	(mV)
I_{bm}	maximum back scattered intensity	(mV)
i	parameter representing the spacial distribution of the particles	
$K_{1...N}$	constants	
k	strength factor	(N/m^2)
k_m	maximum strength factor	(N/m^2)
L	length of the light path	(m)
M	mass	(kg)
M_a	$\int_0^\infty \int_0^\infty (\eta\bar{\eta})^{-a} \quad \psi(\eta) \quad \psi(\bar{\eta})\, d\eta \quad d\bar{\eta}$	
N	stirrer speed; number	(1/s)
N(t)	$\int_0^\infty n(x,t)$ is the total number of agglomerates at time t	(#)
n_i	number of particles with size D_i	(#)
n(x,t)	continuous density distribution function with respect to pellet volume at time t	(#)
O	cross sectional area of the light beam	(m^2)
P	specific power input	(W/kg)
P(d)	probability of a pellet hitting the impeller blade	
$P_k(t)$	cardinal cubic spline functions	
Δp	pressure difference between centre and surface of the pellet	
p	constant in eqn. (2.10)	

p_1	parameter representing particle size distribution	
p_2	parameter representing particle shape	
p_3	parameter representing packing structure	
p_c	capillary pressure	(N/m^2)
p'	turbulent pressure fluctuations	(N/m^2)
$Q_i(t)$	parameters representing time dependence of n	
q	constant in eqn. (2.10)	
R	radius of the particle	(m)
$R(x,\bar{x})$	coalescence frequency function for a pair of particles with volumes x and $\bar{x}$	(1/s)
r	the number of parts into which a pellet breaks	(#)
Re	Reynolds number	
S	degree of saturation	
s	shear rate	$(\frac{1}{s})$
t	time	(s,min)
t_b	characteristic breakage time	(s)
t_z	duration of the zero-growth regime	(s,min)
$\bar{U}^2_{pd}$	variance of the velocity distribution of a particle with size d	(m^2/s^2)
$U' = \sqrt{\bar{U}^2}$	root mean square value of turbulent velocity fluctuations	(m/s)
u	velocity	(m/s)
u_{tip}	tip speed of the stirrer	(m/s)
V	volume	(m^3)
V(t)	volume of crushed material	(m^3)
x	distance parameter in eqn. (2.1)	(m)
x	particle volume	(m^3)
x'	$x\ \xi\ (t)$	(m^3)
α	constant in eqn. (2.1)	
$\alpha(d_1,d_2)$	collision frequency between particles with size d_1 and d_2	(1/s)
$\beta(d_1,d_2)$	coalescence efficiency between particles with size d_1 and d_2	
γ	surface/interfacial tension	(N/m)
$\gamma(d_1,d_2)$	resistance factor for the transport of particles from the bulk of the pellet towards the connecting bridge	
ε	porosity; energy dissipation per unit mann	(W/kg)
η	similarity variable = $\frac{N(t)}{\phi}$. x	(#)
η'	order of the viscous subrange eddies	(m)
θ	contact angle	
λ_s	scale of energy dissipation	(m)
μ	dynamic viscosity	$(N.s/m^2)$
$\mu(t)$	function only depending on t	
ν	kinematic viscosity	(m^2/s)
$\xi(t)$	function only depending on t	
ρ	density	(kg/m^3)
σ	tensile stress	(N/m^2)
σ_D	pressure strength	(N/m^2)
σ_t	tensile strength	(N/m^2)
τ	shear stress; residence time	(N/m^2);(t)
υ_{pi}	Poisson constant	
ϕ	total volume of particles	(m^3)
$\phi(Q_1(t), Q_2(t) \ldots\ldots Q_N(t))$	function representing n(x,t)	
$\psi(\eta)$	similarity variable = $\frac{\phi}{N^2(t)}$. n (x,t)	$(m^3/\#)$

REFERENCES

1. Yusa, M.; H. Suzuki; S. Tanaka; "Separating liquids from solids by pellet flocculation"; J. Am. Water Works Ass. 67 (1975), 397-402.
2. Yusa, M.; "Mechanisms of pelleting flocculation"; Int. J. Min. Proc. 4 (1977), 293-305.
3. Ide, T.; M. Yusa; "Solid-liquid separation by pelleting flocculation process"; Proc. of the 2nd Pacific Chem. Eng. Congr., Denver (USA), august 1977; Vol. I, p. 682-689.
4. Cattermole, A.E.; US Patents 763 259; 763 260; 777 273; 777 274 (1904).
5. Ball, D.F.; "Agglomeration of iron ores"; London, Heinemann, 1973.
6. Roorda, H.J.; O. Burghardt; H.A. Kortmann; M.J. Jipping; T. Kater; "Organic binders for iron-ore agglomeration"; Paper presented at the 11th Int. Min. Proc. Congr., Cagliari (Italy), april 1975; Paper 6.
7. Rumpf, H.; "Die Wissenschaft des Agglomerierens"; Chem. Ing. Techn. 46 (1974), 1-11.
8. Gaudin, A.M.; "Flotation"; New York, McGraw Hill, 1932.
9. Gaudin, A.M.; "Principles of mineral dressing"; New York, McGraw Hill, 1939.
10. Behrenbeck, H.J.; "Die selektieve Agglomeration von Kohlemineralstoffkollektiven in feinsten Steinkohlenschlämmen"; Berlin, Diss. TU, 1973.
11. Farnand, J.R.; H.M. Smith; I.E. Puddington; "Spherical agglomeration of solids in liquid suspension"; Can. J. Chem. Eng. 39 (1961), 94-97.
12. Sutherland, J.P.; "The agglomeration of aqueous suspensions of graphite"; Can. J. Chem. Eng. 40 (1962), 268-272.
13. Zuiderweg, F.J.; N. van Lookeren Campagne; "Pelletizing of soot in waste water of oil gasification plants-the Shell pelletizing separator (S.P.S.)"; The Chem. Engineer (1968), (no. 220), CE 223-227.
14. Meer, D. van der; B.B. Quist; "Agglomeration of suspended solids (crystals) in the Shell pelletizing separator"; De Ingenieur 84 (1972), (no. 45), Ch58-Ch60.
15. Corkill, J.E.M.; "New outlets for asphalt in separation and agglomeration"; Proc. Symp. on New Uses for Asphalt; Amer. Chem. Soc. of Petr. Chem. 13 (1968), (no. 4), C107-C113.
16. Capes, C.E.; J.P. Sutherland; "Formation of spheres from finely divided solids in liquid suspension"; I. & E.C. Proc. Des. Dev. 6 (1967), 146-154.
17. Sirianni, A.F.; C.E. Capes; I.E. Puddington; "Spherical agglomeration of solids in liquid suspension"; Can. J. Chem. Eng. 47 (1969), 166.
18. Sparks, B.D.; F.W. Meadus; "Spherical agglomeration in a conical drum"; Can. J. Chem. Eng. 55 (1977),502-505.
19. Kawashima, Y.; C.E. Capes; "An experimental study of the kinetics of spherical agglomeration in a stirred vessel"; Powder Techn. 10 (1974), 85-92.
20. Kawashima, Y.; C.E. Capes; "Further studies of the kinetics of spherical agglomeration in a stirred vessel"; Powder Techn. 13 (1976), 279-288.
21. Goldberg, A.S.; "Particle technology research review, Vol. I"; London, Powder Advisory Centre, 1973.
22. Farnand, J.R.; F.W. Meadus; P. Tymchuk; I.E. Puddington; "The application of spherical agglomeration to the fractionation of a tin-containing ore"; Can. Metallurgical Quart. 3 (1964), 123-135.
23. Meadus, F.W.; A. Mykytiuk; I.E. Puddington; N.D. MacLeod; "The upgrading of tin ore by continuous agglomeration"; Can. Min. and Metall. Bull. 69 (1966), 986-970.
24. Farnand, J.R.; I.E. Puddington; "Oil-phase agglomeration of germanium-bearing vitrain coal in a shaly sandstone deposit"; Can. Min. Metall. Bull. (1969), (March), 267-271.
25. Farnand, J.R.; F.W. Meadus; E.C. Goodhue; "The benefication of gold ore by oil-phase agglomeration"; Can. Min. Metall. Bull. (1969), (Dec.), 1326-1329.
26. Sparks, B.D.; R.H.T. Wong; "Selective spherical agglomeration of Ilmenite concentrates"; Can. Min. Metall. Bull. (1973), (Jan.), 73-77.
27. Sparks, B.D.; A.F. Sirianni; "Benefication of a phosphoriferous iron ore by agglomeration methods"; Int. J. Min. Proc. 1 (1974), 231-241.
28. Capes, C.E.; "Basic research in particle technology and some novel applications"; Can. J. Chem. Eng. 54 (1976), (febr./apr.), 3-12.
29. Capes, C.E.; A.E. McIlhinney; A.F. Sirianni; "Agglomeration from liquid suspension; research and applications"; Proc. of the 2nd Int. Symp. on Agglomeration, Atlanta, march 1977, Vol. II, p. 910-930; Ed. by K.V.S. Sastry, New York, Am. Inst. Min. Metall. Petr. Eng., 1977.
30. Capes, C.E.; A.E. McIlhinney; R.C. Coleman; "Benefication and balling of coal"; Trans. Soc. Mining Eng. A.I.M.E. (1970),(Sept.), 233-237.
31. Capes, C.E.; A.E. McIlhinney; A.F. Sirianni; I.E. Puddinton; "Agglomeration in coal preparation"; Proc. Inst. Briquetting Agglomeration 12 (1974), 53-62.
32. Capes, C.E.; A.E. McIlhinney; D.S. Russell; "Rejection of trace metals from coal during benefication by agglomeration"; Environm. Sci. & Techn. 8 (1974), (no. 1), 35-38.
33. Capes, C.E.; A.E. Smith; I.E. Puddington; "Economic assessment of the application of oil agglomeration to coal preparation"; C.I.M. Bull. (1974), (July), 115-119.

34. Verschuur, E.; G.R. Davis; "The Shell pelletizing separator: key to a novel process for dewatering and de-ashing slurries of coal fines"; Proc. 7th Int. Coal Preparation Congr., Sydney, 1976; Paper H.1.

35. Bhattacharyya, R.N.; A.K. Moza; G.G. Sarkar; "Role of operating variables in oil-agglomeration of coal"; Proc. of the 2nd Int. Symp. on Agglomeration, Atlanta, march 1977, Vol. II, p. 931-938; Ed. by K.V.S. Sastry, New York, Am. Inst. Min. Metall. Petr. Eng., 1977.

36. Swanson, A.R.; C.N. Bensley; S.K. Nicol; "Some fundamental aspects of the selective agglomeration of fine coal"; Proc. 2nd Int. Symp. on Agglomeration, Atlanta, march 1977, Vol. II, p. 939-951; Ed. by K.V.S. Sastry, New York, Am. Inst. Min. Metall. Petr. Eng., 1977.

37. Bensley, C.N.; A.R. Swenson; S.K. Nicol; "The effect of emulsification on the selective agglomeration of fine coal"; Int. J. Min. Proc. 4 (1977), 173.

38. Kruyt, H.R.; F.G. van Selms; "The influence of traces of water on the plasticity of starch and quartz suspensions in organic media"; Rec. Trav. Chim. 62 (1943), 409-414.

39. Kruyt, H.R.; F.G. van Selms; "The influence of third phase on the rheology of suspensions"; Rec. Trav. Chim. 62 (1943), 415-426.

40. Kao, S.V.; L.E. Nielsen; C.T. Hill; "Rheology of concentrated suspensions of spheres"; J. Colloid & Interf. Sci. 53 (1975), (no. 3), 358-366.

41. Cooper, P.G.; J.G. Rayner; S.L. Nicol; "Flow equation for coagulated suspensions"; Journ. Chem. Soc. Faraday Trans. I (1978), (no. 4), 785-794.

42. Boehm, H.P.; "Funktionelle Gruppen an Festkörperoberflächen"; Chem. Ing. Techn. 46 (1974), 716-726.

43. Nienow, A.W.; "Suspension of solid particles in turbine agitated baffled vessels"; Chem. Eng. Sci. 23 (1968), 1453-1459.

44. Bemer, G.G.; "A simple light backscatter techniques to determine average particle size and concentration in a suspension"; Powder Techn. 20 (1978), 133.

45. Bemer, G.G.; "Light backscattering as an on-line method for determining high slurry concentrations and large particle size"; Powder Techn. 22 (1979), 143-144.

46. Davies, R.; "Review of rapid response instrumentation for the size analysis of airborne and liquidborne particles"; Proc. on the 1973 Int. Conf. on Particle Techn., Chicago, aug. (1973), 116-118.

47. Leschonski, K.; W. Alex; B. Koglin; "Teilchengrössenanalyse"; Chem. Ing. Techn. 47 (1975), 97.

48. Raasch, J.; H. Umhauer; "Grundsätzliche Überlegungen zur Messung der Verteilungen von Partikelgrösse und Partikelgeschwindigkeit disperser Phasen in Strömungen"; Chem. Ing. Techn. 49 (1977), (no. 12), 931-941.

49. Leschonski, K.; "Die On-Line-Messung von Partikelgrössen verteilungen in Gasen und Flüssigkeiten"; Chem. Ing. Techn. 50 (1978), (no. 3), S194-203.

50. Koglin, B.; "Assesment of the degree of agglomeration in suspensions"; Powder Techn. 17 (1977), 219-227.

51. Rhodes, C.A.; I.F. Stowers; L. Hawkins; "In-line dynamic control monitoring of fluids for space systems"; Powder Techn. 14 (1976), 203-208.

52. Tipton, D.F.; "A particle analyzer for stack emissions"; Powder Techn. 14 (1976), 245-252.

53. Cornillaut, J.; "Particle size analyzer"; Appl. Opt. 11 (1972), 265.

54. Sadowski, J.W.; E. Byckling; "Apparatus for real-time measurement of particle size distribution"; Powder Techn. 20 (1978), 273-284.

55. Pfau, B.; "Simultane Geschwindigkeits-, Konzentrations- oder Partikelgrössenmessungen mit Ultraschall in Zweiphasenstromüngen"; Verfahrenstechn. 8 (1974), (no. 2), 54.

56. Pfau, B.; "Kontinuierliche Partikelgrössenmessung mit Ultraschall"; Verfahrenstechn. 8 (1974), 258.

57. Clontz, N.A.; W.L. McCabe; "Contact nucleation of magnesium sulfate heptahydrate"; Chem. Eng. Progr. Symp. Ser. 67 (1971), (no. 110), 6.

58. Johnson, R.T.; R.W. Rousseau; W.L. McCabe; "Factors affecting contact nucleation"; A.I.Ch.E. Symp. Ser. 68 (1972), (no. 12), 31-41.

59. Garside, J.; M.A. Larson; "Direct observation of secondary nuclei production"; Journ. Cryst. Growth 43 (1978), 694.

60. Nienow, A.W.; R. Conti; "Particle abrasion at high solids concentration in stirred vessels"; Chem. Eng. Sci. 33 (1978), 1077-1086.

61. Bemer, G.G.; P. Sonneveld; "The population approach to agglomeration in suspension: a coalescence/breakage model"; To be published.

62. Bemer, G.G. J. Heerens; M. Nienoord; "A method of determining particle-impeller impact forces and collision frequenties"; Chem. Eng. Sci. 34 (1979), 747-749.

63. Beek, W.J.; K.M.K.; Muttzall; "Transport phenomena"; London, Wiley, 1975.

64. Gildemeister, H.H.; "Spannungszustand und Bruchphänomene in prallbeanspruchten Kugeln"; Karlsruhe, Diss., 1976.

65. Berry, D.J.; T. Kelly; "Image analysis methods of particle size measurement and classification"; Proc. of Powtech. '71; Int. Powder Techn. & Bulk Granular Solids Conf., London, p. 49-53.

66. Polke, R.; R. Rieger; "Partikelgrössenanalysen < 10 µm. Messmethoden und Schwierigkeiten"; Chem. Ing. Techn. 50 (1978), (no. 3), S.149-154.

67. Washburn, E.W.; "The dynamics of capillary flow"; Phys. Rev. Ser. 2, 17 (1921), 273.

68. Bartell, F.E.; H.J. Osterhof; "Determination of the wettability of a solid by a fluid"; Ind. Eng. Chem. 19 (1927), 1277.

69. Bruce, W.A.; H.J. Welge; "Restored-state method for determination of oil in place and connate water"; Texas, API Prod. Div. (1947), 22.

70. Kossen, N.W.F.; P.M. Heertjes; "The determination of the contact angle for systems with a powder"; Chem. Eng. Sci. 20 (1965), 593.

71. Sell, P.J.; "Randwinkelmessungen an pulverförmigen Stoffen"; Berichte vom VI Int. Kongr. für grenzflächenaktive Stoffe; Zürich, sept. 1972; Bd. III, Sektion C, p.25-34.

72. Singhal, A.K.; P.M. Dranchuk; "The use of modified threshold pressure for determining the wettability of packs of equal spheres"; Powder Techn. 11 (1975), 45-50.

73. Singhal, A.K.; P.M. Dranchuk, P.M.; "Wettability control of glass beads"; Can. Journ. Chem. Eng. 53 (1975), 3.

74. Gomm, A.S.; F. Hauxwell; J.L. Moilliet; "The estimation of the wettability of small particles by measurements of the apparent boundary tensions at contaminated surfaces"; SCI Monograph no. 25, London, 1967.

75. Newitt, D.M.; J.M. Conway-Jones; "A contribution to the theory and practice of granulation"; Trans. Inst. Chem. Engrs. 36 (1958), 422-442.

76. Kapur, P.C.; D.W. Fuerstenau; "Kinetics of green pelletization"; Trans. Soc. Min. Eng. (1964), (Dec.), 348-355.

77. Capes, C.E.; P.V. Danckwerts; "Granule formation by the agglomeration of damp powders", Part I: The mechanism of granule growth; Trans. Inst. Chem. Engrs. 43 (1965), T116-T123.

78. Capes, C.E.; P.V. Danckwerts; "Granule formation by the agglomeration of damp powders"; Part II: The distribution of granule sizes; Trans. Inst. Chem. Engrs. 43 (1965), T125-T130.

79. Kapur, P.C.; D.W. Fuerstenau; "Size distributions and kinetic relationship in the nuclei region of wet pelletization"; Ind. Eng. Chem. Proc. Des. Dev. 5 (1966), (no. 1), 5-10.

80. Kapur, P.C.; D.W. Fuerstenau; "A coalescence model for granulation"; Ind. Eng. Chem. Proc. Des. Dev. 8 (1969), 56-62.

81. Sherrington, P.J.; "Liquid phase characteristics in fertilizer granulation by a layering processes"; Can. J. Chem. Eng. 47 (1969), 308.

82. Sastry, K.V.S.; D.W. Fuerstenau; "Size distribution of agglomeration in coalescing dispersed phase systems"; Ind. Eng. Chem. Fund. 9 (1970), 145-149.

83. Kapur, P.C.; "The crushing and layering mechanism of granule growth"; Chem. Eng. Sci. 26 (1971), 1093-1099.

84. Butensky, M.; Hyman, D.; "Rotary drum agglomeration. An experimental study of the factors affecting granule size"; Ind. Eng. Chem. Fund. 10 (1971), (no. 2), 212-219.

85. Sastry, K.V.S.; D.W. Fuerstenau; "Principles of agglomerating particulate materials by balling or granulation"; Proc. 12th Binnial Conf. of the Inst. for Briquetting and Agglomeration, Vancouver august 1971.

86. Kapur, P.C.; "Kinetics of granulation by non-random coalescence mechanism"; Chem. Eng. Sci. 27 (1972), 1863-1869.

87. Linkson, P.B.; J.R. Glastonbury; G.J. Duffy; "The mechanism of granule in wet pelletising"; Trans. Inst. Chem. Engrs. 51 (1973), 251.

88. Sastry, K.V.S.; D.W. Fuerstenau; "Mechanisms of agglomerate growth in green pelletization"; Powder Techn. 7 (1973), 97-105.

89. Ouchiyama, N.; T. Tanaka; "Mathematical model in the kinetics of granulation"; Ind. Eng. Chem. Proc. Des. Dev. 13 (1974), (no. 4), 383-389.

90. Ouchiyama, N.; T. Tanaka; "The probability of coalescence in granulation kinetics"; Ind. Eng. Chem. Proc. Des. Dev. 14 (1975), (no. 3), 286-289.

91. Ramabhadran, T.E.; "On the general theory of solid granulation"; Chem. Eng. Sci. 30 (1975), 1027-1033.

92. Pulvermacher, B.; E. Ruckenstein; "Time evolution of the size spectrum in granulation"; The Chem. Eng. Journ. 9 (1975), 21-29.

93. Sastry, K.V.S.; "Similarity size distribution of agglomerates during their growth by coalescence in granulation or green pelletization"; Int. Journ. Min. Proc. 2 (1975), 187-203.

94. Capes, C.E.; R.J. Germain; R.D. Coleman; "Binding liquid requirements for agglomeration by Tumbling"; Ind. Eng. Chem. Proc. Des. Dev. 16 (1977), (no. 4), 517-518.

95. Sastry, K.V.S.; D.W. Fuerstenau; "Kinetics and process analysis of the agglomeration of particulate materials by green pelletization"; Proc. of the 2nd Int. Symp. on Agglomeration; Ed. by K.V.S. Sastry, Atlanta, march 1977, Vol. I, p. 381-402; New York, Am. Inst. Min. Metallurg. Petr. Eng., 1977.

96. Kapur, P.C.; "Role of similarity size spectra in balling and granulation of coarse, liquid deficient powders"; Proc. of the 2nd Int. Symp. on Agglomeration, Ed. by K.V.S. Sastry, Atlanta, march 1977, Vol. I, p. 156-175.; New York, Am. Inst. Min. Metallurg. Petr. Eng., 1977.

97. Rumpf, H.; "Agglomeration"; Ed. by W.A. Knepper, New York, Interscience, 1962.

98. Schubert, H.; "Untersuchungen zur Ertmittlung von Kapillardruck und Zugfestigkeit von feuchten Haufwerken aus körnigen Stoffen"; Universität Karlsruhe, Dissertation, 1972.

99. Rumpf, H.; H. Schubert; "The behaviour of agglomerates under tensile strain"; J. Chem. Eng. Japan 7 (1974), 294-298.

100. Schubert, H.; W. Herrmann; H. Rumpf; "Deformation behaviour of agglomerates under tensile stress"; Powder Techn. 11 (1975), 121-131.

101. Lyne-Smith, K.; G.J. Jarneson; "The rate of agglomeration of solid and liquid particles in a stirred vessel"; Paper presented at the Sixth Ann. Res. Meeting on "Particle Growth Processes" of the Inst. of Chem. Engrs., London, University College, 4-6 April 1979.

102. Pich, J.; S.K. Friedlander; F.S. Lai; "The self-preserving particle size distribution for coagulation by Brownian motion-III"; Aerosol Sci. 1 (1970), 115-126.

103. Ramabhadran, T.E.; T.W. Peterson; J.H. Seinfeld; "Dynamics of aerosol coagulation and condensation"; A.I.Ch.E. Journ. 22 (1976), (no. 5), 840.

104. Middleton, P.; J. Brock; "Simulation of aerosol kinetics";Journ. Colloid & Interf. Sci. 54 (1976), 249-264.

105. Okuyama, K.; Y. Kousaka; Y. Kida; T. Yoshida; "Turbulent coagulation of aerosols in a stirred tank"; Journ. Chem. Eng. Japan 10 (1977), 142-147.

106. Swift, D.L.; S.K. Friedlander; "The coagulation of hydrosols by Brownian motion and laminar shear flow"; Journ. Colloid Sci. 19 (1964), 621.

107. Wang, C.S.; S.K. Friedlander; "The self-preserving particle size distribution for coagulation by Brownian motion"; Journ. Colloid Sci. 24 (1967), 170.

108. Friedlander, S.K.; C.S. Wang; "The self-preserving particle size distribution for coagulatien by Browni n motion"; Journ. Colloid Interf. Sci. 22 (1966), 126-132.

109. Hidy, G.M.; D.K. Lilly; "Solutions to the equations for the kinetics of coagulation"; Journ. Colloid Sci. 20 (1965), 867-874.

110. Hidy, G.M.; "On the theory of the coagulation of noninteracting particles in Bronian motion"; Journ. Colloid Sci. 20 (1965), 123-144.

111. Hulburt, H.M.; T. Akiyama;"Liouville equations for agglomeration and dispersion processes"; Ind. Eng. Chem. Fund. 8 (1969), 319.

112. Bajpai, R.K.; D. Ramkrishna; A. Prokop; "A coalescence redispersion model for drop size distributions in an agitated vessel"; Chem. Eng. Sci. 31 (1976), 913-920.

113. Ramkrishna, D.; "Drop-breakage in agitated liquid-liquid dispersion"; Chem. Eng. Sci. 29 (1974), 987-992.

114. Delichatsios, M.A.; R.F. Probstein; "The effect of coalescence on the average drop size in liquid-liquid dispersions"; Ind. Eng. Chem. Fund. 15 (1976), (no. 2), 134-138.

115. Coulaloglou, C.A.; L.L. Tavlarides; "Description of interaction processes in agitated liquid-liquid dispersions"; Chem. Eng. Sci. 32 (1977), 1289-1297.

116. Stamatoudis, M.; L.L. Tavlarides; "Effects of continuous phase viscosity in liquid-liquid dispersions in agitated vessels"; Paper presented at the 6th CHISA Congr., Praha (Czechoslovakia), aug. 21-25 1978, Paper H2.1.

117. Ramkrishna, D.; J.D. Borwanker; "A puristic analysis of population balance-I"; Chem. Eng. Sci. 28 (1973), 1423-1435.

118. Ramkrishna, D.; J.D. Borwanker; "A puristic analysis of population balance-II"; Chem. Eng. Sci. 29 (1974), 1711-1721.

119. Ramkrishna, D.; B.H. Shah; J.D. Borwanker; "Analysis of population balance-III"; Chem. Eng. Sci. 31 (1976), 435-442.

120. Pulvermacher, B.; E. Ruckenstein; "Similarity solutions of population balances"; Journ. Colloid & Interf. Sci. 46 (1974), 428.

121. Pulvermacher, B.; E. Ruckenstein; "Two kinds of self-preserving size spectra of a cloud of particles"; A.I.Ch.E. Journ. 21 (1975), 128-135.

122. Ramabhadran, T.E.; J.H. Seinfeld; "Self-preserving theory of particulate systems"; Chem. Eng. Sci. 30 (1975), 1019-1025.

123. Abrahamson, J.; "Collision rates of small particles in a vigorously turbulent fluid"; Chem. Eng. Sci. 30 (1975), 1371-1379.

124. Coulaloglou, C.A.; L.L. Tavlarides; M. Stamatoudis; "Theory on drop coalescence in turbulent dispersions"; To be published.

125. Tavlarides, L.L.; M. Stamadoudis;"Analysis of liquid-liquid dispersions with mass-transfer and reaction"; To be published.

126. Brakel, J. van; "Capillary liquid transport in porous media"; Delft, Ph.D Thesis, 1975.

127. Wada, M.; O. Tsuchiya; "The role of hydrophile colloid in iron ore pelletization"; Proc. IXth Int. Min. Proc. Congr., Prague, 1-6 June 1970, p. 23-51.

128. Vervoorn, P.M.M.; "De sterkte van titaandioxyde-granules"; Delft, Ph.D Thesis, 1977.

129. Hinze, J.O.; "Turbulence"; New York, McGraw Hill, 1959.

130. Riet, K, van 't; "Turbine agitator hydrodynamics and dispersion performance"; Delft, Ph.D Thesis, 1975.

131. Tadmor, Z.; "Forces in dispersive mixing"; Ind. Eng. Chem. Fund. 15(1976), 346.

132. Friedlander, S.K.; "Theoretical considerations for the particle size statospheric aerosol"; Journ. Meterol. 18 (1961), 753-759.

133. Ruckenstein, E.; B. Pulvermacher; "Growth kinetics and the size distributions of supported metal crystallites"; Journ. Catalysis 29 (1973), 224-245.

134. Sonneveld, P.; G.G. Bemer; To be published.

135. Capes, C.E.; "A note on size distribution in granulation, balling and wet pelletizing"; The Chem. Eng. (1967), (Apr.), CE78-CE80.

136. Capes, C.E.; A.E. McIlhinney; R.D. Coleman; "Some consideration on the dynamics of balling circuits"; Trans. Soc. Min. Eng. AIME 258 (1975), 204-208.

137. Sastry, K.V.S.; D.W. Fuerstenau; "Laboratory simulation of Closed-circuit Balling drum operation by locked-cycle experiments"; Trans. Soc. Min. Eng. AIME 258 (1975), 335-340.

138. Fuerstenau, D.W.; K.V.S. Sastry; V.N. Setharama; "Investigation of surging in continuous balling circuits by the locked-cycle experimental technique"; C.I.M. Bulletin (1976), (Aug.), 67-72.

139. Narsimhan, G.; J.P. Gupta; D. Ramkrishna; "A model for transitional breakage propbability of droplets in agitated lean liquid-liquid dispersions"; Chem. Eng. Sci. 34 (1979), 257-265.

STELLINGEN

1

Om een bevredigende beschrijving van de natte drukval in gepakte gas-vloeistof kolonnes te verkrijgen is het nodig, maar ook voldoende, aan te nemen dat zich in de pakking kanalen met vernauwingen bevinden.

E. Blass, R. Kurtz; Chem. Ing. Techn. 11 (1977), 44.
G.G. Bemer, G.A.J. Kalis, Trans. I. Chem. E. 56 (1978), 200.

2

In gepakte kolonnes komt het merendeel van de axiale menging in de vloeistoffase op rekening van de sterk gesegregeerde stromingstoestand van de vloeistof.

W. v. Swaay, Diss. Eindhoven, 1967.
G.G. Bemer, F.J. Zuiderweg; Chem. Eng. Sci. 33 (1978), 1637.

3

De ook tegenwoordig nog algemeen gebruikte waarden voor de hoogte van de stofoverdrachtstrap H_{og}, gemeten door Fellinger, zijn te conservatief omdat geen rekening gehouden is met het optreden van Marangoni verschijnselen in het door hem bestudeerde ammoniak-water systeem.

Fellinger, Sc.D Thesis, M.I.T., 1941.
W.L. Bolles, J.R. Fair; I.Chem. E. Symp. Ser. 56 (1979), 33-35.

4

Recentelijk gemeten botsingskrachten en frequenties die optreden bij deeltjesroerder botsingen kunnen als basis dienen voor meer fysisch gefundeerde secundaire kiemvormingsvergelijkingen voor industriele kristallisatoren.

G.G. Bemer; Chem. Eng. Sci. 34 (1979),747

5

Het principe van lichtterugkaatsing kan gebruikt worden bij de verdere ontwikkeling van relatief goedkope 'on-line' methoden ter bepaling van hoge vaste stof koncentraties in gas- of vloeistofstromen.

G.G. Bemer; Powder Techn. 22 (1979),143.

6

Zowel de efficiency als de stabiliteit van kontinue pelletizers wordt waarschijnlijk voor een groot deel bepaald door de volume fractie aan pellets.

dit proefschrift.

7

Bij een juist ontwerp van de pelletizer kan de vereiste verblijftijd aanzienlijk verkort worden door reeds gevormde agglomeraten weer te breken.

dit proefschrift.

8

Het kritisch bestuderen van z.g. traditionele geneeskunde systemen in landen, die op dit moment ontwikkelingslanden worden genoemd, is zowel voor deze landen als voor de ontwikkelde landen van groot belang.

C.A. Gunawardhana; Int. Workshop on Appropriate Technology, 4-7 sept. 1979,Delft.

9

Dat technologie niet waardevrij is maar b.v. economisch, cultureel en doelgroep gebonden, verdient meer aandacht te krijgen in de ingenieursopleiding.

Beleidsplan Centrum voor Aangepaste Technologie, THD, sept. 1979.

10

De verwarring rond het begrip "aangepaste technologie" kan aanzienlijk verminderd worden door aangepaste technologie te beschouwen als die technologie die ontwikkeling bevorderd; hiermee echter is het dilemma of technologie in een specifieke situatie aangepast is of niet, nauwelijks opgelost.

A.K. Reddy, Appropriate Technology; Paper Int. Workshop AT, 4-7 Sept. 1979,Delft.

11

Bij het aangaan van samenwerkingsverbanden tussen technische hogescholen en industrie, verdient gesponserde research de voorkeur boven kontrakt-research.

12

Te stellen dat bij objective fotografie, in tegenstelling tot subjectieve fotografie, het rationele element overheerst is subjectief.

13

Het aanschaffen van goede kookboeken (b.v. van Escoffier) door het Nederlandse Restaurantwezen zou in overeenstemming zijn met de doeleinden van de Wet Investerings Rekening.

G.G. Bemer
september 1979